UNIVERSIDADE FEDERAL DE PERNAMBUCO
CENTRO DE CIÊNCIAS EXATAS DA NATUREZA
PÓS-GRADUAÇÃO EM ESTATÍSTICA

FERNANDA VITAL DE PAULA

EXTENDED CIRCULAR DISTRIBUTIONS: MATHEMATICAL PROPERTIES, INFERENCE AND REGRESSION MODEL

RECIFE

2018

Fernanda Vital de Paula

EXTENDED CIRCULAR DISTRIBUTIONS: MATHEMATICAL PROPERTIES, INFERENCE AND REGRESSION MODEL

Doctoral thesis submitted to the Graduate Program in Statistics, Department of Statistics, Federal University of Pernambuco as a partial requirement for obtaining a doctorate in Statistics.

Advisor: Professor Ph.D. Getúlio José Amorim do Amaral

Co-advisor: Professor Dr. Abraão David Costa do Nascimento

RECIFE

2018

Catalogação na fonte
Bibliotecária Monick Raquel Silvestre da S. Portes, CRB4-1217

P324e Paula, Fernanda Vital de
Extended circular distributions: mathematical properties, inference and regression model / Fernanda Vital de Paula. – 2018.
116 f.: il., fig., tab.

Orientador: Getúlio José Amorim do Amaral.
Tese (Doutorado) – Universidade Federal de Pernambuco. CCEN, Estatística, Recife, 2018.
Inclui referências e apêndices.

1. Estatística. 2. Modelo de regressão. I. Amaral, Getúlio José Amorim do (orientador). II. Título.

310 CDD (23. ed.) UFPE- MEI 2018-044

FERNANDA VITAL DE PAULA

EXTENDED CIRCULAR DISTRIBUTIONS: MATHEMATICAL PROPERTIES, INFERENCE AND REGRESSION MODEL

Tese apresentada ao Programa de Pós-Graduação em Estatística da Universidade Federal de Pernambuco, como requisito parcial para a obtenção do título de Doutor em Estatística.

Aprovada em: 14 de março de 2018.

BANCA EXAMINADORA

Prof. Getúlio José Amorim do Amaral
UFPE

Prof.ª Maria do Carmo Soares de Lima
UFPE

Prof.ª Audrey Helen Maria de Aquino Cysneiros
UFPE

Prof.ª Renata Maria Cardoso Rodrigues de Souza
UFPE

Prof. Marcelo Rodrigo Portela Ferreira
UFPB

Agradecimentos

Aos meus pais, que permitiram que eu chegasse até aqui.

Ao meu orientador, Professor Getúlio José Amorim Amaral, por todos os ensinamentos e incentivo. Pela paciência e disponibilidade. Por acreditar no meu potencial. Pelas reuniões agradáveis e enriquecedoras.

Ao meu coorientador (meu outro orientador), Professor Abraão David Costa do Nascimento, por todos os ensinamentos e motivação. Por ter me considerado como uma orientanda. Pela presença e paciência. Pela confiança. Pelas reuniões aprazíveis e inspiradoras.

Aos membros da banca: Professores Audrey, Marcelo, Maria do Carmo e Renata, pelas valiosas colaborações que fizeram para concretização deste trabalho.

Ao Professor Gauss Moutinho Cordeiro, a quem muito admiro, pelas colaborações na qualificação que convergiram no Capítulo 5, desta tese.

Aos professores do Programa de Pós-Graduação em Estatística, pelos ensinamentos.

A Pernambuco, esse Estado maravilhoso, que me proporcionou experiências incríveis por meio de sua cultura (aqui, agradeço em especial ao Grupo Yalu, pelos fins de semana de maracatu e alegria), de sua tamanha beleza e de pessoas imensamente especiais que encontrei nessas terras e foram essenciais nesta caminhada.

Aos colegas de trabalho e aos alunos da Universidade Federal do Tocantins, pela força, motivação e torcida.

À Universidade Federal do Tocantins, pela oportunidade de me qualificar por meio do afastamento concedido.

À Valéria Bittencourt, secretária da pós-graduação em estatística, pela competência, simpatia e atenção.

Abstract

Circular Statistics is an important branch of the Statistics which has been necessary in various scientific fields such as Biology, Medicine, Geology, Meteorology and others. During the performed researches some gaps were observed in this study branch. Thus, the main objective of this thesis is to collaborate with the enrichment of the literature in Circular Statistics, seeking to fill these gaps. First, the difficulty in obtaining models with asymmetry, different modality scenarios and treatable trigonometric moments was noticed. In this way, a new circular distribution is proposed in the Chapter 2, denominated Exponentialized Cardioid (EC). Some of its mathematical properties are presented, such as trigonometric moments, kurtosis, and asymmetry. In addition, two estimation methods for EC model parameters were studied. Subsequently, the lack of hypothesis tests for parameters of circular distributions, in the context of models distinction, was evidenced in the literature. Apart from, few studies on bootstrap were found in Circular Statistics. Thus, in Chapter 3, we devote attention to make hypothesis inference on EC parameters. In particular, adopting as comparison critera estimated type I error size and test power, we study the performance of tests based on likelihood ratio, Wald, score and gradient statistics and their bootstrap versions putting emphasis to distinguish the EC distribution regard to Cardioid and uniform models, special cases of the former. From the theoretical point of view, an important collaboration was the derivation of the EC Fisher information matrix. The last gap refers to the few models of circular-circular regression in the literature. In Chapter 4, a new circular-circular regression model having distributed EC angular errors is proposed. Its regression curve is expressed in terms of the Möbius Transformation. Futher, a complex version of the EC distribution is also presented, named CEC distribution, and a likelihood-based estimation procedure for parameters of the new model is furnished. The fifth Chapter has the same purpose as Chapter 2. Four new circular distributions, that extend the Cardioid distribution (C) are proposed, called beta Cardioid (βC), Kumaraswamy Cardioid (KwC), gamma Cardioid (ΓC) and Marshall-Olkin Cardioid (MOC). These distributions are rewritten as a family, which is a result of weighting the C probability density function (pdf). General mathematical expressions

for their trigonometric moments and the idea for estimating the parameters of the proposed models by the maximum likelihood method are presented. These four chapters present examples in the area of Meteorology or Biology that point out the success of the new proposed models in the Chapters 2, 4 and 5 and the good performance of the Wald and gradient tests, in the Chapter 3.

Keywords: Circular Statistic. EC distribution. Inference.

Resumo

A Estatística Circular é um ramo importante da Estatística que tem sido necessário em diversos campos científicos como Biologia, Medicina, Geologia, Meteorologia, entre outros. Durante as pesquisas realizadas foram observadas algumas lacunas neste campo de estudo. Dessa forma, o objetivo principal dessa tese é colaborar com o enriquecimento da literatura em Estatística Circular, buscando preencher tais lacunas. Primeiramente, a dificuldade em obter modelos com assimetria, diferentes cenários de modalidade e momentos trigonométricos tratáveis foi notada. Dessa forma, no Capítulo 2 uma nova distribuição circular é proposta, denominada Cardioide Exponencializada (EC). Algumas de suas propriedades matemáticas são apresentadas, como momentos trigonométricos, curtose e assimetria. Além disso, dois métodos de estimação para os parâmetros do EC modelo foram estudados. Posteriormente, a inexistência de testes de hipóteses para parâmetros de distribuições circulares, no contexto de distinção de modelos, foi evidenciada na literatura. Ademais, poucos estudos sobre bootstrap foram encontrados em Estatística Circular. Assim, no Capítulo 3, foi dada atenção à inferência de hipóteses sobre os parâmetros da EC. Em particular, adotando como critérios de comparação o tamanho do erro tipo I e o poder do teste estimados, estudamos o desempenho dos testes baseados na estatísticas de razão de verossimilhança, Wald, escore e gradiente e suas versões bootstrap, com ênfase em distinguir a distribuição EC dos modelos Cardioide (C) e uniforme, casos especiais da primeira. Do ponto de vista teórico, uma importante colaboração foi a derivação da matriz de informação de Fisher da EC. A última lacuna se refere aos poucos modelos de regressão circular-circular existentes na literatura. No Capítulo 4, um novo modelo de regressão circular-circular, com erros angulares assumindo a distribuição EC, é proposto. A curva de regressão é expressa em termos da transformação Möbius. Além disso, uma versão complexa da distribuição EC também é apresentada, denominada distribuição CEC e um procedimento, com base na máxima verossimilhança, é fornecido para estimar os parâmetros do novo modelo. O quinto capítulo tem o mesmo objetivo do Capítulo 2. Quatro novas distribuições circulares flexíveis que estendem a distribuição Cardioide (C) são propostas, denominadas beta Cardioide (βC), Kumaraswamy Cardioide (KwC),

gamma Cardioide (ΓC) e Marshall-Olkin Cardioide (MOC). Estas distribuições são reescritas como ponderações da função densidade de probabilidade da C. As expressões matemáticas para seus momentos trigonométricos e a idéia geral para estimar os parâmetros dos modelos propostos pelo método de máxima verossimilhança são apresentadas. Esses quatro capítulos apresentam exemplos na área de Meteorologia e Biologia que apontam o sucesso dos novos modelos propostos nos Capítulos 2, 4 e 5 e o bom desempenho dos testes Wald e gradiente, no Capítulo 3.

Palavras-chave: Distribuição EC. Estatística circular. Inferência.

List of Figures

List of Tables

List of Abbreviations and Acronyms

βC	beta Cardioid
EC	Exponentiated Cardioid
cdf	cumulative distribution function
KwC	Kumaraswamy Cardioid
FIM	Fisher information matrix
$\hat{l}$	maximized log-likelihoods under H_1
$\tilde{l_a}$	maximized log-likelihoods under H_0 for situation a
$\tilde{l_b}$	maximized log-likelihoods under H_0 for situation b
ML	maximum likelihood
MLE	maximum likelihood estimator
MOC	Marshall-Olkin Cardioid
MSE	mean square error
MT	Möbius transformation
pdf	probability density function
QLSE	quantile least squares estimator
SE	standard errors
T_{1a}	likelihood ratio test for situation a
T_{1b}	likelihood ratio test for situation b
T_{2a}	Wald test for situation a
T_{2b}	Wald test for situation b
T_{3a}	score test for situation a
T_{3b}	score test for situation b
T_{4a}	gradient test for situation a
T_{4b}	gradient test for situation b
vM	von Mises
vMM	modified von Mises
wC	wrapped Cauchy
ΓC	gamma Cardioid

Contents

1 Introduction

Circular statistics is a particular branch of the Statistics that deals with data that can be represented as angles or, equivalently, as points on the circumference of the unit circle. According to Fisher (1995), this branch is situated somewhere between the analysis of linear and spherical data.

Examples of circular data include directions measured using instruments such as a compass, protractor, weather vane, sextant or theodolite. It is usual to record such directions as angles expressed in degrees or radians measured either clockwise or counterclockwise from some origin, referred to as the zero direction. The requirements to specify the position of the origin and the direction taken to be positive do not arise for data on the real line; the origin is 0, values to the left of 0 are negative and those to the right are positive. For circular data, each angle defines a point on the circumference of the unit circle, just as each value of a linear variable defines a point on the real line. As the absolute value of a linear variable increases we move further away from the origin. So, on the real line, a value of 360 is relatively close to a value of 355 but relatively far from the origin. The situation is very different for circular variables. Whilst an angle of 355 corresponds to a point on the circumference of the unit circle that is close to that corresponding to 360, the angles 0 and 360 define the exact same point. It is this periodic nature of circular data that forces us to abandon standard statistical techniques designed for linear data in favor of those which respect the periodicity of circular data (Pewsey *et al.*, 2014).

Pewsey *et al.* (2014) still mentions that the support for circular data is the unit circle as opposed to the real line which is the support for linear data. Whilst measured directions recorded as angles constitute one type of circular data, not all circular data are necessarily initially measured

or recorded as angles. As example, each time of day measured on a 24 hours can be converted to an angle measured in degrees by multiplying the time in hours by 360/24. Those angles can then be used to define points around the circumference of the unit circle.

The circular data are of interest in many contexts (Pewsey *et al.*, 2014). Some examples include

- the bonding angles of molecules (Viftrup *et al.*, 2007),
- the direction of the wind (Davis, 1986),
- time patterns in crime incidence (Brunsdon and Corcoran, 2006),
- time patterns of events in the field of cyber security (Pan *et al.*, 2017),
- the incidence throughout the years of measles (Guo *et al.*, 2010).

Other applications from astronomy, geology, medicine, meteorology, oceanography, physics and psychology are referred to in Fisher (1995) and Mardia and Jupp (1999). According to Morellato *et al.* (2010), variables that characterize the phenology of species, such as powering onset during the year, are of great interest to biologists. Many of these examples illustrate the importance of circular statistics in environmental and climate-change analysis. Circular statistics have also been applied by Mardia *et al.* (2007) and Boomsma *et al.* (2008) in the areas of bioinformatics and proteomics.

Due to the importance of analyzing circular data in the area of Statistics, there are seven books devoted to this topic more depth: Mardia (1972), Batschelet (1981), Upton and Fingleton (1989), Fisher (1995), Mardia and Jupp (1999), Jammalamadaka and Sengupta (2001) and Pewsey *et al.* (2014). Mardia and Jupp (1999) is a heavily revised, updated and extended version of Mardia (1972), which, together with Jammalamadaka and Sengupta (2001), provide the most theoretical treatments of the subject. The last is the only one of them that includes any code, but the S-Plus based on the CircStats package to which it refers is of rather limited scope, before the publication of Pewsey *et al.* (2014) which includes the R code for applications of

techniques presented in other literatures. Aspects of robust or Bayesian methods are considered in Mardia and Jupp (1999) and Jammalamadaka and Sengupta (2001). Time series or spatial analysis for circular data are covered by Fisher (1995).

Construction of a tractable circular model with an asymmetric shape has been a problem in statistics of circular data. To tackle this problem, some asymmetric extensions of well-known circular models have been proposed in the literature. Malsimov (1967), Yfantis and Borgmann (1982) and Gatto and Jammalamadaka (2007) discussed an extension of the vM distribution, generated through maximization of Shannon's entropy with restrictions on certain trigonometric moments. Batschelet (1981) proposed a mathematical method of skewing circular distributions that has seen renewed interest very recently. In Fernández-Durán (2004), the author proposed the non-negative trigonometric moment distributions. Pewsey (2008) presented a four parameter family of distributions on the circle by wrapping the stable distribution and Jammalamadaka and Kozubowsky (2004) by wrapping the classical exponential and Laplace distributions. Kato and Jones (2010) proposed a family of distributions arising from the Möbius transformation which includes the vM and wrapped Cauchy distributions. Umbach and Jammalamadaka (2009) introduced the idea of Azzalini (1985) to circular distributions that typically results in an asymmetric distribution. Kato and Jones (2013) proposed a mathematical tractability model, obtained from the wrapped Cauchy, by applying Brownian motion. Unlike familiar symmetric distributions, it is often difficult to deal with skew models in statistical analysis. This difficulty is partly due to the lack of some mathematical properties that many of the well known symmetric models have. For example, existing asymmetric models often have complex normalizing constants and trigonometric moments, which could cause trouble in analysis (Kato and Jones, 2013).

In relation to statistical inference for the parameters of circular distributions, Jammalamadaka and Sengupta (2001) cites that not much is known in terms of optimal tests for the parameters of other circular distributions, besides the vM. Such a distribution is called *circular Normal distribution* to emphasize its importance and similarities to the Normal distribution on the real line. The author still indicates SenGupta and Pal (2001) for a discussion on Wrapped Stable distributions.

As regards circular regression models, three types can be cited: linear-circular, circular-linear and circular-circular. The study of the latter has received very little attention (Pewsey *et al.*, 2014), although the regression of a circular variable on a circular variable often arises in practice. Many examples can be cited including the spawning time of a particular fish on the time of the low tide, wind directions at different times and the orientation of a bird nest on orientation of river. In circular-circular regression, an angular random variable is modelled in terms of other circular random variable and both are measured assuming the same zero direction and rotation sense (Sarma and Jammalamadaka, 1993). Such particularities makes the problem more complicated than the usual linear regression.

Therefore, the idea of the thesis is to contribute to fill these gaps in the literature of circular statistics with respect to the:

- proposition of new circular models with asymmetry, different modality scenarios and treatable properties;
- statistical inference for the parameters of a circular distributions; and
- proposition of circular-circular regression models.

These contributions resulted in six chapters, including this introductory chapter. The four independent following chapters are connected by a single object of study: a new circular distribution. In Chapter 2, the new model is proposed, called Exponentiated Cardioid (EC) and their properties such as trigonometric moments, kurtosis and skewness are derived. A discussion about the modality of the studied model is also presented. To fit the EC model, two estimation methods are presented based on maximum likelihood and quantile least squares procedures. The performance of proposed estimators is evaluated in a Monte Carlo simulation study and the proposed model is applied to a dataset about wind directions.

In Chapter 3, the EC distribution is considered in order to study the Type I error rate and the power of the likelihood ratio, Wald, score and gradient tests and their bootstrap versions to distinguish the EC distribution from the Cardioid and uniform distributions. In addition, an

important property of the proposed model is derived (Fisher information matrix) and the tests and their bootstrap versions are applied to datasets.

In Chapter 4, the EC distribution is assumed as distribution for the angular errors of the a proposed circular-circular regression model. Its regression curve is expressed in terms of the Möbius transformation. Futher, the complex version of the EC distribution is introduced, named CEC distribution. The maximum likelihood method is presented to estimate the model parameters. The usefulness of the new model is illustrated using wind direction real data. Its performance is compared with those due to models having the vM, wrapped Cauchy and modified vM error distributions as error angular components. Results indicate that the our proposal may be the best regression model.

Four new circular distributions that extend the C distribution are introduced in Chapter 5, called beta Cardioid (βC), Kumaraswamy Cardioid (KwC), gamma Cardioid (ΓC) and Marshall-Olkin Cardioid (MOC). These distributions are rewritten as a family, which is a result of weighting the C pdf. General mathematical expressions for their trigonometric moments and the idea for estimating the parameters of the proposed models by the maximum likelihood method are presented. The usefulness of the new distributions is illustrated using two applications to real data. Finally, in Chapter 6, some conclusions and ideas for further work are presented.

2 A new extended Cardioid model: an application to wind data

Resumo

A distribuição Cardioide é um modelo relevante no tratamento de dados circulares. Porém, este modelo não é adequado para cenários onde existe assimetria ou multimodalidade. Para resolver esse problema, um modelo extendido da Cardioide é proposto, chamado distribuição Cardioide exponencializada (EC). Além disso, algumas de suas propriedades como momentos trigonométricos, curtose, e assimetria são derivadas. Uma discussão sobre a modalidade do modelo estudado é também apresentada. Para ajustar o modelo EC, são apresentados dois métodos de estimação, a máxima verossimilhança e mínimos quadrados quantílicos. A performance dos estimadores é avaliada em um estudo de simulação, adotando viés e erro quadrático médio, como comparação. Finalmente, o modelo proposto é aplicado a um conjunto de dados no contexto de direções de vento. Resultados indicam que a distribuição EC pode superar distribuições clássicas com suporte circular tais como a Cardioide e a vM.

Palavras-chave: Cardioide exponencializada. Direção do vento. Modalidade. Momentos trigonométricos.

Abstract

The Cardioid distribution is a relevant model for circular data. However, this model is not suitable for scenarios where there is asymmetry or multimodality. In order to solve this problem, an extended Cardioid model is proposed, which is called Exponentiated Cardioid (EC) distribu-

tion. Moreover, some of its properties, such as trigonometric moments, kurtosis and skewness are derived. A discussion about the modality of the studied model is also presented. To fit the EC model, two estimation methods are presented based on maximum likelihood and quantile least squares procedures. The performance of proposed estimators is evaluated in a Monte Carlo simulation study, adopting both average bias and square error as comparison criteria. Finally, the proposed model is applied to a dataset in the wind direction context. Results indicate that the EC distribution may outperform some classical distributions with circular support such as the Cardiod and the von Mises.

Key-words: Exponentiated Cardioid. Modality. Trigonometric moments. Wind direction.

2.1 Introduction

Circular data have been obtained from various fields such as in Biology (Batschelet, 1981), Zoology (Boles and Lohmann, 2003), Geology (Rao and Sengupta, 1972) and others. Some examples are related to birds navigational, variation in the onset of leukaemia, orientation data in textures and wind directions. The periodic nature of circular data imposes a specific treatment which is appropriate for non-euclidean space. Even though symmetry is assumed by several circular models, there are many practical situations where asymmetric distributions are necessary. Thus, a new tractable flexible circular model will be presented in this chapter.

There are some generators for representing circular and directional data. Among them, the simplest is known as *perturbation procedure* proposed by Jeffreys (1961) and it is based on the product of an existing circular density and a function chosen such that the resulting expression is also a circular density (Pewsey *et al.*, 2014). The Cardioid and sine-skewed (Abe and Pewsey, 2009) distributions are particular cases of this method. The Cardioid distribution was introduced by Jeffreys (1961) as cosine perturbation of the continuous circular uniform distribution and has probability density function (pdf) given by

$$f_C(\theta) = \frac{1}{2\pi}\{1 + 2\rho\cos(\theta - \mu)\},$$

where $0 \leq \mu < 2\pi$ is the mean direction parameter and $|\rho| \leq \frac{1}{2}$ is the concentration param-

eters. Further, the circular uniform distribution is obtained when $\rho = 0$. Other generator is stemmed from the real line around the circumference, called *wrapping models* (Jammalamadaka and Sengupta, 2001). The wrapped Cauchy and normal models are examples of this method. Generators defined by transforming the argument of some existing densities, say $g(\theta)$, replacing its argument, θ, by functions of it, can also be mentioned. Some distribution generators in this way are Jones-Pewsey (Abe *et al.*, 2013), Inverse Batschelet (Jones and Pewsey, 2012), Papakonstantinou (Abe *et al.*, 2009) (generated from Cardioid) and Batshelet (Batschelet, 1981) (from Von Mises) families. Moreover, the von Mises (vM) distribution is particularly useful in this chapter because its wide application to circular data. Its pdf is given by (for $0 \leq \theta < 2\pi$)

$$f_V(\theta) = [2\pi I_0(\rho)]^{-1} \exp[\rho \cos(\theta - \mu)],$$

where $0 \leq \mu < 2\pi$, $\rho \geq 0$ and $I_0(\rho) = \int_0^{2\pi} \exp[\rho \cos(\phi - \mu)] d\phi$ is the modified Bessel function of the first kind and order zero.

A further form to construct a circular model is the called *Möbius transformation* (see more details in Hardy and Wright (1979)). An example is the proposed family in Kato and Jones (2010), derived from vM distribution. Another method is based on the transformation of a bivariate linear random variable to its directional component. The obtained models are called *offset* distributions (Mardia and Sutton, 1975).

The previous generators results in, generally, symmetrical and unimodal distributions. However, circular data are seldom symmetrically distributed (Pewsey, 2008), besides presenting possible multimodality as the wind directions used in the application of this chapter, in the subsection 2.5.2. Therefore, tractable models with asymmetric shape and modality scenarios are required in several applications into the circular context. Some asymmetric extensions have been proposed in the literature. Among them, finite mixtures of unimodal models (Mardia and Sutton, 1975) and the application of multiplicative mixing, as that used by Gatto and Jammalamadaka (2007) to extended the vM law. Pewsey *et al.* (2014) also made reference to the non-negative trigonometric moment distributions (Fernández-Durán, 2004). Regarding the modality, the bimodal generalized skew-normal and sine-skewed circular distributions were proposed by Hernández-Sánchez

and Scarpa (2012) and Abe and Pewsey (2009), respectively.

In the Euclidean space, there are several ways to extend well-defined models. One of them is by exponentiating a cumulative distribution function (cdf), say F, by a positive real number β, $F(\cdot)^\beta$, see AL-Hussaini and Ahsanullah (2015). The review carried out indicates that this approach has not been previously used in the circular data context.

In this chapter, the methodology described by AL-Hussaini and Ahsanullah (2015) is used to obtain a new asymmetric circular distribution, called the EC model. The additional parameter may add events of amodality and bimodality to the baseline unimodal C, as it will be shown. Expressions for its trigonometric moments are also obtained. Two estimation procedures for the EC parameters are presented: maximum likelihood estimator (MLE) and quantile least squares estimator (QLSE). In order to compare those estimators, a Monte Carlo simulation study is performed. The numerical results indicate that the ML estimates have smaller mean square errors than those of QLS estimates in almost all considered cases. Finally, in order to illustrate the EC distribution potentiality, a comparison of its fit to those due to C and vM distributions is provided. Results of Kuiper and Watson goodness-of-fit statistics indicate that our proposal outperforms the other alternatives.

This chapter is organized as follows. In Sections 2.2 and 2.3, the EC distribution and some of its mathematical properties are presented, respectively. Section 2.4 deals with estimation procedures. Finally, numerical results obtained from real data studies are presented and discussed in Section 2.5.

2.2 The proposed model

The EC distribution has cdf given by (for $0 < \theta \leq 2\pi$)

$$F(\theta;\beta,\rho,\mu) = \left\{ \frac{\theta}{2\pi} + \frac{\rho}{\pi}[\text{sen}(\theta-\mu) + \text{sen}(\mu)] \right\}^{\beta}, \tag{2.1}$$

where $0 < \mu \leq 2\pi$, $0 \leq \rho \leq 0.5$ and $\beta > 0$ and, therefore, its pdf is

$$f(\theta;\beta,\rho,\mu) = \frac{\beta}{2\pi} \left\{ \frac{\theta}{2\pi} + \frac{\rho}{\pi}[\text{sen}(\theta-\mu) + \text{sen}(\mu)] \right\}^{\beta-1} [1 + 2\rho\cos(\theta-\mu)]. \tag{2.2}$$

This situation is denoted as $\Theta \sim EC(\beta, \rho, \mu)$. As special cases, the Cardioid distribution follows for $\beta = 1$ and the uniform distribution is obtained when $\beta = 1$ and $\rho = 0$. In this position, it is important to mention that the Cardioid extension by exponentiation requires to replacement zero by 2π in the EC support comparatively to that of the Cardioid model. This change avoids an undefinition at zero.

Figure 2.1 displays EC pdf curves and their associated histograms drawn from generated data for several parametric points. It is noticeable bimodal and asymmetric events in contrast with its baseline at $\beta = 1$. Moreover, higher values of ρ indicate more concentrated scenarios, as illustrated in Figure 2.1(d).

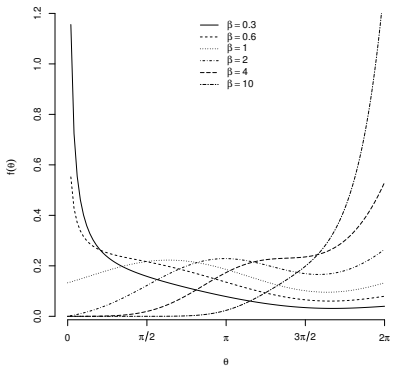

(a) For $\rho = 0.2$ and $\mu = 2$.

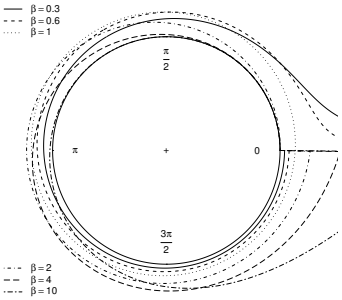

(b) For $\rho = 0.2$ and $\mu = 2$.

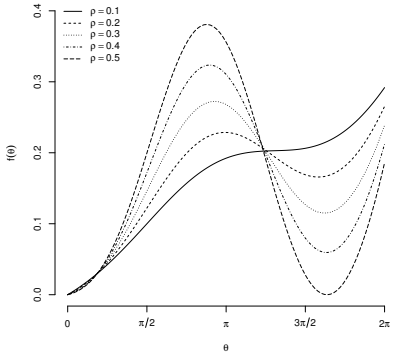

(c) For $\beta = 2$ and $\mu = 2$.

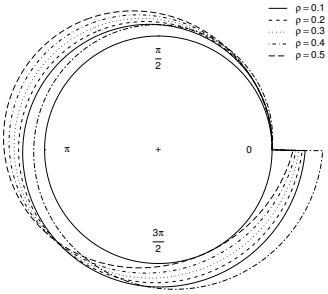

(d) For $\beta = 2$ and $\mu = 2$.

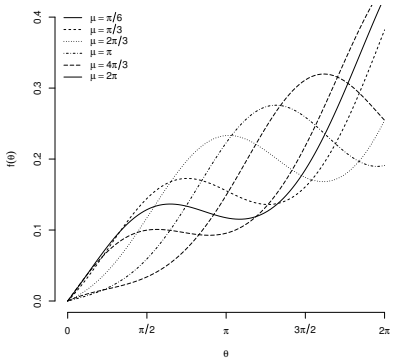

(e) For $\beta = 2$ and $\rho = 0.2$.

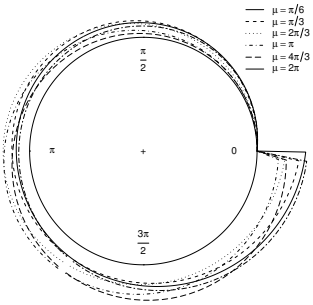

(f) For $\beta = 2$ and $\rho = 0.2$.

Figure 2.1: Theoretical and empirical EC densities for some parametric points.

2.2.1 *Modality essays*

The flexibility of the EC distribution is partially portrayed in Table 2.1. It is known that the Cardioid model ($\beta = 1$) is unimodal. In contrast, the EC distribution can be classified as amodal, unimodal and bimodal for different values of β, ρ and μ. This fact shows that our proposal has greater flexibility than its corresponding baseline.

Theorem 2.2.1 characterizes the EC modes. The proof is presented in Appendix A.

Theorem 2.2.1. *Let $\Theta \sim EC(\beta, \rho, \mu)$. If $\beta \geq 1$, then the equations $f'(\theta) = 0$ and $F(\theta) = \frac{\theta}{2\pi}$ are equivalent, where F is the EC cdf.*

Table 2.1: Modality of the EC distribution, for different values of the parameters, where ∅=Amodal, ◊=Unimodal and ■=Bimodal.

$\beta = 0.3$	ρ				
μ	$\frac{1}{10}$	$\frac{1}{5}$	$\frac{3}{10}$	$\frac{2}{5}$	$\frac{1}{2}$
$\frac{\pi}{6}$	◊	◊	◊	◊	◊
$\frac{\pi}{3}$	◊	◊	◊	◊	◊
$\frac{2\pi}{3}$	◊	◊	◊	◊	◊
π	∅	∅	∅	∅	∅
$\frac{4\pi}{3}$	∅	◊	◊	◊	◊
2π	◊	◊	◊	◊	◊

$\beta = 0.6$	ρ				
μ	$\frac{1}{10}$	$\frac{1}{5}$	$\frac{3}{10}$	$\frac{2}{5}$	$\frac{1}{2}$
$\frac{\pi}{6}$	◊	◊	◊	◊	◊
$\frac{\pi}{3}$	◊	◊	◊	◊	◊
$\frac{2\pi}{3}$	◊	◊	◊	◊	■
π	∅	◊	◊	◊	◊
$\frac{4\pi}{3}$	◊	◊	◊	◊	◊
2π	◊	◊	◊	◊	◊

$\beta = 1.0$	ρ				
μ	$\frac{1}{10}$	$\frac{1}{5}$	$\frac{3}{10}$	$\frac{2}{5}$	$\frac{1}{2}$
$\frac{\pi}{6}$	◊	◊	◊	◊	◊
$\frac{\pi}{3}$	◊	◊	◊	◊	◊
$\frac{2\pi}{3}$	◊	◊	◊	◊	◊
π	◊	◊	◊	◊	◊
$\frac{4\pi}{3}$	◊	◊	◊	◊	◊
2π	◊	◊	◊	◊	◊

$\beta = 2.0$	ρ				
μ	$\frac{1}{10}$	$\frac{1}{5}$	$\frac{3}{10}$	$\frac{2}{5}$	$\frac{1}{2}$
$\frac{\pi}{6}$	◊	■	■	■	■
$\frac{\pi}{3}$	◊	■	■	■	■
$\frac{2\pi}{3}$	◊	■	■	■	■
π	■	■	■	■	◊
$\frac{4\pi}{3}$	◊	◊	◊	■	■
2π	◊	■	■	■	■

$\beta = 4.0$	ρ				
μ	$\frac{1}{10}$	$\frac{1}{5}$	$\frac{3}{10}$	$\frac{2}{5}$	$\frac{1}{2}$
$\frac{\pi}{6}$	◊	◊	■	■	■
$\frac{\pi}{3}$	◊	◊	■	■	■
$\frac{2\pi}{3}$	◊	◊	■	■	■
π	◊	■	■	■	◊
$\frac{4\pi}{3}$	◊	◊	◊	◊	◊
2π	◊	◊	■	■	■

$\beta = 10.0$	ρ				
μ	$\frac{1}{10}$	$\frac{1}{5}$	$\frac{3}{10}$	$\frac{2}{5}$	$\frac{1}{2}$
$\frac{\pi}{6}$	◊	◊	◊	■	■
$\frac{\pi}{3}$	◊	◊	◊	■	■
$\frac{2\pi}{3}$	◊	◊	◊	■	■
π	◊	◊	◊	■	◊
$\frac{4\pi}{3}$	◊	◊	◊	◊	◊
2π	◊	◊	◊	■	■

2.3 Moments

Expressions for the first two trigonometric moments of the EC model are derived in this section. Moreover, standard descriptive measures for the proposed model are obtained from them. In general, EC trigonometric moments do not present closed-form expressions. Thus, they are represented through expansions in terms of a proposed special function as follows.

Theorem 2.3.1. *Let $\Theta \sim EC(\beta, \rho, \mu)$. Its cdf can be represented as*

$$F(\theta) = \sum_{k=0}^{\infty} \sum_{s=0}^{k} t_{k,s} \theta^{\beta-k} [\sin(\theta-\mu)]^s \left\{ [\sin(\theta-\mu)]^{k-2s} M_0 + [\sin(\mu)]^{k-2s} M_1 \right\},$$

where $M_0 = \mathbb{I}(|\sin(\theta-\mu)| \geq |\sin(\mu)|)$, $M_1 = \mathbb{I}(|\sin(\theta-\mu)| < |\sin(\mu)|)$, $\mathbb{I}(.)$ refers to the indicator function and $t_{k,s}$ is given by

$$t_{k,s}(\beta, \rho, \mu) = \binom{\beta}{k} \binom{k}{s} \left(\frac{1}{2\pi}\right)^{\beta-k} \left(\frac{\rho}{\pi}\right)^k (sen(\mu))^s.$$

Using integration by parts, it follows that

$$\mathbb{E}\{\cos[p(\Theta-\mu)]\} = \int_0^{2\pi} \cos[p(\theta-\mu)] dF(\theta) = \cos(p\mu) + \int_0^{2\pi} p\{[\sin[p(\theta-\mu)]\} F(\theta) d\theta$$

and

$$\mathbb{E}\{\text{sen}[p(\Theta-\mu)]\} = \int_0^{2\pi} \text{sen}[p(\theta-\mu)] dF(\theta) = -\text{sen}(p\mu) - \int_0^{2\pi} p\{[\cos[p(\theta-\mu)]\} F(\theta) d\theta$$

It is known the nth central trigonometric moment of the EC is given by

$$\mu_p = \mathbb{E}\{\cos[p(\Theta-\mu)]\} + i\mathbb{E}\{\text{sen}[p(\Theta-\mu)]\}.$$

When $p = 1$, applying the Theorem 2.3.1, the EC first moment is given by

$$\mu_1 = \mathbb{E}\{\cos[(\Theta-\mu)]\} + i\mathbb{E}\{\text{sen}[(\Theta-\mu)]\} = \alpha_1 + i\beta_1.$$

The terms α_1 and β_1 are determined at the following corollary.

Corollary 2.3.2. *Let $\Theta \sim EC(\beta, \rho, \mu)$. The components of the first central trigonometric moment are given by*

$$\alpha_1 = \cos(\mu) + \sum_{k=0}^{\infty}\sum_{s=0}^{k} t_{k,s}\left\{A(\beta-k,0,k-s+1)M_0 + [\sin(\mu)]^{k-2s}A(\beta-k,0,s+1)M_1\right\}$$

and

$$\beta_1 = -\sin(\mu) - \sum_{k=0}^{\infty}\sum_{s=0}^{k} t_{k,s}\left\{A(\beta-k,1,k-s)M_0 + [\sin(\mu)]^{k-2s}A(\beta-k,1,s)M_1\right\},$$

where

$$A(a,b,c) = \int_0^{2\pi} \theta^a[\cos(\theta-\mu)]^b[\sin(\theta-\mu)]^c d\theta.$$

The details for derivation of the above expressions are presented in Appendix B. To illustrate the use of the Corollary 2.3.2, for the Cardioid distribution ($\beta = 1$, $A(0,0,1) = A(0,1,1) = A(0,1,0) = 0$, $M_0 = 0$ and $M_1 = 1$ or $M_0 = 0$ and $M_1 = 1$), it follows that

$$\begin{aligned}
\alpha_1 =& \cos(\mu) + T_{0,0}\{A(1,0,1)M_0 + A(1,0,1)M_1\} + T_{1,0}\{A(0,0,2)M_0 \\
&+ \sin(\mu)^{-1}A(0,0,1)M_1\} + T_{1,1}\{A(0,0,1)M_0 + \sin(\mu)^{-1}A(0,0,2)M_1\} \\
=& \cos(\mu) + (2\pi)^{-1}\{-2\pi\cos(\mu)(M_0+M_1)\} + \frac{\rho}{\pi}\pi M_0 + \frac{\rho\sin(\mu)}{\pi}[\pi\sin(\mu)^{-1}]M_1 \\
=& \rho
\end{aligned}$$

and

$$\begin{aligned}
\beta_1 =& -\sin(\mu) - T_{0,0}\{A(1,1,0)M_0 + A(1,1,0)M_1\} - T_{1,0}\{A(0,1,1)M_0 \\
&+ \sin(\mu)A(0,1,0)M_1\} - T_{1,1}\{A(0,1,0)M_0 + \sin(\mu)^{-1}A(0,1,1)M_1\} \\
=& -\sin(\mu) + (2\pi)^{-1}\{2\pi\sin(\mu)(M_0+M_1)\} \\
=& 0,
\end{aligned}$$

which corresponds to the components of the first central trigonometric moment of the Cardioid distribution (Fisher, 1995). In a similar manner, the second moment is

$$\mu_2 = \mathbb{E}\{\cos[2(\Theta - \mu)]\} + i\mathbb{E}\{\sin[2(\Theta - \mu)]\} = \alpha_2 + i\beta_2.$$

The terms α_2 and β_2 are determined as follows.

Corollary 2.3.3. *Let $\Theta \sim EC(\beta, \rho, \mu)$. The components of the second central trigonometric moment are given by*

$$\begin{aligned}\alpha_2 = &\cos(2\mu) + 4\sum_{k=0}^{\infty}\sum_{s=0}^{k} t_{k,s}\{A(\beta - k, 1, k - s + 1)M_0 \\ &+ [\sin(\mu)]^{k-2s} A(\beta - k, 1, s + 1)M_1\}\end{aligned}$$

and

$$\begin{aligned}\beta_2 = &-\sin(2\mu) - 2\sum_{k=0}^{\infty}\sum_{s=0}^{k} t_{k,s}\{[2A(\beta - k, 2, k - s) - A(\beta - k, 0, k - s)]M_0 \\ &+ [\sin(\mu)]^{k-2s}[2A(\beta - k, 2, s) - A(\beta - k, 0, s)]M_1\}.\end{aligned}$$

Some standard circular measures are functions of the first and second trigonometric moments. The second column of Table 2.2 presents expressions (in terms of ρ_1, α_2 and β_2) for mean resultant length, circular variance, standard deviation, dispersion, skewness and kurtosis of any circular model. Using results of Corollaries 5.3.2 and 5.3.4, these quantities can be obtained to the EC model. The ranges to each resulting EC quantities are given in the third column in Table 2.2. The used notation is the same as in Fisher (1995), where $\rho_i = \sqrt{\alpha_i^2 + \beta_i^2}$ for $i = 1, 2$.

In order to illustrate the presented measures, Figure 2.2 displays the plots of the skewness and kurtosis of Cardioid, EC and vM distributions, which characterize the distribution shape. The special case of the Cardioid ($\beta = 1$) is highlighted. It may be observed the Cardioid (skewness, kurtosis) pair is overlapped to that of the vM law and the EC pair region covers the two first. From perspective of this diagram, our model seems to extend the former models. Additionally, Cardioid and vM skewnesses assume null values, as expected.

Table 2.2: Ranges of some standard circular measures of the EC distribution.

Measure	Expression	Range
Mean Resultant Length	ρ_1	$[0, 1]$
Circular Variance	$1 - \rho_1$	$[0, 1]$
Circular Standard Deviation	$\sqrt{-2 \log \rho_1}$	$[0, \infty)$
Circular Dispersion	$(1 - \alpha_2)/(2{\rho_1}^2)$	$[0, \infty)$
Circular Skewness	$\beta_2/(1 - \rho_1)^{\frac{3}{2}}$	$(-\infty, \infty)$
Circular Kurtosis	$(\alpha_2 - {\rho_1}^4)/(1 - \rho_1)^2$	$(-\infty, \infty)$

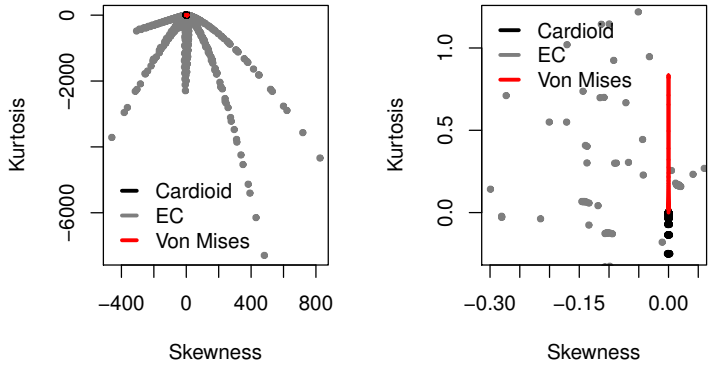

Figure 2.2: Skewness and kurtosis maps for EC, Cardioid and von Mises distributions.

2.4 Estimation Procedures

2.4.1 *Maximum Likelihood Estimation*

Let $\theta_1, \theta_2, \ldots, \theta_n$ be observed sample n-points from $\Theta \sim \mathrm{EC}(\beta, \rho, \mu)$. Then the log-likelihood function at $\boldsymbol{\delta} = (\beta, \rho, \mu)^\top$ is given by

$$\begin{aligned} l(\boldsymbol{\delta}) =& n \log \beta + (\beta - 1) \sum_{i=1}^{n} \log \left\{ \frac{\theta_i}{2\pi} + \frac{\rho}{\pi} [\sin(\theta_i - \mu) + \sin \mu] \right\} \\ & - n \log(2\pi) + \sum_{i=1}^{n} \log\{1 + 2\rho \cos(\theta_i - \mu)\}. \end{aligned}$$

Therefore, the ML estimates for β, ρ and μ, say $\hat{\beta}$, $\hat{\rho}$ and $\hat{\mu}$, can be defined as solutions of the following non-linear system (see Nocedal and Wright (2006)). Let

$$\left. \frac{\partial \ell(\boldsymbol{\delta})}{\partial \beta} \right|_{\boldsymbol{\delta} = \hat{\boldsymbol{\delta}}} = \frac{n}{\beta} + \sum_{i=1}^{n} \log \left\{ \frac{\theta_i}{2\pi} + \frac{\rho}{\pi} [\sin(\theta_i - \mu) + \sin \mu] \right\} = 0, \tag{2.3}$$

$$\left.\frac{\partial \ell(\boldsymbol{\delta})}{\partial \rho}\right|_{\boldsymbol{\delta}=\hat{\boldsymbol{\delta}}} = \sum_{i=1}^{n}\left\{(\beta-1)\frac{\sin(\theta_i-\mu)+\sin\mu}{\theta_i+2\rho[\sin(\theta_i-\mu)+\sin\mu]}+\frac{\cos(\theta_i-\mu)}{1+2\rho\cos(\theta_i-\mu)}\right\}=0 \tag{2.4}$$

and

$$\left.\frac{\partial \ell(\boldsymbol{\delta})}{\partial \mu}\right|_{\boldsymbol{\delta}=\hat{\boldsymbol{\delta}}} = \sum_{i=1}^{n}\left\{(\beta-1)\frac{-\cos(\theta_i-\mu)+\cos\mu}{\theta_i+2\rho[\sin(\theta_i-\mu)+\sin\mu]}+\frac{\sin(\theta_i-\mu)}{1+2\rho\cos(\theta_i-\mu)}\right\}=0. \tag{2.5}$$

This system can be reduced to others under equations 2.4 and 2.5, replacing the ML estimate $\hat{\beta}$, which is obtained from (2.3) by

$$\hat{\beta}(\rho,\mu) = -\frac{n}{\sum_{i=1}^{n}\log\left\{\frac{\theta_i}{2\pi}+\frac{\rho}{\pi}[\sin(\theta_i-\mu)+\sin\mu]\right\}}. \tag{2.6}$$

Thus, the ML estimates for ρ and μ are obtained numerically from

$$\left.\frac{\partial \ell(\boldsymbol{\delta})}{\partial \rho}\right|_{\boldsymbol{\delta}=\hat{\boldsymbol{\delta}}} = 0 \quad \text{and} \quad \left.\frac{\partial \ell(\boldsymbol{\delta})}{\partial \mu}\right|_{\boldsymbol{\delta}=\hat{\boldsymbol{\delta}}} = 0.$$

2.4.2 *Quantile least squares method*

The QLSE for $\boldsymbol{\delta}$ can be defined as solutions from minimization of the sum of squares of the differences between theoretical and empirical quantiles. Consider $\theta_{1:n},\cdots,\theta_{n:n}$ as observed order statistics drawn from $n-$points random sample of $\Theta \sim EC(\beta,\rho,\mu)$, where $\theta_{k:n}$ is the kth order statistics. Thus, the QLS estimates for EC parameters consist in argument that minimizes the following goal function:

$$q(\boldsymbol{\delta}) = \sum_{i=1}^{n}\left[\frac{i}{n}-\left\{\frac{\theta_{i:n}}{2\pi}+\frac{\rho}{\pi}[\sin(\theta_{i:n}-\mu)+\sin(\mu)]\right\}^{\beta}\right]^2. \tag{2.7}$$

Equivalently to discussed in previous section, the QLS estimates for β, ρ and μ can be defined as solutions of the following non-linear equations system:

$$\frac{\partial q(\boldsymbol{\delta})}{\partial \beta} = \sum_{i=1}^{n}\left[\frac{i}{n}-F(\theta_{1:n})\right]F_C(\theta_{1:n})^{2\beta-1}\log[F_C(\theta_{1:n})]=0, \tag{2.8}$$

$$\frac{\partial q(\boldsymbol{\delta})}{\partial \rho} = \sum_{i=1}^{n}\left[\frac{i}{n}-F(\theta_{1:n})\right]F_C(\theta_{1:n})^{\beta-1}\frac{1}{\pi}[\sin(\theta_{1:n}-\mu)+\sin\mu]=0 \tag{2.9}$$

and

$$\frac{\partial q(\boldsymbol{\delta})}{\partial \mu} = \sum_{i=1}^{n} \left[\frac{i}{n} - F(\theta_{1:n}) \right] F_C(\theta_{1:n})^{\beta-1} \frac{\rho}{\pi} [\cos(\theta_{1:n} - \mu) - \cos \mu] = 0, \tag{2.10}$$

where F_C represents the Cardioid cdf and F is given in (2.1).

2.5 Numerical results

2.5.1 *Simulation Study*

In this subsection, a Monte Carlo simulation study is performed to assess and compare the two proposed estimators. To that end, five thousand replications are considered and, on each one of them, average bias and square error for both procedures were quantified, as comparison criteria.

Initially, a discussion about the effect of the use of (2.6) is presented in estimation process by maximum likelihood. That is, the impact of the reduction of the non-linear system from three to two equations in the ML estimation was quantified through the mean square error (MSE) of the estimates obtained by considering both forms of obtaining. Here, a sample size $n = 100$ and four parametric points were considered. Results are displayed in Table 2.3 and indicate that the use of (2.6) may imply in more accurate estimates. The most pronounced improvement can be observed to estimate ρ. Moreover, the estimation considering (2.6) had the mean execution of 83 seconds, while the other was in mean higher, making in 116 seconds. From now on, the best ML estimates for β, ρ and μ are used.

Now, the two methods of the previous sections are compared. Results are presented in Tables 2.4 and 2.5. They are indexed in terms of mean direction and resultant lenght in ascending order for the sample sizes $n = 30$, 50 and 100.

Regard to choose parametric scenarios, vectors (β, ρ, μ) are selected such that they have different mean directions and resultant lengths. For this, the 180 parametric vectors of Table 2.1 were ordered according to their directional average. Subsequently, seven of these 180 vectors were chosen so that the first and last have the lowest and highest directional mean and the other five are equally spaced according to their directional mean. The same process was performed according to

Table 2.3: MSEs for the ML estimates obtained by the equations 2.3, 2.4 and 2.5 (MSE) and ML estimates obtained by the equations 2.4 and 2.5 after β (2.6) substitution (MSE'), by the Monte Carlo method, over 5.000 replications. The size of the sample was set to 100.

(β, ρ, μ)	MSE	MSE'
$\left(1, \frac{1}{2}, 2\pi\right)$	$(0.0071, 0.2991, 0.0000)$	$(0.0000, 0.0000, 0.0000)$
$\left(4, \frac{3}{10}, \frac{2\pi}{3}\right)$	$(0.6449, 13.7865, 0.0764)$	$(0.5101, 0.0030, 0.0516)$
$\left(1, \frac{3}{10}, \frac{4\pi}{3}\right)$	$(0.0658, 0.5818, 0.1883)$	$(0.0293, 0.0073, 0.0936)$
$\left(4, \frac{1}{2}, \frac{\pi}{3}\right)$	$(0.2384, 11.4078, 0.0119)$	$(0.1761, 0.0001, 0.0056)$

the mean result length from the vectors. The idea of this procedure was to verify if the variation of the mean direction or resultant length influenced the estimation of the parameters, using the average bias and MSE as evaluation criterion besides comparing the ML and QLS estimates.

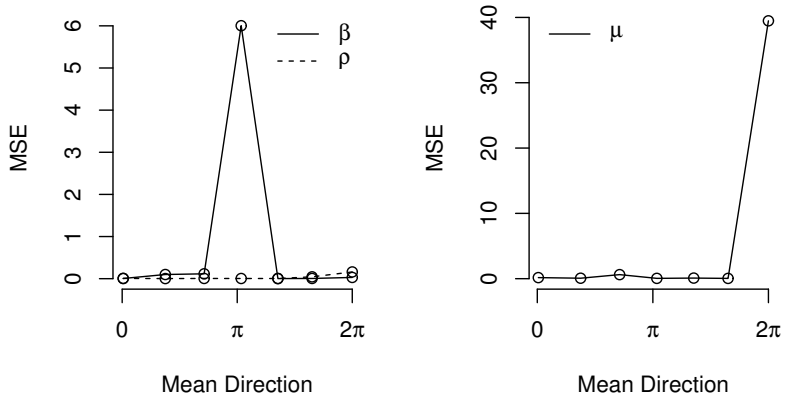

Figure 2.3: MSE for the ML estimates of the seven parametric vectors chosen according to the mean direction.

The obtained results for three of the considered seven parametric vectors are shown in the Table 2.4. The vectors of the first column are sorted by mean direction. It can be seen that the MSE decreases with increasing sample size, as expected. For the majority of cases, MLE performs better than QLSE, presenting estimates with lower MSE. Similar results are shown in

Table 2.4: Average bias and MSE for the ML and QLS estimates for different parametric vectors, by the Monte Carlo method, over 5.000 replications. Sample sizes of 30, 50 and 100 were considered.

(β, ρ, μ)	Method	n	Bias	MSE
$\left(1, \frac{1}{2}, 2\pi\right)$	MLE	30	$(0.0315, 0.0000, 0.0000)$	$(0.0272, 0.3683, 0.0000)$
		50	$(0.0170, 0.0000, 0.0000)$	$(0.0000, 0.0000, 0.0000)$
		100	$(0.0094, 0.0000, 0.0000)$	$(0.0000, 0.0000, 0.0000)$
	QLSE	30	$(0.0685, 0.0000, 0.0000)$	$(0.0213, 0.3398, 0.0000)$
		50	$(0.0546, 0.0000, 0.0000)$	$(0.0129, 0.3176, 0.0000)$
		100	$(0.0421, 0.0000, 0.0000)$	$(0.0071, 0.2991, 0.0000)$
$\left(1, \frac{3}{10}, \frac{4\pi}{3}\right)$	MLE	30	$(0.1343, 0.0128, -0.1473)$	$(0.2093, 0.0173, 0.5766)$
		50	$(0.0703, 0.0011, -0.0873)$	$(0.0842, 0.0126, 0.2838)$
		100	$(0.0330, -0.0030, -0.0361)$	$(0.0293, 0.0073, 0.0936)$
	QLSE	30	$(0.0823, 0.0419, -0.1351)$	$(0.3230, 0.9282, 0.5750)$
		50	$(0.0337, 0.0254, -0.1035)$	$(0.1420, 0.6792, 0.3726)$
		100	$(0.0185, 0.0104, -0.0679)$	$(0.0658, 0.5818, 0.1883)$
$\left(4, \frac{1}{2}, \frac{\pi}{3}\right)$	MLE	30	$(0.0683, -0.0089, -0.0067)$	$(0.6570, 0.0006, 0.0215)$
		50	$(0.0249, -0.0068, -0.0045)$	$(0.3651, 0.0003, 0.0123)$
		100	$(0.0112, -0.0041, -0.0025)$	$(0.1761, 0.0001, 0.0056)$
	QLSE	30	$(-0.3654, -0.0311, -0.0570)$	$(1.0033, 10.6952, 0.0581)$
		50	$(-0.2616, -0.0236, -0.0362)$	$(0.4815, 10.9000, 0.0293)$
		100	$(-0.1544, -0.0165, -0.0191)$	$(0.2384, 11.4078, 0.0119)$

the Table 2.5, where the parametric vectors of the first column are sorted by mean resultant length.

Figures 2.3 and 2.5 show the MSEs for the three parameter vectors considered in Table 2.4 and others four for the ML and QLS estimates, respectively. Figures 2.4 and 2.6 show the MSEs for the ML and QLS estimates, respectively, on points in Table 2.5 and others. In Figure 2.3, the first point is the vector $\left(0.6, 0.2, \frac{\pi}{6}\right)$ whose mean direction is 0.0279, while $(2, 0.3, \frac{2\pi}{3})$, with mean direction 1.1777, is the second point.

Regard to quantify the impact over varying of mean direction, fourth and seventh points impose difficulties to both methods for estimating β or ρ and μ, respectively. However, the impact over ML estimates are smaller than on the QLS estimates. For varying of mean resultant length, the hardest scenario is the sixth point and the same conclusion can be obtained. In particular, poor QLS estimates for ρ at third, sixth and seventh points are found, according to the Figure 2.6, in contrast with respective ML estimates. Additionally, such points refer to $\beta = 4$,

Table 2.5: Average bias e MSE for the MLE and QLSE for different values of β, ρ and μ, by the Monte Carlo method, over 5.000 replications. Sample sizes of 30, 50 and 100 were considered.

(β, ρ, μ)	Method	n	Bias	MSE
$\left(0.3, \frac{1}{2}, \frac{4\pi}{3}\right)$	MLE	30	$(0.0131, -0.0076, 0.0135)$	$(0.0041, 0.0007, 0.0242)$
		50	$(0.0069, -0.0049, 0.0017)$	$(0.0021, 0.0002, 0.0113)$
		100	$(0.0036, -0.0029, -0.0035)$	$(0.0010, 0.0001, 0.0048)$
	QLSE	30	$(0.0064, -0.0219, -0.0045)$	$(0.0098, 0.0185, 0.0739)$
		50	$(0.0038, -0.0156, 0.0017)$	$(0.0035, 0.0128, 0.0378)$
		100	$(0.0036, -0.0111, 0.0043)$	$(0.0012, 0.0105, 0.0191)$
$\left(4, \frac{3}{10}, \frac{\pi}{3}\right)$	MLE	30	$(0.3223, 0.0178, 0.0031)$	$(1.5698, 0.0096, 0.1673)$
		50	$(0.1696, 0.0106, -0.0062)$	$(0.7629, 0.0060, 0.0969)$
		100	$(0.0852, 0.0050, -0.0052)$	$(0.3411, 0.0032, 0.0440)$
	QLSE	30	$(-0.0977, 0.0034, -0.1103)$	$(3.2670, 15.5235, 0.3313)$
		50	$(-0.1147, 0.0027, -0.1092)$	$(1.1496, 13.9908, 0.1954)$
		100	$(-0.0603, 0.0006, -0.0639)$	$(0.5405, 13.7842, 0.0832)$
$\left(10, \frac{1}{2}, 2\pi\right)$	MLE	30	$(0.3154, 0.0000, 0.0000)$	$(3.9682, 0.0000, 0.0000)$
		50	$(0.1698, 0.0000, 0.0000)$	$(2.1771, 0.0000, 0.0000)$
		100	$(0.0935, 0.0000, 0.0000)$	$(1.0645, 0.0000, 0.0000)$
	QLSE	30	$(0.3048, 0.0000, 0.0000)$	$(0.2787, 96.3191, 0.0000)$
		50	$(0.3012, 0.0000, 0.0000)$	$(0.2685, 96.2410, 0.0000)$
		100	$(0.2861, 0.0000, 0.0000)$	$(0.2405, 95.9267, 0.0000)$

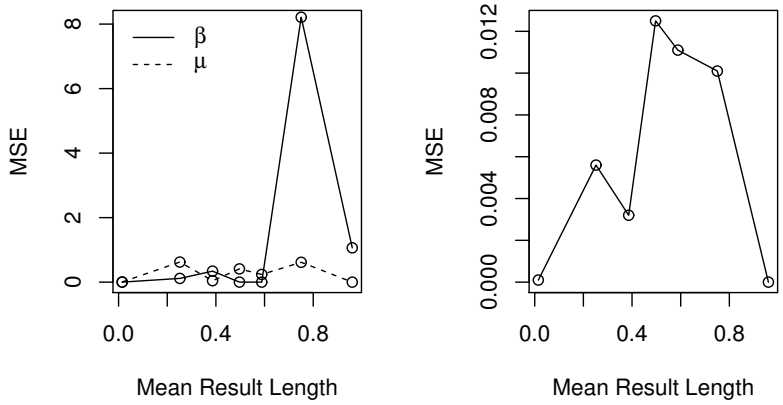

Figure 2.4: MSE for the ML estimates of the seven parametric vectors chosen according to the mean resultant length.

$\beta = 4$ and $\beta = 10$, respectively, which indicates that high values to β difficult the estimation of ρ.

Other interesting evidence can be found in the Figure 2.6, where the behavior of the MSEs

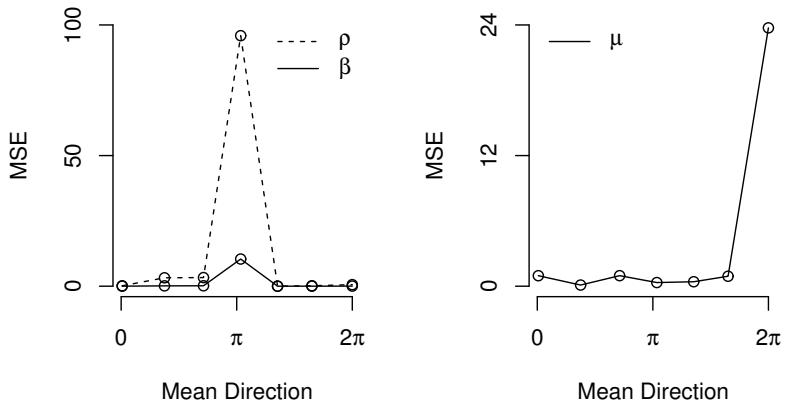

Figure 2.5: MSE for the QLS estimates of the seven parametric vectors chosen according to the mean direction.

for the estimates of ρ is approximately monotone.

In general, the MLE is better than the QLSE in most considered cases, comparing the MSEs of the estimates. The QLSE is better in the estimation of large β ($\beta = 10$) and small ρ ($\rho = \frac{1}{5}$), as can be seen in the Table 2.6.

Table 2.6: MSE for the ML and QLS estimates for different values of β, ρ and μ, by the Monte Carlo method, over 5.000 replications and sample size $n = 100$.

(β, ρ, μ)	ML	QLS
$\left(0.3, \frac{1}{5}, \frac{2\pi}{3}\right)$	$(0.0014, 0.0125, 0.4106)$	$(0.0019, 0.0104, 0.4729)$
$\left(0.3, \frac{1}{5}, \frac{\pi}{6}\right)$	$(0.0011, 0.0111, 0.2384)$	$(0.0013, 0.0106, 0.3574)$
$\left(10, \frac{1}{2}, 2\pi\right)$	$(1.0645, 0.0000, 0.0000)$	$(0.2405, 95.9267, 0.0000)$

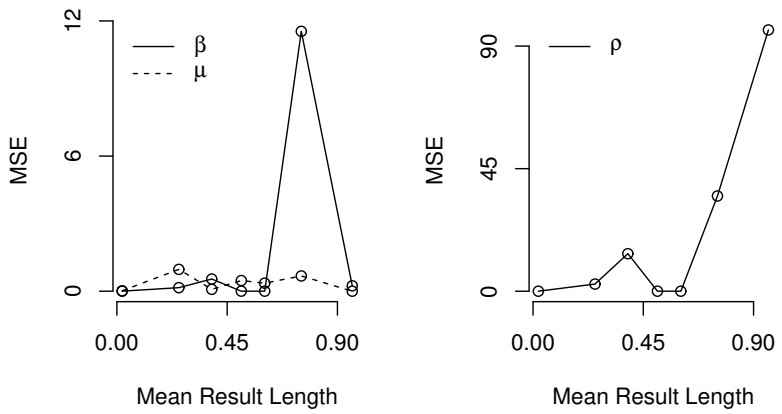

Figure 2.6: MSE for the QLS estimates of the seven parametric vectors chosen according to the mean resultant length.

2.5.2 *Application*

In order to illustrate the potentiality of the EC distribution, an application to real data was provided. Further, its performance is compared with other due to the Cardioid and vM models. ML estimates are used to fit considered models to data. All the computations are done using function `maxLik` at the R statistical software (R Core Team, 2017).

The dataset consists of 21 wind directions, at a weather station in Milwaukee, at 6.00 am, on consecutive days (Johnson and Wehrly, 1977). The independence of the data was verified by the Box-Pierce (Ljung-Box) test (Box and Pierce, 1970), useful for examining the null hypothesis of independence in time series and results can be checked in Figure 2.7, under a nominal value of 0.05.

The Figure 2.8 shows a qualitative analysis of skewness and kurtosis of the data, represented by blue color. Sample skewness and kurtosis from under study dataset are 0.4313 and 0.2480, respectively. It noticeable that the EC model may provide better fit than those due to Cardioid and vM distributions. Likelihood ratio test was also applied to compare the Cardioid ($H_0 : \beta = 1$) and EC ($H_0 : \beta \neq 1$) distributions. The p-value obtained was 0.0027, indicating the EC model as the best descriptor for these wind directions.

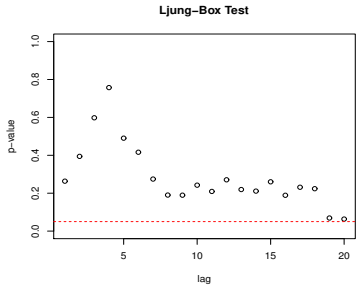

Figure 2.7: Ljung-Box test statistic.

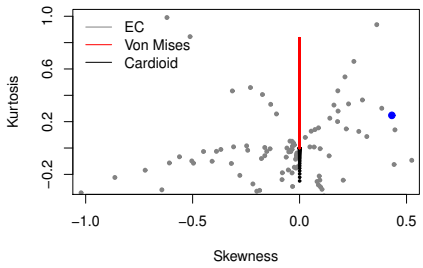

Figure 2.8: Data skewness and kurtosis.

Table 2.7: ML estimates of the model parameters for the data, the corresponding standard errors (given in parentheses) and the Kuiper and Watson statistics.

Model	β	ρ	μ	Kuiper	Watson
Cardioid	–	0.2436	4.6708	1.0388	0.0592
	–	(0.1463)	(0.6835)		
EC	2.8757	0.2164	1.1782	0.7369	0.0257
	–	(0.1465)	(0.6168)		
vM	–	0.5322	5.0092	1.1590	0.0711
	–	(0.3250)	(0.5899)		

First, the ML estimates and their SEs (given in parentheses) were evaluated and, subsequently, the values of the Kuiper (K) and Watson (W) statistics are obtained. These aderence measures may be found in Jammalamadaka and Sengupta (2001) and they are given by

$$K = \sqrt{n}\left\{\max_{1\leq i\leq n}\left(U_{(i)} - \frac{i-1}{n}\right) + \max_{1\leq i\leq n}\left(\frac{i}{n} - U_{(i)}\right)\right\}$$

and

$$W = \sum_{i=1}^{n} \left[\left(U_{(i)} - \frac{i - 0.5}{n} \right) - \left(\overline{U} - 0.5 \right) \right]^2 + \frac{1}{12n},$$

where $U_{(i)} = F(\alpha_{(i)})$ in terms of the order statistics $\alpha_{(1)} \leq \alpha_{(2)} \leq \cdots \leq \alpha_{(n)}$. In general, smaller values of them are associated to better fits. Table 2.7 displays results.

In order to do a qualitative comparison, Figure 2.9 presents empirical and fitted densities. Results confirm what is concluded from Table 2.7.

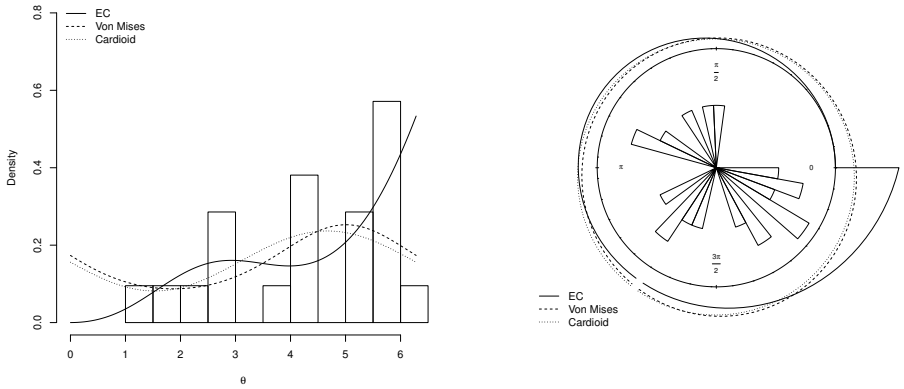

Figure 2.9: Fitted densities of the EC, Cardioid and von Mises models for the data.

2.6 Concluding remarks

An extended Cardioid model was proposed, called the *Exponentiated Cardioid* distribution. Our proposal has shown to be able to describe circular asymmetric data, as well as amodality, unimodality and bimodality scenarios. Expressions for the EC trigonometric moments by means of expansions were derived and a discussion about its mode was presented. Two estimation procedures for the EC parameters were proposed regard to maximum likelihood and quantile least square frameworks. The performance of these estimates was evaluated from a Monte Carlo simulation study. Finally, an application to real wind data was made and results have indicated that the EC model may outperform the classic Cardioid and vM distributions.

3 Inference and hypothesis tests for the exponentiated Cardioid distribution

Resumo

O modelo Cardioide exponencializado (EC), proposto no Capítulo 2, foi usado com sucesso para descrever fenômenos assimétricos e multimodais no círculo, superando algumas lacunas deixadas pelas distribuições clássicas uniforme e Cardioide (C). Este capítulo fornece e compara procedimentos de inferência baseados em hipóteses para os parâmetros da EC sob perspectivas asintótica e bootstrap. Nós consideramos os testes da razão de verossimilhança, Wald, escore e gradiente. Primeiro, nós derivamos uma expressão fechada para a matriz de informação de Fisher da EC. Usando tamanhos do teste e poderes empíricos como critério de comparação, quantificamos o desempenho dos testes propostos através de um estudo de Monte Carlo. Aplicações a dados reais ilustram o uso dos testes propostos para o modelo EC em contraste com as distribuições uniforme e C. Resultados sugerem que o teste gradiente supera o restante e substituindo a estrutura assintótica pelo bootstrap uma melhora significativa na tomada de decisão pode ser obtida.

Palavras-chave: Bootstrap vs. assintótico. Cardioide Exponencializada. Informação de Fisher. Testes de hipóteses.

Abstract

The exponentiated Cardioid (EC) model proposed in the Chapter 2 has been successfully used to describe asymmetry and multimodal phenomena in the circle, outperforming some gaps left by the uniform and Cardioid (C) classic distributions. This chapter provides and compares

hypothesis-based inference procedures for the EC parameters under both bootstrap and asymptotic perspectives. We consider likelihood ratio, Wald, score, and gradient tests. First we derive a closed-form expression for the EC Fisher information matrix. Using empirical test sizes and powers as comparison criteria, we quantify the performance of employed tests through a Monte Carlo study. Applications to real data illustrate the use of proposed tests for the EC model in contrast with the uniform and C distributions. Results advocate the gradient test outperforms the remainder and replacing the asymptotic framework by bootstrap can improve meaningfully the decision taking.

Keywords: Bootstrap vs. Asymptotic. Exponentiated Cardioid. Fisher information matrix. Hypothesis tests.

3.1 Introduction

In order to describe directional spectra of ocean waves, Jeffreys (1961) pioneered the Cardioid (C) distribution, which has cumulative distribution function (cdf) and probability density function (pdf) given by, respectively,

$$G(\theta) \,=\, \frac{\theta}{2\,\pi} \,+\, \frac{\rho}{\pi}\,[\,\sin(\theta-\mu) \,+\, \sin(\mu)\,] \tag{3.1}$$

and

$$g(\theta) \,=\, \frac{1}{2\pi}[\,1 \,+\, 2\,\rho\,\cos(\theta-\mu)\,]$$

where $\theta, \mu \in [0, 2\pi)$ and $|\rho| < 1/2$. Some works have addressed inference procedure (Rao *et al.*, 2011; Jones and Pewsey, 2005) and mathematical properties (Rao *et al.*, 2011; Wang and Shimizu, 2012) for this model. However, the C model is not able to describe non-symmetric behaviors. To outperform this gap, Wang and Shimizu (2012) have derived a new angular distribution from applying the Möbius transformation into the C model and Abe *et al.* (2009) studied the Papakonstantinou's family, which also extends (3.1). Despite excellent advances made in terms of mathematical properties, these extensions present hard analytic formulas for their densities. On

the other hand, the Chapter 2 have introduced a simple extension for the C distribution called exponentiated Cardioid (EC) distribution, which can describe asymmetric and some bimodal cases as well.

Given the flexibility of the EC distribution for circular phenomena, proposing hypothesis-based inference procedures to distinguish the former from C and uniform models is an important stage to be defined. Due to their well-known first order asymptotic properties, we work with the likelihood ratio (LR) (Neyman and Pearson, 1928), Wald (Wald, 1943), score (Rao, 1948), and gradient (Terrell, 2002) tests. It is known they are biased under small and moderate sample sizes; in particular, considerable distortions in their power functions are often found in practice. Thus, we aim to answer "what is the test which yields mildest distortions in terms of its asymptotic distribution?"

The bootstrap framework can be understood like a computationally intensive way to improve inference methods (estimators and hypothesis tests) before small and moderate size samples. The bootstrap method is based on resampling and allows to replicate interest measures without knowing their asymptotic or exact distributions (Cribari-Neto and Cordeiro, 1996). Parametric bootstrap refers to sampling from a parametric model with parameters estimated from data under study (Efron, 1979). With respect to applying bootstrap to hypothesis tests, the critical values of respective statistics are obtained from the empirical distributions of sample test statistics defined in all considered replications (Cribari-Neto and Queiroz, 2014). Using bootstrap often yields significance levels that differ from advertised level by $O(n^{-2})$ as compared to $O(n^{-1})$ for tests based on non-pivotal statistics (Fisher and Hall, 1990).

In the circular data context, a detailed discussion of bootstrap methods was given by Fisher (1995). Fisher and Hall (1992) have furnished other review about bootstrap methods for directional data. Referring to hypothesis tests equipped with a bootstrap framework, Fisher (1995) proposed some tests for mean direction. From our research on the existing literature, there are not works which have addressed performance studies (adopting test size and power as figures of merit) among asymptotic and bootstrap tests for circular data. In the context of models having support in the Euclidean space (particularly dispersion models), Lemonte and Ferrari (2012)

proposed a size and power study and used the von Mises distribution as illustration.

This chapter aims to propose and compare hypothesis-based inference procedures for the EC distribution. We look for contrasting the EC model versus the C and uniform distributions, assumptions used in practice with the circular data processing (Fernandez *et al.*, 1997; Tietjen, 1978). To that end, we propose a closed-form expression for the EC Fisher information matrix (FIM). Four pivotal statistics are considered on both asymptotic and bootstrap perspectives: LR, Wald, score, and gradient statistics. Through Monte Carlo experiments, the performance of the associated tests is quantified adopting estimated sizes and powers as comparison criteria. Tests are applied to real data as well. Results indicate the gradient test as the best tool among considered ones to discriminate models in the EC distribution and adding the bootstrap methodology may indeed improve the performance of tests.

The subsequent sections are organized as follows. Section 3.2 presents some likelihood-based inference tools for the EC model. The LR, Wald, score, and gradient tests for such model are described in Section 3.3. Section 3.4 tackles numerical results of this chapter. Finally, main conclusions are elected in Section 3.5.

3.2 Likelihood-based tools for the EC model

The Chapter 2 introduced a new three-parameter model having pdf given by: For $0 < \theta \leq 2\pi$,

$$f(\theta;\beta,\rho,\mu) = \frac{\beta}{2\pi}\left\{\frac{\theta}{2\pi} + \frac{\rho}{\pi}[\text{sen}(\theta-\mu)+\text{sen}(\mu)]\right\}^{\beta-1}[1+2\rho\cos(\theta-\mu)],$$

where $0 < \mu \leq 2\pi$, $|\rho| \leq 1/2$, and $\beta > 0$. This situation is denoted as $\Theta \sim EC(\beta,\rho,\mu)$. Some evidences were provided to confirm the EC model may assume asymmetric and bimodal behaviors. Taking (i) $\beta = 1$ and (ii) $\beta = 1$ and $\rho = 0$, the EC model collapses in the C and uniform laws, respectively. These two models have been widely applied in circular data Chu *et al.* (2015); Coles *et al.* (2004); Flohr *et al.* (2014); Solman and Kingstone (2014). In what follows, some likelihood-based tools which were not proposed in the Chapter 2 and are important to determine inferential procedures are derived.

Let $\Theta_1,\ldots,\Theta_n$ be a n-points *random sample* (independent and identically distributed) from

$\Theta \sim \text{EC}(\beta, \rho, \mu)$. Then the EC log-likelihood function, say ℓ, at $\boldsymbol{\delta} = (\beta, \rho, \mu)^\top$ can be expressed as

$$\begin{aligned}\ell(\boldsymbol{\delta}) =& n \log \beta + (\beta - 1) \sum_{i=1}^{n} \log \left\{ \frac{\Theta_i}{2\pi} + \frac{\rho}{\pi}[\sin(\Theta_i - \mu) + \sin(\mu)] \right\} - n \log(2\pi) \\ &+ \sum_{i=1}^{n} \log\{1 + 2\rho \cos(\Theta_i - \mu)\}. \end{aligned} \tag{3.2}$$

Thus, the maximum likelihood estimators (MLEs) for β, ρ, and μ can be defined as $\widehat{\boldsymbol{\delta}} = \arg\max_{\boldsymbol{\delta} \in \boldsymbol{\Delta}} \ell(\boldsymbol{\delta})$ for $\boldsymbol{\Delta}$ being the parametric space or, equivalently, as solutions of the following system of non-linear equations:

$$(U_\beta, U_\rho, U_\mu) \,:=\, \left(\frac{\partial \boldsymbol{\delta}}{\partial \beta}, \frac{\partial \boldsymbol{\delta}}{\partial \rho}, \frac{\partial \boldsymbol{\delta}}{\partial \mu} \right) \,=\, (0, 0, 0),$$

where

$$U_\beta = \frac{n}{\beta} + \sum_{i=1}^{n} \log \left\{ \frac{\Theta_i}{2\pi} + \frac{\rho}{\pi}[\sin(\Theta_i - \mu) + \sin(\mu)] \right\},$$

$$U_\rho = 2 \sum_{i=1}^{n} \left\{ (\beta - 1) \frac{\sin(\Theta_i - \mu) + \sin(\mu)}{\Theta_i + 2\rho[\sin(\Theta_i - \mu) + \sin(\mu)]} + \frac{\cos(\Theta_i - \mu)}{1 + 2\rho \cos(\Theta_i - \mu)} \right\}, \tag{3.3}$$

and

$$U_\mu = 2\rho \sum_{i=1}^{n} \left\{ (\beta - 1) \frac{-\cos(\Theta_i - \mu) + \cos(\mu)}{\Theta_i + 2\rho[\sin(\Theta_i - \mu) + \sin(\mu)]} + \frac{\sin(\Theta_i - \mu)}{1 + 2\rho \cos(\Theta_i - \mu)} \right\}. \tag{3.4}$$

This system can be reduced by applying the following expression of $\hat{\beta}$ in (3.3) and (3.4):

$$\hat{\beta} \,=\, \hat{\beta}(\rho, \mu) \,:=\, -\frac{n}{\sum_{i=1}^{n} \log \left\{ \frac{\Theta_i}{2\pi} + \frac{\rho}{\pi}[\sin(\Theta_i - \mu) + \sin(\mu)] \right\}}. \tag{3.5}$$

Finally, ML estimates for ρ and μ may also be obtained numerically from

$$U_\rho \Big|_{\beta = \hat{\beta}(\rho, \mu)} = 0 \quad \text{and} \quad U_\mu \Big|_{\beta = \hat{\beta}(\rho, \mu)} = 0.$$

In the remainder of this chapter, we refer to $[U_\beta, U_\rho, U_\mu]^\top$ as the score vector.

Other important quantity in statistical inference is the Fisher information matrix (FIM) defined by

$$\boldsymbol{K} \,=\, \boldsymbol{K}(\boldsymbol{\delta}) \,:=\, \mathbb{E}\left(\frac{\partial \ell}{\partial \boldsymbol{\delta}} \frac{\partial \ell}{\partial \boldsymbol{\delta}^\top} \right) \,=\, \mathbb{E}\left(-\frac{\partial^2 \ell}{\partial \boldsymbol{\delta} \partial \boldsymbol{\delta}^\top} \right),$$

where the last identity follows if satisfied conditions on Lehmann and Casella (2006). It is known that the ML estimate for $\boldsymbol{\delta}$, $\widehat{\boldsymbol{\delta}}$, holds the following asymptotic result: For $n \to \infty$,

$$\sqrt{n}\,(\,\hat{\boldsymbol{\delta}}\,-\,\boldsymbol{\delta}\,) \xrightarrow{\mathcal{D}} \mathbb{N}_3\left(\mathbf{0}, \boldsymbol{K}_1^{-1}(\boldsymbol{\delta})\right),$$

where $\boldsymbol{K}_1(\boldsymbol{\delta}) := \boldsymbol{K}(\boldsymbol{\delta})/n$ is the unit Fisher information and $\mathbb{N}_p$ represents the p-variate normal distribution. Deriving $\boldsymbol{K}$ is often a hard task for several distributions. When the FIM is analytically intractable, the observed information matrix, $\boldsymbol{J} := \left\{-\partial^2 \ell/\partial\boldsymbol{\delta}\partial\boldsymbol{\delta}^\top\right\}$, is used as an estimator for $\boldsymbol{K}$. In what follows, we present the elements of $\boldsymbol{J} = \{J_{ij}\}_{i,j=1,2,3}$ and $\boldsymbol{K} = \{K_{ij}\}_{i,j=1,2,3}$ for the EC model.

Differencing the score vector, the elements of $\boldsymbol{J}$ are given by:

$$J_{11} = \frac{n}{\beta^2}, \quad J_{12} = J_{21} = -2\sum_{i=1}^{n} \frac{\sin(\Theta_i - \mu) + \sin(\mu)}{\Theta_i + 2\rho[\sin(\Theta_i - \mu) + \sin(\mu)]},$$

$$J_{13} = J_{31} = 2\rho\sum_{i=1}^{n} \frac{\cos(\Theta_i - \mu) - \cos(\mu)}{\Theta_i + 2\rho[\sin(\Theta_i - \mu) + \sin(\mu)]},$$

$$J_{22} = 4\sum_{i=1}^{n}\left\{(\beta-1)\left\{\frac{\sin(\Theta_i - \mu) + \sin(\mu)}{\Theta_i + 2\rho[\sin(\Theta_i - \mu) + \sin(\mu)]}\right\}^2 + \left\{\frac{\cos(\Theta_i - \mu)}{1 + 2\rho\cos(\Theta_i - \mu)}\right\}^2\right\},$$

$$J_{23} = J_{32} = 2\sum_{i=1}^{n}\left\{(\beta-1)\Theta_i\frac{\cos(\Theta_i - \mu) - \cos(\mu)}{\{\Theta_i + 2\rho[\sin(\Theta_i - \mu) + \sin(\mu)]\}^2} - \frac{\sin(\Theta_i - \mu)}{\{1 + 2\rho\cos(\Theta_i - \mu)\}^2}\right\},$$

and

$$J_{33} = 2\rho\sum_{i=1}^{n}\left\{(\beta-1)\frac{\Theta_i[\sin(\Theta_i - \mu) + \sin(\mu)] + 4\rho[1 - \cos(\Theta_i)]}{\{\Theta_i + 2\rho[\sin(\Theta_i - \mu) + \sin(\mu)]\}^2} + \frac{2\rho + \cos(\Theta_i - \mu)}{\{1 + 2\rho\cos(\Theta_i - \mu)\}^2}\right\}.$$

Now, we are in position of discussing an expression for $\boldsymbol{K}$. First, we propose the following theorem.

Theorem 3.2.1. *Let $\Theta \sim EC(\beta, \rho, \mu)$. Thus,*

$$\mathbb{E}\left\{\, G^{-1}(\Theta)\,\right\} \,=\, \frac{\beta}{(\beta-1)} \quad \textit{for} \quad \beta > 1$$

and

$$\mathbb{E}\left\{ G^{-2}(\Theta) \right\} = \frac{\beta}{(\beta-2)} \quad \textit{for} \quad \beta > 2,$$

where $G(\cdot)$ is the C cdf.

Its proof is given in Appendix C. Theorem 3.2.1 expresses moment expressions for two transformations of the EC model. It will be used for deriving $\boldsymbol{K}$ of the EC distribution.

Now, consider the functions

$$I_{p,k,s,t}(\beta,\rho,\mu) = \int_0^{2\pi} \theta^p \left[\sin(\theta-\mu)\right]^k G(\theta)^{\beta-s}\, g(\theta)^t \,\mathrm{d}\theta$$

and

$$V_{p,k,s,t}(\beta,\rho,\mu) = \int_0^{2\pi} \theta^p \left[\cos(\theta-\mu)\right]^k G(\theta)^{\beta-s}\, g(\theta)^t \,\mathrm{d}\theta,$$

where $g(\cdot)$ is the C pdf. The functions $I_{j,k,s,t}$ and $V_{j,k,s,t}$ are well-defined for $p \in \mathbb{R}$, $k \geq 1$, $s \leq \beta + 3$, and $t \in \mathbb{R}$. Figure 3.2 displays curves of the special functions for some values, which are used into the FIM. It can be observed that both functions are well-defined for the derivation of $\mathbf{K}$. From Theorem 3.2.1, the elements of the FIM are given by the bellow theorem.

Theorem 3.2.2. *Let $\boldsymbol{\Theta} = (\Theta_1, \ldots, \Theta_n)^\top$ be a random sample from $\Theta \sim EC(\beta,\rho,\mu)$. Its FIM, $\boldsymbol{K} = \{K_{ij}\}_{i,j=1,2,3}$, is determined by:*

$$K_{11} = \frac{n}{\beta^2}, \qquad K_{12} = -\frac{n\beta}{\pi}\left[\frac{\sin(\mu)}{\beta-1} + I_{0,1,2,1}(\beta,\rho,\mu)\right],$$

$$K_{13} = \frac{n\beta\rho}{\pi}\left[\frac{\cos(\mu)}{1-\beta} + V_{0,1,2,1}(\beta,\rho,\mu)\right],$$

$$K_{22} = \frac{n\beta}{\pi^2}\left[\frac{(\beta-1)[\sin(\mu)]^2}{\beta-2} + (\beta-1)I_{0,2,3,1} + 2(\beta-1)\sin(\mu)I_{0,1,3,1} + V_{0,2,1,-1}\right],$$

$$K_{23} = \frac{n\beta}{2\pi^2}\left[(1-\beta)\cos(\mu)I_{1,0,3,1} - I_{0,1,1,-1} + (\beta-1)V_{1,1,3,1}\right],$$

and

$$K_{33} = \frac{n\beta\rho}{2\pi^2}\{(\beta-1)\{I_{1,1,3,1} + \sin(\mu)\{I_{1,0,3,1} + 4\rho I_{0,1,3,1}\} - 4\rho\cos(\mu)V_{0,1,3,1}\} + 2\rho V_{0,0,1,-1} + V_{0,1,1,-1}\} + \frac{2n\rho^2\beta(\beta-1)}{\pi^2(\beta-2)}.$$

An outline of the proof of this theorem is given in Appendix D.

3.3 Some hypothesis tests for the EC model

In this section, we present some hypothesis tests for the EC model. As discussed, this distribution has as particular cases the C ($\beta = 1$) and uniform ($\beta = 1$ and $\rho = 0$) laws and our exposition is focused on two situations:

- Situation a: $H_0 : \beta = 1$ vs. $H_1 : \beta \neq 1$;
- Situation b: $H_0 : \boldsymbol{\lambda} = \boldsymbol{\lambda}_0$ vs. $H_1 : \boldsymbol{\lambda} \neq \boldsymbol{\lambda_0}$, where $\boldsymbol{\lambda} = [\beta\ \rho]^\top$ and $\boldsymbol{\lambda}_0 = [1\ 0]^\top$.

To contrast the EC, C, and uniform models, we consider the four tests: LR (T_{1j}), Wald (T_{2j}), score (T_{3j}), and gradient (T_{4j}) for $j \in \{a, b\}$. Next, the notation T_{ij} indicates the ith (for $i = 1, 2, 3, 4$) test at the jth situation.

The work proposed by Abe *et al.* (2009) was the single study we found in the literature discussing hypothesis tests for the C or uniform distributions. Authors adopted the LR test to distinguish between the C model and one of its extensions proposed by Papakonstantinou. Although important properties have been derived for such extension, the analytic expression of its density is hard (dependent of the Bessel function of the first kind) comparatively to the EC model. In this chapter, we focus on hypothesis-based inference procedures for the EC model.

3.3.1 *The likelihood ratio test*

The LR statistic, T_{1a}, is defined in terms of the maximum restricted (under null hypothesis, H_0) and unrestricted (under alternative hypothesis, H_1) log-likelihoods given by $\widetilde{\ell} := \ell(1, \widetilde{\rho}, \widetilde{\mu}|\boldsymbol{\Theta})$ and $\widehat{\ell} := \ell(\widehat{\beta}, \widehat{\rho}, \widehat{\mu}|\boldsymbol{\Theta})$, respectively, where $\boldsymbol{\Theta} = (\Theta_1, \ldots, \Theta_n)^\top$ is a n-points random sample from

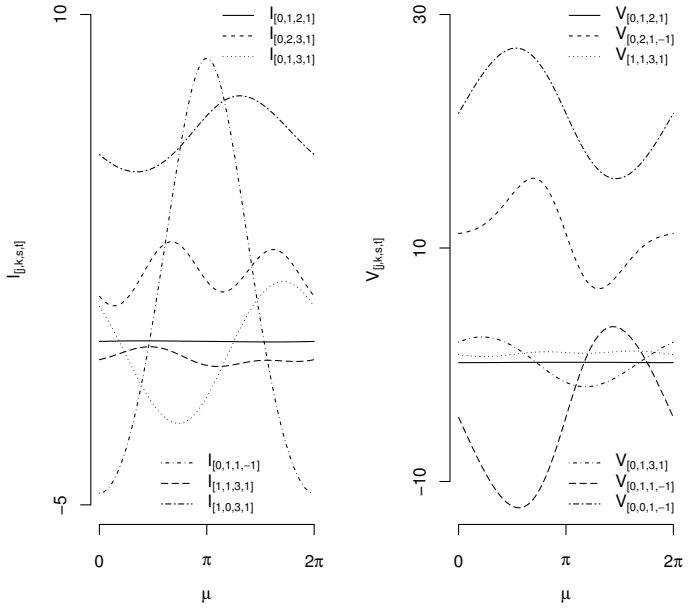

(a) Special functions for $\beta = 2$ and $\rho = 0.2$.

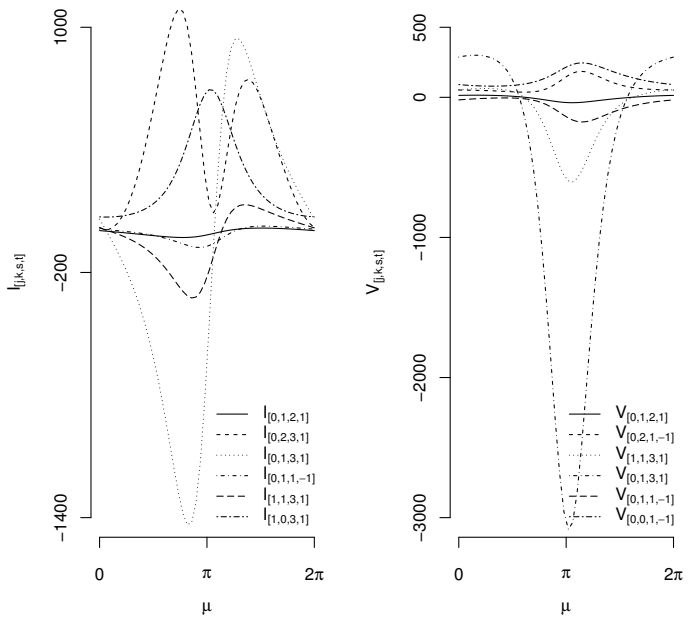

(b) Special functions for $\beta = 0.3$ and $\rho = 0.3$.

Figure 3.1: Illustration of the special functions.

$\Theta \sim \text{EC}(\beta, \rho, \mu)$, $\tilde{\cdot}$ denotes the restricted ML estimate and $\hat{\cdot}$ is its original version. Thus, setting $\tilde{\ell}_a$ as the maximized log-likelihood under H_0 at the situation a,

$$T_{1a} \,=\, 2\,(\hat{\ell} - \tilde{\ell}_a),$$

where

$$\tilde{\ell}_a \,=\, -n\,\log(2\pi) \,+\, \sum_{i=1}^{n} \log\{\,1 \,+\, 2\,\tilde{\rho}\,\cos(\Theta_i - \tilde{\mu})\,\}$$

and

$$\begin{aligned}\hat{\ell} \,=& n\,\log\hat{\beta} \,+\, (\hat{\beta}-1)\,\sum_{i=1}^{n}\log\left\{\frac{\Theta_i}{2\pi} \,+\, \frac{\hat{\rho}}{\pi}[\sin(\Theta_i - \hat{\mu}) + \sin(\hat{\mu})]\right\} \,-\, n\,\log(2\pi) \\ &+ \sum_{i=1}^{n}\log\{\,1 \,+\, 2\,\hat{\rho}\,\cos(\Theta_i - \hat{\mu})\,\}. \end{aligned} \tag{3.6}$$

For the situation b, it follows that

$$T_{1b} \,=\, 2\,(\hat{\ell} \,-\, \tilde{\ell}_b\,),$$

where the restricted log-likelihood ($\tilde{\ell}_b$) is a constant, $\tilde{\ell}_b \,=\, -n\log(2\pi)$.

3.3.2 *The Wald test*

The Wald test is based on ML estimates under H_1. As under the null hypothesis there is one restriction for the situation a, the Wald statistic is given by:

$$T_{2a} = (\hat{\beta}-1)^2\hat{I}_{11}^{-1} = n\left(\frac{\hat{\beta}-1}{\hat{\beta}}\right)^2.$$

where $\hat{\beta}$ is given in (3.5).

For the situation b, it holds that

$$T_{2b} = (\widehat{\boldsymbol{\lambda}} - \boldsymbol{\lambda}_0)^\top \widehat{\boldsymbol{I}}_\lambda^{-1}(\widehat{\boldsymbol{\lambda}} - \boldsymbol{\lambda}_0),$$

where $\hat{\boldsymbol{I}}_\lambda$ is the limit covariance matrix of the ML estimate for $\boldsymbol{\lambda}$, $\widehat{\boldsymbol{\lambda}} = [\hat{\beta}, \hat{\rho}]^\top$, evaluated under $\widehat{\boldsymbol{\delta}}$; that is, $\widehat{\boldsymbol{I}}_\lambda := \boldsymbol{I}_\lambda(\widehat{\boldsymbol{\delta}})$, where

$$\boldsymbol{I}_\lambda \,=\, \begin{bmatrix} I_{11} & I_{12} \\ I_{21} & I_{22} \end{bmatrix}.$$

3.3.3 *The score test*

The score statistic for the situation a is obtained by evaluating U_β and I_{11} at $\beta = 1$, $\tilde{\rho}$, and $\tilde{\mu}$. Thus,

$$T_{3a} \,=\, U_{\tilde{\beta}}^2\, \tilde{I}_{11} \,=\, \frac{1}{n}\left(n + \sum_{i=1}^{n} \log\left\{\frac{\Theta_i}{2\pi} + \frac{\tilde{\rho}}{\pi}\left[\sin(\Theta_i - \tilde{\mu}) + \sin(\tilde{\mu})\right]\right\}\right)^2.$$

For the situation b, this statistic is given by:

$$T_{3b} \,=\, \tilde{\boldsymbol{u}}_\lambda^\top\, \tilde{\boldsymbol{I}}_\lambda\, \tilde{\boldsymbol{u}}_\lambda,$$

where $\tilde{\boldsymbol{u}}_\lambda = [\tilde{U}_\beta\ \tilde{U}_\rho]^\top$ denotes the two first entries of the score vector evaluated at the restricted ML estimate for $\boldsymbol{\delta}$.

There is a limitation when calculating T_{3b} with respect to obtaining $\tilde{\mu}$, since $\tilde{\ell}_b$ is a constant function. In the numerical study of this chapter, $\tilde{\mu}$ is estimated from the C model, as a possible approximation. The same strategy is used for the calculation of T_{4b} as well.

3.3.4 *The gradient test*

The gradient statistic for the situation a is given by:

$$T_{4a} \,=\, U_{\tilde{\beta}}\,(\hat{\beta} - 1) \,=\, \left(n + \sum_{i=1}^{n} \log\left\{\frac{\Theta_i}{2\pi} + \frac{\tilde{\rho}}{\pi}\left[\sin(\Theta_i - \tilde{\mu}) + \sin(\tilde{\mu})\right]\right\}\right)\,(\hat{\beta} - 1).$$

For situation b,

$$T_{4b} = \tilde{\boldsymbol{u}}_\lambda^\top\,(\hat{\boldsymbol{\lambda}} - \boldsymbol{\lambda}_0) = (\hat{\beta} - 1)\,\left[n \,+\, \sum_{i=1}^{n} \log(\Theta_i) - n\log(2\pi)\right] \,+\, 2\,\hat{\rho}\,\sum_{i=1}^{n}\cos(\Theta_i - \tilde{\mu}).$$

Under the null hypothesis, the statistics T_{1a}, T_{2a}, T_{3a}, and T_{4a} follow χ_1^2, while the ones for situation b are asymptotically distributed as χ_2^2.

3.3.5 *Bootstrap tests*

Parametric bootstrap refers to sampling from a parametric model with parameters estimated from data under study (Efron, 1979). The bootstrap scheme we use in the synthetic study is described by the following steps (Cribari-Neto and Queiroz (2014); Davison and Hinkley (2003)):

1. Let $\boldsymbol{\theta} = (\theta_1, \ldots, \theta_n)^\top$ be a possible observation of a random sample from $\Theta \sim \text{EC}(\beta, \rho, \mu)$. Calculate the test statistic of interest, denoted by $T_{ij}(\boldsymbol{\theta}) := T_{ij}$ for $i = 1, 2, 3, 4$ and $j = a, b$.

2. Generate n-points bootstrap samples, say $\boldsymbol{\theta}_b^* = (\theta_1^*, \ldots, \theta_n^*)^\top$ for $b = 1, \ldots, B$, of the EC model estimated (under H_0) from the original sample, $\boldsymbol{\theta}$.

3. Estimate the model using $\boldsymbol{\theta}_b^*$ and compute the bootstrap bth statistic, say $T_{ij}(\boldsymbol{\theta}_b^*)$.

4. Repeat the steps (2) and (3) for a large number B of times.

5. Compute the p-value, p^*, as

$$p^* = \frac{\sum_{b=1}^{B} \mathbb{I}(\, T_{ij}\,(\boldsymbol{\theta}_b^*) > T_{ij}\,(\boldsymbol{\theta})\,)}{B}, \tag{3.7}$$

   where $\mathbb{I}(.)$ refers to the indicator function.

Finally, as decision rule, if $p^* < \alpha$ then reject H_0.

3.4 Numerical results

In this section, we carry out a synthetic study and an application involving two real data sets. We aim to compare the performance of the four hypothesis tests for the EC model discussed previously under asymptotic and bootstrap perspectives. The EC distribution has as particular cases the C ($\beta = 1$) and uniform ($\beta = 1$ and $\rho = 0$) laws and we consider the following hypotheses in our discussion:

- Situation a: $H_0 : \beta = 1$ vs. $H_1 : \beta \neq 1$;

- Situation b: $H_0 : \boldsymbol{\lambda} = \boldsymbol{\lambda}_0$ vs. $H_1 : \boldsymbol{\lambda} \neq \boldsymbol{\lambda}_0$.

To quantify the performance under moderate and small size ($n = 20, 50, 100, 150$) samples, we use 5.000 Monte Carlo and $B = 1.000$ bootstrap replications. To the end of study, rejection

rates of the null hypothesis subject to data come from H_0 (named as estimated test size) and H_1 (estimated test power) are computed. It is expected that empirical sizes are close to the nominal values (assumed as $\alpha = 1\%, 5\%, 10\%$) and, fixed $\alpha = 5\%$ for all hypothesis tests, estimated powers are as great as possible. Further, the variations $\mu = \pi/6$, $2\pi/3$, $4\pi/3$, $7\pi/4$ (points in each quadrant of the circle) and $\rho = 0.0$, 0.1, 0.2, 0.3, 0.4, 0.5 (from the state "uniformly distributed in the circle" to "highly concentrated") are adopted to quantify empirical sizes; while $\beta \in (0.1, 3.4)$ (from "amodal/unimodal pdfs" to "bimodal", see Chapter 2) is used to measure empirical powers.

3.4.1 *Performance for asymptotic distribution-based percentiles*

Situation a

Table 3.1 reports estimated sizes for $\rho = 0.3$, $\mu = 2\pi/3$ and $n = 20, 50, 100, 150$. In general, the null hypothesis rejection rates approach the adopted nominal levels as the sample size increases for all the tests. For small samples, all tests were liberal with emphasis on the Wald test; whereas the score and gradient tests presented the best performance in the majority of cases.

Table 3.1: Rejection rate (%) under the null hypothesis for the situation a, considering $\rho = 0.3$, $\mu = \frac{2\pi}{3}$, and different sample sizes.

	$\alpha = 10\%$				$\alpha = 5\%$				$\alpha = 1\%$			
n	T_{1a}	T_{2a}	T_{3a}	T_{4a}	T_{1a}	T_{2a}	T_{3a}	T_{4a}	T_{1a}	T_{2a}	T_{3a}	T_{4a}
20	12.68	16.76	13.20	10.58	6.48	12.92	7.60	5.24	1.16	10.06	2.76	1.24
50	12.30	12.28	11.50	11.66	6.80	7.76	6.04	6.20	1.32	3.96	1.26	1.04
100	10.68	10.26	10.32	10.62	5.44	5.08	5.04	5.38	1.20	1.36	1.14	1.08
150	9.84	9.86	10.04	9.68	5.18	4.78	5.02	5.12	0.88	0.86	0.96	0.98

Figure 3.2 shows the estimated power function of the four tests at $\alpha = 5\%$. From what is expected (since all test statistics follow the chi-square limit distribution), curves became similar as the sample size increases. For $n = 20$ and $\beta > 1$, the Wald test presented the smallest power function. The gradient test was the most powerful, followed by the LR and score tests for all considered sample sizes. On the other hand, for $0 < \beta < 0.39$, the score test was the most powerful, followed by the Wald, LR, and gradient tests. In the neighborhood of $\beta = 1$, this

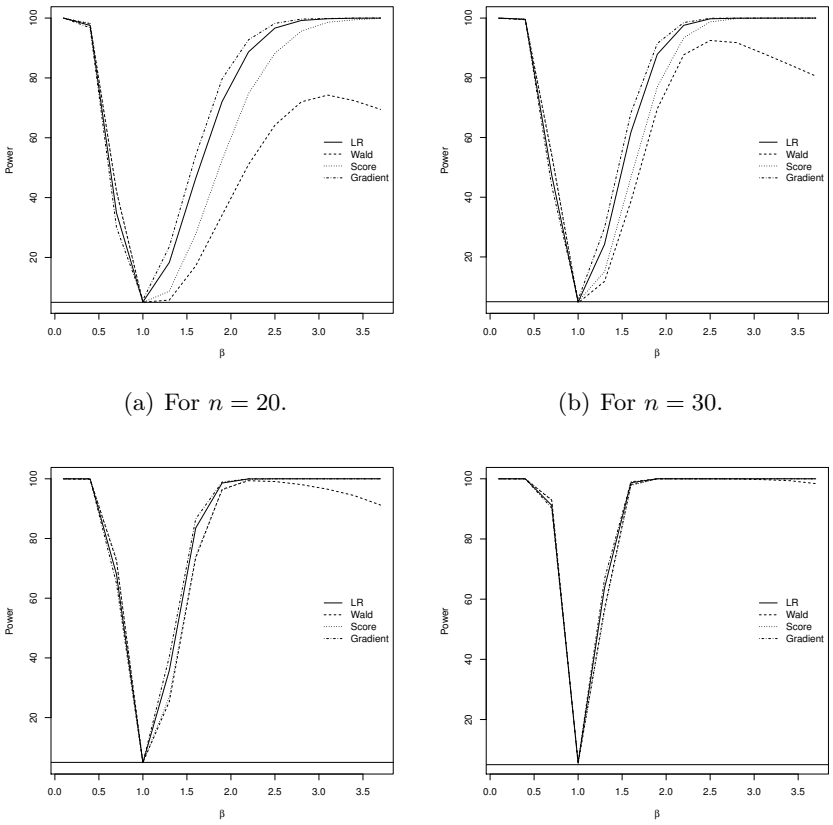

(a) For $n = 20$.

(b) For $n = 30$.

(c) For $n = 50$.

(d) For $n = 100$.

Figure 3.2: Estimated power curves on situation a for different sample sizes, considering $\alpha = 5\%$, $\rho = 0.3$, and $\mu = \frac{\pi}{6}$.

study suggests the gradient and score tests as the best options to discriminate the C and EC distributions. On the other hand, with respect to the power function, the score test is the most powerful for $\beta < 1$; while, for $\beta > 1$, the gradient test is the best.

Further, other scenarios were considered to quantify the test size for variation of μ and ρ at $n = 20$. Results are presented in Table 3.2. It was observed the Wald test is the most liberal when μ is in the $2st$ and $3st$ quadrants of the circle; while, for μ in the $1st$ and $4st$ quadrants, gradient and score tests are most liberal, respectively. With respect to most conservative tests, the Wald ($1st$ and $4st$) and score tests ($3st$) stand out, considering $\alpha = 10\%$. For the majority of cases, the empirical test size increases as the concentration parameter, ρ, increases.

Regarding the variation of μ, one noticed that all tests were more liberal when μ belongs to the $2st$ and $3st$ quadrants. For instance, assuming $\rho = 0.3$, $\alpha = 10\%$, and μ such as in Table 3.2, the LR test provided the estimated sizes 10.22%, 12.68%, 12.56%, and 9.80%. This seems indicating the more μ moves away from the origin of the circle, the type I error rate is higher.

Situation b

Here, the same scenarios of the situation a are used. However, with respect to the equivalent of Table 3.2, n is changed instead of ρ, which is equal to zero according to H_0. Results we provide are exhibited in Table 3.3. As expected, type I error rate for all the tests approach slowly of the adopted nominal levels when the sample size increases.

One observed that the score test is the most liberal for 10% and 5% significance levels, while the Wald test is most liberal for 1% level. We noted also that the Wald test is the most conservative for 10% and 5% significance levels and the LR test is less liberal for 1%. For the variation of the mean, it was noticed that all tests are more liberal when the EC average belongs to the $2st$ and $3st$ quadrants. As an example, for the $n = 50$ and $\alpha = 10\%$, the LR test presented type I error rate of 10.38%, 12.74%, 12.02% and 10.18%, respectively. The same was observed in the situation a.

Figure 3.3 shows the behavior of the power of the four tests at $\alpha = 5\%$. One noted the power

Table 3.2: Rejection rate (%) under the null hypothesis for the situation a, considering $n = 20$ and different values of (μ, ρ).

	$\mu = \frac{\pi}{6}$											
	$\alpha = 10\%$				$\alpha = 5\%$				$\alpha = 1\%$			
ρ	T_{1a}	T_{2a}	T_{3a}	T_{4a}	T_{1a}	T_{2a}	T_{3a}	T_{4a}	T_{1a}	T_{2a}	T_{3a}	T_{4a}
0.0	11.20	8.18	8.32	12.72	6.08	3.58	3.86	7.44	1.40	0.72	0.70	2.38
0.1	10.78	8.38	8.80	11.38	5.68	4.44	4.42	6.58	1.26	1.00	1.06	2.20
0.2	10.04	8.60	9.78	10.64	5.40	4.66	5.18	6.28	1.12	1.34	1.46	1.80
0.3	10.22	7.90	10.64	10.84	5.12	4.20	5.66	5.78	1.12	1.24	1.78	1.64
0.4	9.72	7.64	13.40	10.38	5.04	4.00	8.06	5.56	1.02	1.22	2.84	1.30
0.5	9.74	5.22	19.02	9.38	4.46	2.78	12.68	4.90	1.06	0.68	6.26	1.10
	$\mu = \frac{2\pi}{3}$											
	$\alpha = 10\%$				$\alpha = 5\%$				$\alpha = 1\%$			
ρ	T_{1a}	T_{2a}	T_{3a}	T_{4a}	T_{1a}	T_{2a}	T_{3a}	T_{4a}	T_{1a}	T_{2a}	T_{3a}	T_{4a}
0.0	13.74	11.92	10.88	12.76	7.66	7.14	5.60	7.12	2.10	3.52	1.64	2.40
0.1	11.96	13.78	10.64	11.14	6.30	9.50	6.10	5.58	1.40	5.68	1.98	1.50
0.2	12.40	15.76	11.14	10.50	5.98	11.62	6.34	4.96	1.34	7.92	2.18	1.36
0.3	12.68	16.76	13.20	10.58	6.48	12.92	7.60	5.24	1.16	10.06	2.76	1.24
0.4	11.34	14.50	13.96	9.40	6.00	11.94	9.00	4.78	1.06	9.92	3.42	1.04
0.5	7.60	6.50	15.66	7.64	3.74	4.76	10.32	3.68	0.68	3.68	4.62	0.58
	$\mu = \frac{4\pi}{3}$											
	$\alpha = 10\%$				$\alpha = 5\%$				$\alpha = 1\%$			
ρ	T_{1a}	T_{2a}	T_{3a}	T_{4a}	T_{1a}	T_{2a}	T_{3a}	T_{4a}	T_{1a}	T_{2a}	T_{3a}	T_{4a}
0.0	10.98	12.84	11.00	7.70	5.98	8.24	6.32	3.54	1.58	4.56	2.42	0.34
0.1	10.56	12.42	10.20	9.40	5.34	9.14	6.38	4.72	1.08	5.26	3.08	0.86
0.2	11.44	13.06	9.74	10.60	5.48	9.80	5.92	5.94	1.08	5.82	2.92	1.48
0.3	12.56	14.60	8.50	13.04	6.32	11.24	5.66	7.22	1.12	7.22	2.90	2.42
0.4	14.64	16.72	6.20	18.04	7.36	12.74	4.64	12.10	1.50	7.60	2.80	5.22
0.5	20.16	18.60	3.58	29.84	11.52	14.04	2.68	23.30	2.72	7.48	1.74	13.88
	$\mu = \frac{7\pi}{4}$											
	$\alpha = 10\%$				$\alpha = 5\%$				$\alpha = 1\%$			
ρ	T_{1a}	T_{2a}	T_{3a}	T_{4a}	T_{1a}	T_{2a}	T_{3a}	T_{4a}	T_{1a}	T_{2a}	T_{3a}	T_{4a}
0.0	7.24	10.10	8.06	6.86	3.34	6.00	4.50	2.82	0.50	2.58	1.88	0.28
0.1	8.68	10.24	9.34	8.56	4.46	6.82	5.36	3.68	0.84	3.50	2.34	0.52
0.2	9.44	9.00	9.96	9.62	4.66	5.50	5.72	4.66	0.78	2.42	2.32	0.84
0.3	9.80	8.16	10.34	10.68	4.72	4.56	6.02	5.34	0.74	1.70	2.18	1.30
0.4	9.56	6.82	11.38	10.58	4.42	3.86	6.60	5.34	0.90	1.20	2.26	1.52
0.5	10.18	5.80	13.56	10.78	5.14	2.50	7.70	6.30	1.04	0.96	3.10	1.60

Table 3.3: Rejection rate (%) under the null hypothesis for the situation b, considering $n = 20$ and different values of μ.

	$\mu = \frac{\pi}{6}$											
	$\alpha = 10\%$				$\alpha = 5\%$				$\alpha = 1\%$			
n	T_{1a}	T_{2a}	T_{3a}	T_{4a}	T_{1a}	T_{2a}	T_{3a}	T_{4a}	T_{1a}	T_{2a}	T_{3a}	T_{4a}
20	11.60	13.40	13.90	11.28	6.46	8.60	7.46	6.04	1.74	4.04	2.56	1.68
50	10.38	10.60	12.78	9.92	5.74	6.54	6.76	5.38	1.20	2.02	1.32	1.36
100	11.46	10.84	13.56	11.30	6.18	5.80	6.80	6.06	1.36	1.60	1.44	1.42
500	10.56	9.18	12.70	10.08	5.24	4.44	6.24	5.00	0.90	0.84	1.20	0.90
	$\mu = \frac{2\pi}{3}$											
	$\alpha = 10\%$				$\alpha = 5\%$				$\alpha = 1\%$			
n	T_{1a}	T_{2a}	T_{3a}	T_{4a}	T_{1a}	T_{2a}	T_{3a}	T_{4a}	T_{1a}	T_{2a}	T_{3a}	T_{4a}
20	14.58	15.12	13.44	15.08	8.68	10.16	6.80	8.28	2.72	5.18	2.22	2.94
50	12.74	12.64	12.84	12.72	7.36	8.02	6.88	7.64	1.64	2.54	1.50	2.36
100	12.46	11.46	13.12	13.10	6.88	6.28	7.00	7.60	1.68	1.62	1.26	2.14
500	11.96	10.30	13.26	12.48	5.96	5.04	6.54	6.64	1.20	1.06	1.08	1.56
	$\mu = \frac{4\pi}{3}$											
	$\alpha = 10\%$				$\alpha = 5\%$				$\alpha = 1\%$			
n	T_{1a}	T_{2a}	T_{3a}	T_{4a}	T_{1a}	T_{2a}	T_{3a}	T_{4a}	T_{1a}	T_{2a}	T_{3a}	T_{4a}
20	13.12	12.78	15.18	11.10	7.44	8.56	8.16	5.74	1.98	4.02	2.58	1.36
50	12.02	12.54	14.34	11.18	6.70	7.76	7.58	6.10	1.58	2.64	1.96	1.50
100	12.32	11.74	14.48	11.32	6.88	6.46	7.58	6.48	1.70	1.90	1.56	1.54
500	11.12	10.04	13.90	10.64	5.88	5.22	7.00	5.62	1.30	1.08	1.26	1.16
	$\mu = \frac{7\pi}{4}$											
	$\alpha = 10\%$				$\alpha = 5\%$				$\alpha = 1\%$			
n	T_{1a}	T_{2a}	T_{3a}	T_{4a}	T_{1a}	T_{2a}	T_{3a}	T_{4a}	T_{1a}	T_{2a}	T_{3a}	T_{4a}
20	11.12	11.10	13.50	10.88	5.86	7.20	6.78	5.44	1.36	3.02	1.70	1.06
50	10.18	10.44	13.44	10.64	5.62	6.44	7.04	5.96	1.28	2.14	1.56	1.32
100	10.98	9.92	13.68	11.32	5.84	5.32	7.12	6.28	1.26	1.52	1.32	1.38
500	10.62	8.80	13.76	11.18	5.44	4.42	6.82	5.74	1.12	0.82	1.16	1.22

of the tests increases considerably and the curves are close with the increase of the sample size. The gradient test was more powerful for $\beta > 1$, followed by the LR, score, and Wald tests for all considered sample sizes. There is a disagreement in the neighborhood to the right of $\beta = 1$ for the $n = 20$, $n = 30$ and $n = 50$ where the Wald test was more powerful. While on the left of $\beta = 1$, the score test has shown the more power for β close to zero and the Wald test was the most powerful in the neighbored of $\beta = 1$, followed by the score, LR and gradient tests.

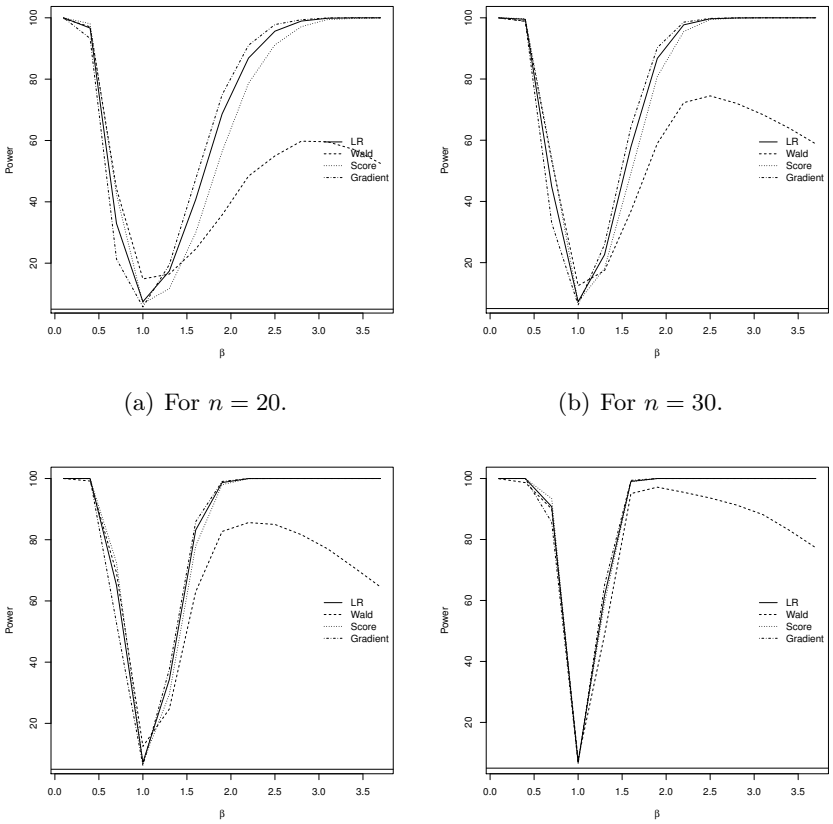

(a) For $n = 20$. (b) For $n = 30$.

(c) For $n = 50$. (d) For $n = 100$.

Figure 3.3: Estimated power curves on situation b for different sample sizes, considering $\alpha = 5\%$, $\rho = 0.3$, and $\mu = \frac{4\pi}{3}$.

3.4.2 *Performance for parametric bootstrap-based percentiles*

As previously mentioned, for small samples, the asymptotic χ^2 distribution may not be a good approximation to the exact null distribution of the statistics under discussion. Figure 3.4(a)

shows the χ^2_1 q-q plot of T_{1a}, while Figure 3.4(b) displays the χ^2_2 q-q plot of T_{4b}. Kolmogorov-Smirnov test results was performed, giving p-values of 2.2×10^{-16} for both situations; i.e., approximating the asymptotic distributions of T_{1a} and T_{4b} by the chi-square law is not adequate. The parametric bootstrap versions of the tests are alternatives to outperform this problem and we study their applications to tests for the EC model.

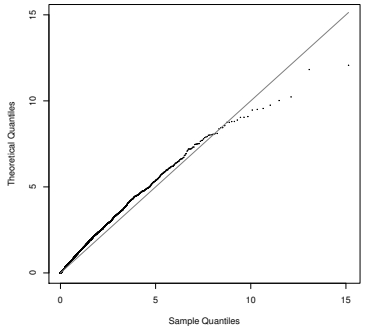

(a) Q-q plot of T_{1a} for twenty EC$(1, 2\pi/3, 0.3)$ generated observations.

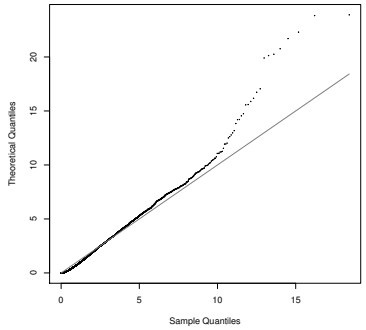

(b) Q-q plot of T_{4b} for twenty EC$(1, 4\pi/3, 0)$ generated observations.

Figure 3.4: Illustration of bias for the asymptotic distribution of T_{ij}.

By simplicity issues, we approach the use of bootstrap for the situation a, which is the most common in practice. From results of Table 3.4, null rejection rates for all the tests approach well the corresponding nominal levels as the sample size increases, as expected. The bootstrap-based LR and Wald tests were the most liberal for small samples. The score test approaches the nominal levels more slowly.

Table 3.4: Rejection rate (%) under the null hypothesis for the situation a and boostrap-based percentiles, considering $\rho = 0.3$, $\mu = \frac{2\pi}{3}$, and different sample sizes

	$\alpha = 10\%$				$\alpha = 5\%$				$\alpha = 1\%$			
n	T_{1a}	T_{2a}	T_{3a}	T_{4a}	T_{1a}	T_{2a}	T_{3a}	T_{4a}	T_{1a}	T_{2a}	T_{3a}	T_{4a}
20	11.28	12.52	9.12	10.72	5.48	6.64	4.36	5.38	1.10	1.24	0.58	1.10
50	10.88	10.00	9.96	9.84	5.26	5.00	4.52	4.84	1.00	0.86	0.66	0.86
100	9.92	9.64	9.82	10.04	4.70	4.54	4.80	4.84	0.98	0.72	0.96	0.94
150	9.40	9.70	9.76	9.34	4.94	5.02	5.08	4.86	0.82	0.82	0.84	0.88

The other scenarios considered in Section 3.4.1 were studied here as well. Table 3.5 presents such results under the bootstrap perspective. The Wald test was the most liberal in all the considered quadrants, for $\alpha = 10\%$ and $\alpha = 5\%$. For $\alpha = 1\%$, the ratio likelihood test was the most liberal. For the majority of cases, the type I error rate tends to increase as the parameter ρ increases. It is also possible to observe that the bootstrap version of tests corrected the inaccuracy presented by the type I error rate for the extremes of the ρ range. For instance, for $\mu = \frac{4\pi}{3}$, $\rho = 0.5$ and $\alpha = 5\%$, $T_{4a} = 23.30\%$ while for the bootstrap version results in 5.18%.

For the variation of μ, it was noticed that T_{2a} and T_{3a}, most of the times, are more liberal when μ belongs to the $2st$ and $3st$ quadrants and T_{1a} and T_{2a}, when μ is in the $1st$ and $4st$ quadrants. For instance, for the $\rho = 0.4$ and $\alpha = 5\%$, the Wald test presented type I error rate 5.14%, 6.98%, 5.60% and 4.78% and the LR test obtained type I error rate 4.76%, 5.68%, 3.80% and 4.04%. In general, the bootstrap version of the tests was more conservative than the usual tests, for $n = 20$; mainly, for test score.

In terms of the power, results for the bootstrap tests are presented in Figure 3.5, fixing $\alpha = 5\%$. It was observed that the power increases considerably and the curves are close when the sample size increases. For $n = 20$, one noted that, for a small variation on $\beta > 1$, the Wald and score tests have power smaller than $\alpha = 5\%$. Besides that, the power curve of the Wald and score tests approach faster, compared to the usual tests. The gradient test is the more powerful for $\beta > 1$, followed by the LR, score and Wald tests for all sample sizes considered. While for $\beta < 1$, the score test has shown the lowest power for β close to zero, the Wald test is less powerful in the vicinity of $\beta = 1$.

3.4.3 *Application*

Now, the tests T_{ij} for the EC model are submitted to three databases: two real sets and one synthetic. The first of them is defined by twenty one wind directions, measured from a weather station in Milwaukee at 6.00 a.m. on consecutive days (Johnson and Wehrly, 1977). The second database represents 9 orientations of core samples at the location 4 of the Pacheco Pass area of the Diablo Range (California, USA) (Upton and Fingleton, 1989). Upton and Fingleton have been

Table 3.5: Rejection rate (%) under the null hypothesis for the situation a and boostrap-based percentiles, considering $n = 20$ and different values of (μ, ρ)

	$\mu = \frac{\pi}{6}$											
	$\alpha = 10\%$				$\alpha = 5\%$				$\alpha = 1\%$			
ρ	T_{1a}	T_{2a}	T_{3a}	T_{4a}	T_{1a}	T_{2a}	T_{3a}	T_{4a}	T_{1a}	T_{2a}	T_{3a}	T_{4a}
0.0	9.78	9.50	9.02	9.98	5.28	4.80	4.22	5.20	1.10	0.82	0.92	1.10
0.1	9.36	9.12	8.18	9.52	4.76	4.18	3.84	4.90	0.88	0.34	0.50	0.96
0.2	9.00	10.20	8.40	9.18	4.62	4.88	3.94	4.90	0.96	0.78	0.64	1.08
0.3	9.62	10.68	7.96	9.62	4.72	5.26	3.56	4.72	0.88	0.78	0.42	0.90
0.4	9.30	10.06	7.90	9.34	4.76	5.14	3.22	4.80	1.04	0.88	0.44	0.96
0.5	9.54	8.72	10.32	8.90	4.56	4.28	4.94	4.34	0.96	0.96	0.80	0.78
	$\mu = \frac{2\pi}{3}$											
	$\alpha = 10\%$				$\alpha = 5\%$				$\alpha = 1\%$			
ρ	T_{1a}	T_{2a}	T_{3a}	T_{4a}	T_{1a}	T_{2a}	T_{3a}	T_{4a}	T_{1a}	T_{2a}	T_{3a}	T_{4a}
0.0	10.62	8.64	9.54	10.80	5.38	3.84	4.38	5.44	1.22	0.24	0.66	1.42
0.1	10.02	9.90	9.20	10.36	4.84	4.90	4.58	4.76	1.12	0.66	0.58	1.16
0.2	10.44	10.92	8.90	10.04	5.00	5.46	4.22	4.58	1.04	0.76	0.40	0.98
0.3	11.28	12.52	9.12	10.72	5.48	6.64	4.36	5.38	1.10	1.24	0.58	1.10
0.4	11.42	12.62	8.88	10.68	5.68	6.98	3.80	5.14	1.08	1.36	0.48	1.00
0.5	9.04	7.82	9.26	9.32	4.44	4.16	4.18	4.68	0.80	1.06	0.70	0.66
	$\mu = \frac{4\pi}{3}$											
	$\alpha = 10\%$				$\alpha = 5\%$				$\alpha = 1\%$			
ρ	T_{1a}	T_{2a}	T_{3a}	T_{4a}	T_{1a}	T_{2a}	T_{3a}	T_{4a}	T_{1a}	T_{2a}	T_{3a}	T_{4a}
0.0	10.00	9.90	10.26	8.76	5.22	4.46	4.78	3.96	1.14	0.80	0.64	0.58
0.1	9.12	8.98	9.98	8.62	4.68	4.74	5.04	3.94	0.90	0.82	1.00	0.50
0.2	9.44	9.20	9.94	8.32	4.40	4.42	4.90	3.44	0.84	0.80	0.98	0.38
0.3	9.58	10.18	9.82	8.08	4.38	5.12	5.02	3.30	0.66	0.96	0.94	0.28
0.4	9.10	10.32	8.78	7.92	3.80	5.60	4.74	2.78	0.78	0.86	0.94	0.16
0.5	10.60	10.86	5.44	11.44	5.22	5.44	3.14	5.18	1.24	1.02	0.62	0.60
	$\mu = \frac{7\pi}{4}$											
	$\alpha = 10\%$				$\alpha = 5\%$				$\alpha = 1\%$			
ρ	T_{1a}	T_{2a}	T_{3a}	T_{4a}	T_{1a}	T_{2a}	T_{3a}	T_{4a}	T_{1a}	T_{2a}	T_{3a}	T_{4a}
0.0	8.10	8.94	8.54	7.78	3.74	4.28	4.10	3.36	0.62	0.86	0.70	0.58
0.1	8.82	9.62	9.14	8.14	4.62	5.06	4.58	3.62	1.04	0.92	0.66	0.32
0.2	9.14	9.52	9.18	9.06	4.48	4.64	4.52	3.92	0.74	0.70	0.76	0.30
0.3	9.06	9.86	8.76	9.24	4.46	4.74	4.12	4.02	0.70	0.64	0.46	0.42
0.4	8.86	10.14	8.04	8.96	4.04	4.78	3.54	3.98	0.76	0.60	0.48	0.72
0.5	9.24	9.14	8.80	8.98	4.34	4.28	3.66	4.56	0.78	0.78	0.50	0.70

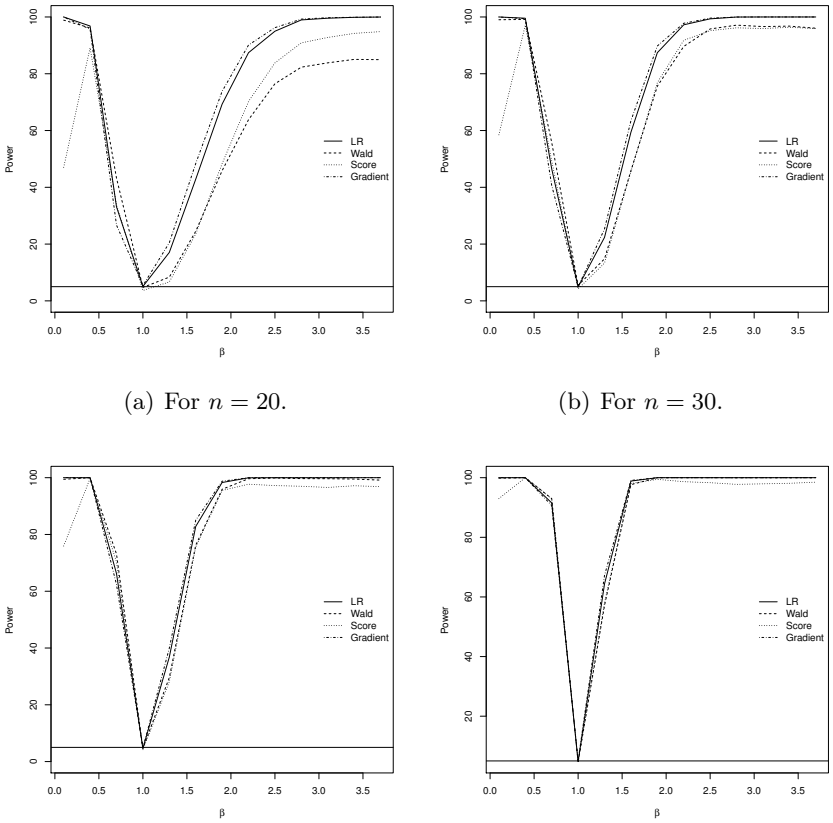

(a) For $n = 20$.

(b) For $n = 30$.

(c) For $n = 50$.

(d) For $n = 100$.

Figure 3.5: Estimated power curves on situation a via boostrap for different sample sizes, considering $\alpha = 5\%, \rho = 0.3$, and $\mu = \frac{\pi}{6}$.

indicated the C distribution for describing these orientations. In order to align this application to the previous synthetic study, we also consider a third dataset having 30 observations, generated from the uniform distribution. The datasets measured in degrees are given bellow.

Data Set 1	356	97	211	232	343	292	157	302	335	302	324
	85	324	340	157	238	254	146	232	122	329	
Data Set 2	8	194	352	304	50	320	350	314	50		
Data Set 3	231	212	346	333	58	152	232	172	11	224	276
	64	153	231	315	64	211	96	58	100	92	219
	223	60	296	298	85	86	161	349			

Here, we aim to quantify the potentiality of discussed tests according to a and b situations for real data. For the situation a, first and second datasets represent alternative and null hypotheses, respectively. Thus, it is expected H_0 is only rejected for dataset 1. On the other hand, with respect to the situation b, datasets 1 and 3 indicate H_1 and H_0, respectively. For this case, one expects to reject H_0 only for dataset 1.

First, we fit EC, Cardioid and uniform models, according to the Table 3.6. Results indicate acceptable adjustments, although some difficulties have been found to estimate ρ in small samples (a longer discussion about it was furnished in the Chapter 2). As qualitative evidence of these fits, empirical and fitted pdfs are presented in Figure 3.6. It is noticeable the EC model tends to approach the C and uniform laws for second and third databases; while, the former is meaningfully different of other two for the first database.

Adopting the level of significance of 10%, it can be observed that only the Wald test and its bootstrap version do not reject the null hypothesis for dataset 1 in the situation b; that is, they do not reject the uniform assumption when these data are strongly asymmetric (see Figures 3.6(a) and 3.6(b)). Therefore, this test is not indicated when one wishes to distinguish between uniform and EC distributions in small samples.

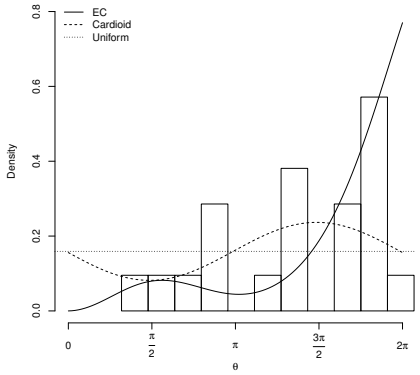

(a) Original histogram for dataset 1.

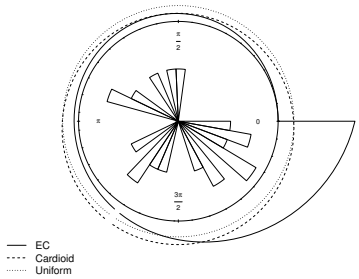

(b) Circular histogram for dataset 1.

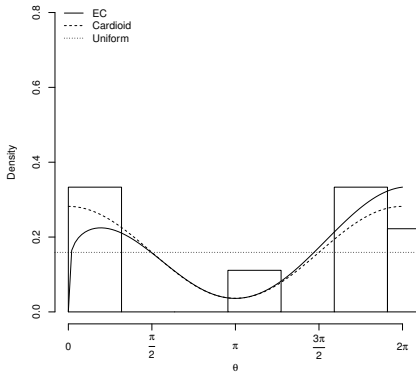

(c) Original histogram for dataset 2.

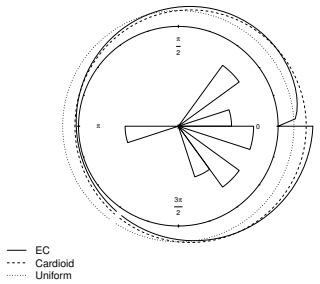

(d) Circular plot for dataset 2.

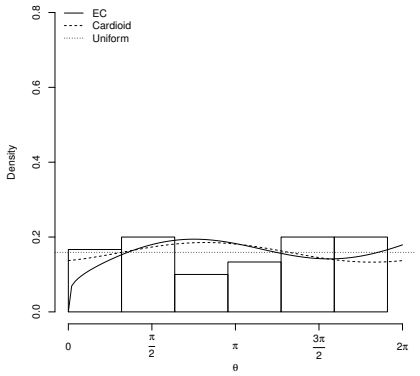

(e) Original histogram for dataset 3.

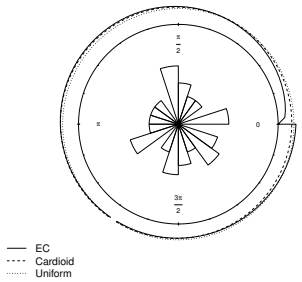

(f) Circular plot for dataset 3.

Figure 3.6: Fitted EC, C, and uniform densities for three databases.

Table 3.6: ML estimates (SEs) for parameters for considered models

Model	Parameter	Dataset 1	Dataset 2	Dataset 3
Cardioid	ρ	0.2436	0.3859	–
		(0.1239)	(0.1411)	–
	μ	4.6708	0.0002	–
		(0.6135)	(0.3601)	–
Exponentiated Cardioid	β	2.8764	1.1755	1.2067
		(0.8929)	(0.3956)	(0.2202)
	ρ	0.2166	0.3911	0.1166
		(0.1185)	(0.1431)	(0.0000)
	μ	1.1789	0.0002	1.8655
		(0.5902)	(0.0000)	(0.0000)

Table 3.7: P-values of the asymptotic (T_{ij}) and bootstrap (T^*_{ij}) hypothesis tests

	Situation a			Situation b	
	Dataset1	Dataset2		Dataset1	Dataset3
T_{1a}	0.0028	0.6381	T_{1b}	0.0031	0.6264
T_{2a}	0.0359	0.6971	T_{2b}	0.1100	0.6695
T_{3a}	0.0360	0.6058	T_{3b}	0.0459	0.8692
T_{4a}	0.0002	0.6285	T_{4b}	0.0000	0.5827
T^*_{1a}	0.0020	0.6623	T^*_{1b}	0.0030	0.8032
T^*_{2a}	0.0719	0.6723	T^*_{2b}	0.1459	0.6214
T^*_{3a}	0.0559	0.6464	T^*_{3b}	0.0120	0.6074
T^*_{4a}	0.0020	0.6623	T^*_{4b}	0.0010	0.7892

3.5 Concluding remarks

The Chapter 2 showed convincing evidence the exponentiated Cardioid (EC) distribution may assume asymmetric and bimodal behaviors, unlikely the uniform and Cardioid (C) particular models, which have been widely used in the circular data practice. Testing hypothesis mapped from circular models is a mandatory activity in several applications. This chapter has presented hypothesis-based inference procedures to choose among the EC, C, and uniform laws by means of LR, Wald, score and gradient tests on both asymptotic and bootstrap perspectives. First a closed-form expression for the EC Fisher information matrix has been derived. In order to quantify the performance of tests, a Monte Carlo simulation study has been presented, adopting empirical test size and power as comparison criteria. The gradient and score tests have presented the best performance in different situations. Finally, the asymptotic and bootstrap tests have been applied to real datasets. Results indicated the gradient test as the best discriminant tool and the use of bootstrap has improved meaningfully the performance of considered tests.

4 A circular-circular regression model for the exponentiated Cardioid model

Resumo

O modelo Cardioide exponencializado (EC) foi introduzido no Capítulo 2 e empregado com sucesso para descrever dados circulares. Ao contrário do modelo Cardioide, a distribuição EC apresenta comportamentos assimétricos e bimodais. Compreender a relação entre duas variáveis circular é necessário na prática. Neste Capítulo, propomos um modelo de regressão circular-circular com o erro aleatório assumindo a distribuição EC. Para este fim, empregamos o mapeamento do círculo de Möbius como mecanismo técnico. Primeiro, derivamos o modelo complexo associado aos erros angulares cujo argumento segue a distribuição EC. Um procedimento baseado no método da máxima verossimilhança é desenvolvido para estimar os parâmetros do modelo proposto. Finalmente, uma aplicação a um conjunto de dados de direções do vento é realizada. Os resultados indicam que o novo modelo pode superar três outros que possuem a ditribuição von Mises, wrapped Cauchy e von Mises modificada como suposições para distribuição dos erros angulares.

Palavras-chave: Distribuição EC. Modelos complexos. Regressão circular-circular. Transformação de Möbius.

Abstract

The exponentiated Cardioid (EC) model has been introduced in the Chapter 2 and successfully employed for describing circular data. Unlike the Cardioid model, the EC distribution may fit

asymmetric and bimodal behaviors. Understanding the relation between two circular variables is required in practice. In this chapter, we propose a circular-circular regression model with the random error having EC distributed angular component. This model uses the Möbius circle as a usel tool. First we derive the complex model associated to the error variable whose argument follows the EC distribution. A point estimation procedure via maximum likelihood is developed for the parameters of our proposal. Finally, an application to wind directions data is performed. Results indicate our model may outperform three other models having the von Mises, wrapped Cauchy and modified von Mises distributions as angular assumptions for the error variable.

Keywords: Circular-circular regression. Complex models. EC distribution. Möbius transformation.

4.1 Introduction

Regression models in the Circular Statistics area are often designed under three perspectives in terms of response and explanatory variables, say response-exploratory: circular-linear, linear-circular and circular-circular. Illustrating the first kind, the effect of the wind speed over the angle of the fire propagation was quantified by Li *et al.* (2017). With respect to the second kind, Kucwaj *et al.* (2017) proposed to measure the altimetric (positive-valued measurement) obtained from satellite signals conditioned to the phase delay, captured by signal before and after of sensoring an under study surface. SenGupta and Kim (2016) studied the relation between gene locations for two circular genomes representing the third branch. In this chapter, we provide advances on this last kind.

In circular-circular regressions, an angular random variable is modelled in terms of other circular random variable and both are measured assuming the same zero direction and rotation sense (Sarma and Jammalamadaka, 1993). However, the study of this topic has received very little attention (Pewsey *et al.*, 2014). The classical regression analysis among real-valued variables cannot be applied for the circular-circular case because the former is specific for the Euclidean space.

The concept of circular-circular regression was introduced by Sarma and Jammalamadaka (1993). In Rivest (1997), the circular dependent variable is regressed on an independent variable by decentering the dependent variable. Other models for this purpose are explained by Minh and Farnum (2003) and Hussin *et al.* (2004). SenGupta *et al.* (2013) discussed inverse circular-circular regression. Downs and Mardia (2002), Kato *et al.* (2008) and Kato and Jones (2010) presented a mathematical treatment about a circular-circular regression by using the Möbius transformation (MT) like link function. Earlier works on circular-circular regression models have been tackled by Fisher (1995).

The MT that maps the unit disc to itself was used for studying two circular variables in Downs and Mardia (2002), Kato *et al.* (2008) and Kato and Jones (2010). These works have assumed the von Mises (vM), wrapped Cauchy (wC) and modified von Mises (vMM) models as error angular components, respectively. As one of the earlier works to adopt the MT, McCullagh *et al.* (1996) has investigated using the Cauchy distribution as one input to such transformation. The MT was also used in the context of spherical regression by Chang (1986) and by Minh and Farnum (2003) to induce probability distributions on the circle. Jones (2004) and Seshadri (1991) propsed the Möbius distribution to generate new family of distributions. Jha and Biswas (2017) introduced multiple circular-circular regression models using the MT.

The expontentiated Cardioid (EC) distribution was introduced in the Chapter 2 as an extension to the Cardioid distribution. This model is very useful since it is suitable for asymmetry and bimodality situations. Thus, we advocate that using this model as the distribution of angular error in regression models can be advantageous. In this chapter we propose a new circular-circular regression model having EC distributed angular errors. Its regression curve is expressed in terms of the MT. Futher, we also introduce the complex version of the EC distribution, named CEC distribution. A likelihood-based estimation procedure for the parameters of the new model is furnished. To illustrate the proposed model potentiality, we compare its performance applied to wind direction real data with those due to models having the vM, wC and vMM error distributions as error angular components. Results indicate that our proposal may be the best regression strategy.

The subsequent sections are organized as follows. In Section 4.2, the MT and some of its properties are discussed. The EC model is presented as well as its complex form in Section 4.3. Section 4.4 presents the used estimation procedure. In Section 4.5 our model is applied to wind directions data and compared with others models. Finally, 4.6 summarizes the main findings of the chapter.

4.2 Möbius transformation

Let u be a variable with support in the unit circle or, equivalently, in the unit norm complex plane. Suppose β_0 and β_1 are complex parameters with $|\beta_0| = 1$. Then the link function of the regression model proposed in this chapter is given by

$$v = \beta_0 \frac{u + \beta_1}{1 + \overline{\beta_1} u}, \tag{4.1}$$

where $|u| = 1$. The mapping with $|\beta_1| \neq 1$ is called the MT. It is known that this transformation is a one-to-one mapping which carries the unit circle onto itself, i.e. $|v| = 1$.

Theorem 4.2.1. $|v| = 1$.

Proof. Let $u = e^{i\theta_1}$ and $\beta_1 = ae^{i\theta_2}$. Without loss of generality, we assume that $\beta_0 = 1$. It follows from (a), the modulus of the complex ratio is ratio between modules Ahlfors (1979) that

$$|v| = \left| \frac{u + \beta_1}{1 + \overline{\beta_1} u} \right| \overset{(a)}{=} \frac{|u + \beta_1|}{|1 + \overline{\beta_1} u|} = \frac{\sqrt{[\cos(\theta_1) + a\cos(\theta_2)]^2 + [\sin(\theta_1) + a\sin(\theta_2)]^2}}{\sqrt{[1 + a\cos(\theta_1 - \theta_2)]^2 + [a\sin(\theta_1 - \theta_2)]^2}} = 1.$$

□

Reparametrized MT can be used by putting $(u, v) = (e^{ia}, e^{ib})$, $\beta_1 = re^{i\theta}$ $(r \geq 0,\ 0 \leq \theta < 2\pi)$ and $\beta_0' = \mathrm{Arg}(\beta_0)$:

$$e^{ib} = e^{i\beta_0'} \frac{e^{ia} + re^{i\theta}}{1 + re^{i(a-\theta)}} \quad \text{or} \quad b = \beta_0' + \theta + 2\arctan\left[w_r \tan\left\{ \frac{1}{2}(a - \theta) \right\} \right],$$

where $w_r = (1 - r)/(1 + r)$.

Some interesting results about the MT can be checked in Kato *et al.* (2008). It is worth mentioning that β_0 is a rotation parameter. Already β_1 can be intuitively interpreted as the

parameter that attracts the points on the circle toward $\beta_1/|\beta_1|$. The concentration of points about $\beta_1/|\beta_1|$ increases as $|\beta_1|$ increases.

For the possible forms assumed by the MT, it is important to note the symmetry between the curves $v(\beta_0, \beta_1, u)$ and $v(\overline{\beta_0}, \overline{\beta_1}, \overline{u})$ in relation to $u = 0$ and $v = 0$. This behavior is illustrated in Figure 4.1(a) and proved in the following Theorem. The Figure 4.1(b) exhibits some possible forms of the MT.

Theorem 4.2.2. $-Arg[v(\overline{\beta_0}, \overline{\beta_1}, \overline{u})] = Arg[v(\beta_0, \beta_1, u)]$.

Proof. Let $u = e^{ia}$ and $\beta_1 = re^{ib}$. It follows that

$$\begin{aligned}
-\text{Arg}[v(\overline{\beta_0}, \overline{\beta_1}, \overline{u})]) &= -\text{Arg}\left(\overline{\beta_0}\frac{\overline{u} + \overline{\beta_1}}{1 + \beta_1\overline{u}}\right) = -[\text{Arg}(\overline{\beta_0}) + \text{Arg}(\overline{u} + \overline{\beta_1}) - \text{Arg}(1 + \beta_1\overline{u})] \\
&= \text{Arg}(\beta_0) - \arctan\left(-\frac{\sin a + r\sin b}{\cos a + r\cos b}\right) + \arctan\left(\frac{r\sin(b-a)}{1 + r\cos(b-a)}\right) \\
&= \text{Arg}(\beta_0) + \arctan\left(\frac{\sin a + r\sin b}{\cos a + r\cos b}\right) - \arctan\left(\frac{r\sin(b-a)}{1 + r\cos(b-a)}\right) \\
&= \text{Arg}\left(\beta_0\frac{u + \beta_1}{1 + \overline{\beta_1}u}\right) \\
&= \text{Arg}[v(\beta_0, \beta_1, u)].
\end{aligned}$$

□

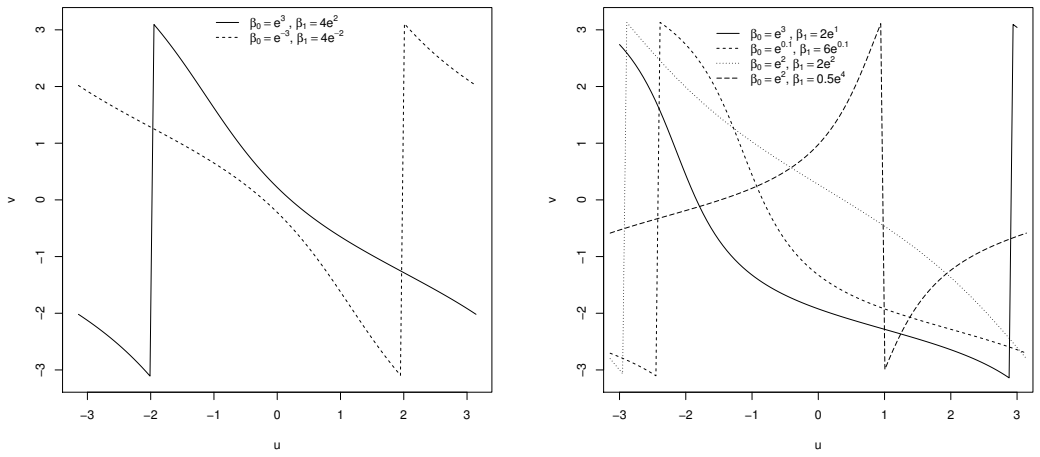

Figure 4.1: Plots of the regression curve.

Figure 4.2 illustrates the MT and the Theorem 4.2.2 given the complex input $u = 0.54+0.84\,i$, $\beta_0 = -0.99 + 0.14\,i$ and $\beta_1 = -0.21 + 0.45\,i$.

To that end the following six operations are done:

- $u \overset{1}{\Rightarrow} u + \beta_1 \overset{2}{\Rightarrow} \frac{u+\beta_1}{1+\overline{\beta}_1 u} \overset{3}{\Rightarrow} \beta_0 \frac{u+\beta_1}{1+\overline{\beta}_1 u}$,
- $\bar{u} \overset{4}{\Rightarrow} \bar{u} + \overline{\beta}_1 \overset{5}{\Rightarrow} \frac{\bar{u}+\overline{\beta}_1}{1+\beta_1 \bar{u}} \overset{6}{\Rightarrow} \overline{\beta}_0 \frac{\bar{u}+\overline{\beta}_1}{1+\beta_1 \bar{u}}$.

The resulting angles were -1.64 and 1.64, respectively, which show that the results differ only by a signal, according to the symmetry of the Theorem 4.2.2.

4.3 Exponentiated Cardioid model

The EC distribution was introduced in Chapter 2 as an extension to the Cardioid distribution. Such a model has the advantage of allowing the description of asymmetric and some bimodality phenomena. This new three-parameter model has probability density function (pdf) given by (for $0 < \theta \leq 2\pi$)

$$f(\theta;\beta,\rho,\mu) = \frac{\beta}{2\pi}\left\{\frac{\theta}{2\pi} + \frac{\rho}{\pi}[\text{sen}(\theta-\mu) + \text{sen}(\mu)]\right\}^{\beta-1}[1 + 2\rho\cos(\theta-\mu)], \tag{4.2}$$

where $0 < \mu \leq 2\pi$, $0 \leq \rho \leq 0.5$ and $\beta > 0$.

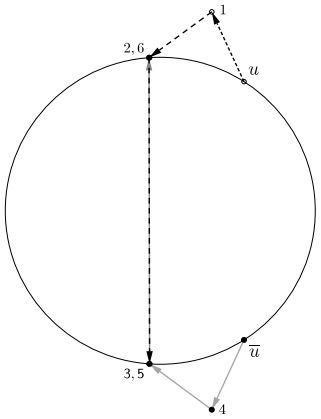

Figure 4.2: Symmetry in the Möbius transformation.

Since the MT is suitable to the complex plane, it is important to define the complex distribution whose the angular component is the EC distribution. This situation is denoted as $Z \sim CEC(\beta, \phi)$; i.e., if $\Theta \sim EC(\mu, \rho, \beta)$, then $Z = \mathrm{e}^{i\,\Theta} \sim CEC(\beta, \phi)$ such that $\phi = \rho\,\mathrm{e}^{i\,\mu}$. In follow theorem, we derive the density of Z.

Theorem 4.3.1. *Defining* $\mathbb{I}_1 = \mathbb{I}_{(-\pi+\mu,\mu)\vee(\pi+\mu,2\pi+\mu)}(\theta)$*, if* $Z \sim CEC(\beta, \phi)$*, its pdf is given by*

$$f(z) = -\beta \frac{|z-\phi|^2 + |1-|\phi|^2| - 3}{(2\pi)^\beta} \times \left[Arg(z) + (-1)^{\mathbb{I}_1} 2\rho \left(\sqrt{1 - \left[\frac{-|z-\phi|^2 + 1 + |\phi|^2}{2|\phi|} \right]^2} + \sin[Arg(\phi)] \right) \right]^{\beta-1},$$

with $z = e^{i\theta}$*,* $\phi = \rho e^{i\mu}$*,* $0 < \rho \leq 0.5$ *and* $0 < \theta, \mu \leq 2\pi$*.* $|\cdot|$ *and* $Arg(\cdot)$ *indicate the modulus and argument of a complex number, respectively.*

The proof is presented in Appendix E.

4.4 Circular-circular regression model and likelihood-based estimation

The considered regression model is given by

$$Y = \beta_0 \frac{x + \beta_1}{1 + \overline{\beta_1} x} \epsilon, \quad |x| = 1,$$

where $\beta_0, \beta_1 \in \mathbb{C}$ such that $|\beta_0| = 1$, $\epsilon \sim \text{CEC}(\beta, \phi)$ and $\text{Arg}(Y) = \text{cons} + \text{Arg}(\epsilon)$, with cons $= \text{Arg}(\beta_0) + \arctan\left[\frac{\text{Im}(x)+\text{Im}(\beta_1)}{\text{Re}(x)+\text{Re}(\beta_1)}\right] - \arctan\left[\frac{\text{Im}(\overline{\beta_1}x)}{1+\text{Re}(\overline{\beta_1}x)}\right]$ and $\text{Arg}(\epsilon) \sim EC(\mu, \rho, \beta)$, where $\text{Im}(\cdot)$ and $\text{Re}(\cdot)$ are real and imaginary parts of the considered complex number.

A manner to obtained ML estimates for the parameters involved in the proposed regression model is through of the angular errors distribution. Let $\text{Arg}(\epsilon_1)$, $\text{Arg}(\epsilon_2)$, ..., $\text{Arg}(\epsilon_n)$ be an observed sample of size n from $\text{Arg}(\epsilon) \sim \text{EC}(\beta, \rho, \mu)$. The log-likelihood function at $\boldsymbol{\delta} = (\beta, \rho, \mu, \beta_0', r, \beta_1')^\top$, ℓ, can be expressed as

$$\begin{aligned}\ell(\boldsymbol{\delta}) =& n\log\beta + (\beta-1)\sum_{i=1}^{n}\log\left\{\frac{\text{Arg}(\epsilon_i)}{2\pi} + \frac{\rho}{\pi}\{\sin[\text{Arg}(\epsilon_i)-\mu] + \sin\mu\}\right\} - n\log(2\pi) \\ &+ \sum_{i=1}^{n}\log\{1 + 2\rho\cos[\text{Arg}(\epsilon_i)-\mu]\},\end{aligned} \tag{4.3}$$

where $\epsilon_i = y_i(1+\overline{\beta}_1 x_i)/\beta_0(x_i+\beta_1)$.

To facilitate the derivation of ML estimates, reparametrizations are often used. We adopt $(x_i, y_i) = (e^{i\theta_{1i}}, e^{i\theta_{2i}})$, $\beta_1 = re^{i\beta_1'}$ ($r \geq 0,\ 0 \leq \theta < 2\pi$), $\beta_0' = \text{Arg}(\beta_0)$ and $\beta_1' = \text{Arg}(\beta_1)$. Defining

$$\psi_i = \begin{cases} \arctan\left(\frac{S_i}{C_i}\right), \text{if } S_i > 0 \text{ and } C_i > 0, \\ \arctan\left(\frac{S}{C_i}\right) + \pi, \text{if } C_i < 0, \\ \arctan\left(\frac{S}{C}\right) + 2\pi, \text{if } S_i < 0 \text{ and } C_i > 0, \end{cases}$$

where $S_i = -\sin(\theta_{1i}) - 2r\sin(\beta_1') + r^2\sin(-2\beta_1' + \theta_{1j})$ and $C_i = \cos(\theta_{1i}) + 2r\cos(\beta_1') + r^2\cos(-2\beta_1' + \theta_{1i})$, it follows that

$$\text{Arg}(\epsilon_i) = \begin{cases} \theta_{2i} - \beta_0' + \psi_i, \text{if } 0 < \theta_{2i} - \beta_0' + \psi_i \leq 2\pi, \\ \theta_{2i} - \beta_0' + \psi_i + 2\pi, \text{if } \theta_{2i} - \beta_0' + \psi_i \leq 0, \\ \theta_{2i} - \beta_0' + \psi_i - 2\pi, \text{if } \theta_{2i} - \beta_0' + \psi_i > 2\pi. \end{cases}$$

Therefore, the ML estimates for β, ρ, μ, β_0', r and β_1' are solutions of the following system of non-linear equations:

$$U_\beta = \frac{\partial\ell(\boldsymbol{\delta})}{\partial\beta} = \frac{n}{\beta} + \sum_{i=1}^{n}\log\left\{\frac{\text{Arg}(\epsilon_i)}{2\pi} + \frac{\rho}{\pi}\{\sin[\text{Arg}(\epsilon_i)-\mu] + \sin\mu\}\right\} = 0,$$

$$U_\rho = \frac{\partial \ell(\boldsymbol{\delta})}{\partial \rho} = 2\sum_{i=1}^{n}\left\{(\beta-1)\frac{\sin[\mathrm{Arg}(\epsilon_i)-\mu]+\sin\mu}{\mathrm{arg}(\epsilon_i)+2\rho\{\sin[\mathrm{Arg}(\epsilon_i)-\mu]+\sin\mu\}}+\frac{\cos[\mathrm{Arg}(\epsilon_i)-\mu]}{1+2\rho\cos[\mathrm{Arg}(\epsilon_i)-\mu]}\right\}=0,$$

$$U_\mu = \frac{\partial \ell(\boldsymbol{\delta})}{\partial \mu} = 2\rho\sum_{i=1}^{n}\left\{(\beta-1)\frac{-\cos[\mathrm{Arg}(\epsilon_i)-\mu]+\cos\mu}{\mathrm{Arg}(\epsilon_i)+2\rho\{\sin[\mathrm{Arg}(\epsilon_i)-\mu]+\sin\mu\}}+\frac{\sin[\mathrm{Arg}(\epsilon_i)-\mu]}{1+2\rho\cos[\mathrm{Arg}(\epsilon_i)-\mu]}\right\}=0,$$

$$U_{\beta_0'} = \frac{\partial \ell(\boldsymbol{\delta})}{\partial \beta_0'} = 2\rho\sum_{i=1}^{n}\left\{(1-\beta)\frac{\cos[\mathrm{Arg}(\epsilon_i)-\mu]}{\mathrm{Arg}(\epsilon_i)+2\rho\{\sin[\mathrm{Arg}(\epsilon_i)-\mu]+\sin\mu\}}+\frac{\sin[\mathrm{Arg}(\epsilon_i)-\mu]}{1+2\rho\cos[\mathrm{Arg}(\epsilon_i)-\mu]}\right\}=0,$$

$$U_r = \frac{\partial \ell(\boldsymbol{\delta})}{\partial r} = \sum_{i=1}^{n}A_i\left\{(\beta-1)\frac{1+2\rho\cos[\mathrm{Arg}(\epsilon_i)-\mu]}{\mathrm{Arg}(\epsilon_i)+2\rho\{\sin[\mathrm{Arg}(\epsilon_i)-\mu]+\sin\mu\}}-\frac{2\rho\sin[\mathrm{Arg}(\epsilon_i)-\mu]}{1+2\rho\cos[\mathrm{Arg}(\epsilon_i)-\mu]}\right\}=0$$

and

$$U_{\beta_1'} = \frac{\partial \ell(\boldsymbol{\delta})}{\partial \beta_1'} = \sum_{i=1}^{n}B_i\left\{(\beta-1)\frac{1+2\rho\cos[\mathrm{Arg}(\epsilon_i)-\mu]}{\mathrm{Arg}(\epsilon_i)+2\rho\{\sin[\mathrm{Arg}(\epsilon_i)-\mu]+\sin\mu\}}-\frac{2\rho\sin[\mathrm{Arg}(\epsilon_i)-\mu]}{1+2\rho\cos[\mathrm{Arg}(\epsilon_i)-\mu]}\right\}=0,$$

where $A_i = (C_i^2+S_i^2)^{-1}[-2\sin(\beta_1')+2r\sin(-2\beta_1'+\theta_{1i})]C - S[2\cos(\beta_1')+2r\cos(-2\beta_1'+\theta_{1i})]$ and $B_i = (C_i^2+S_i^2)^{-1}[-2r\cos(\beta_1')-2r^2\cos(-2\beta_1'+\theta_{1i})]C - S[-2r\sin(\beta_1')+2r^2\sin(-2\beta_1'+\theta_{1i})]$.

This system of equations can be reduced by applying the following expression for $\hat{\beta}$ in the last identities:

$$\hat{\beta}(\rho,\mu,\beta_0',r,\beta_1') = -\frac{n}{\sum_{i=1}^{n}\log\left\{\frac{\mathrm{Arg}(\epsilon_i)}{2\pi}+\frac{\rho}{\pi}[\sin(\mathrm{Arg}(\epsilon_i)-\mu)+\sin\mu]\right\}}. \tag{4.4}$$

Thus, the ML estimates for ρ, μ, β_0', r and β_1' are obtained numerically from

$$\left.\frac{\partial \ell(\boldsymbol{\delta})}{\partial \rho}\right|_{\beta=\hat{\beta}(\rho,\mu,\beta_0',r,\beta_1')}=0,\quad \left.\frac{\partial \ell(\boldsymbol{\delta})}{\partial \mu}\right|_{\beta=\hat{\beta}(\rho,\mu,\beta_0',r,\beta_1')}=0,\quad \left.\frac{\partial \ell(\boldsymbol{\delta})}{\partial \beta_0'}\right|_{\beta=\hat{\beta}(\rho,\mu,\beta_0',r,\beta_1')}=0,$$

$$\left.\frac{\partial \ell(\boldsymbol{\delta})}{\partial r}\right|_{\beta=\hat{\beta}(\rho,\mu,\beta_0',r,\beta_1')}=0 \text{ and } \left.\frac{\partial \ell(\boldsymbol{\delta})}{\partial \beta_1'}\right|_{\beta=\hat{\beta}(\rho,\mu,\beta_0',r,\beta_1')}=0.$$

In the remainder of this chapter, we refer to $[U_\beta, U_\rho, U_\mu, U_{\beta_0'}, U_r, U_{\beta_1'}]^\top$ as the score vector.

4.5 A Real Data Set

In order to illustrate the potentiality of the proposed model, an application to real data was made. Further, its performance was compared with three other models, where the vM, wC and vMM distributions were assumed for $\mathrm{Arg}(\epsilon_i)$. Their respective densities are given by.

$$f_{vM} = \frac{1}{2\pi I_0(\kappa)}\exp\{\kappa\cos(\theta-\mu)\},\ 0\le\theta,\mu<2\pi \text{ and } \kappa\ge 0,$$

$$f_{wC} = \frac{1}{2\pi}\frac{1-\rho^2}{1+\rho^2-2\rho\cos(\theta-\mu)},\ 0 \leq \theta, \mu < 2\pi \text{ and } 0 \leq \rho < 1 \text{ and}$$

$$f_{vMM} = \frac{1-\rho^2}{2\pi I_0(\kappa)} \exp\left[\frac{\kappa\{\xi\cos(\theta-\eta)-2\rho\cos(\beta)\}}{1+\rho^2-2\rho\cos(\theta-\gamma)}\right]\frac{1}{1+\rho^2-2\rho\cos(\theta-\gamma)},\ 0 \leq \theta < 2\pi,$$

where $\xi = \sqrt{\rho^4+2\rho^2\cos(2\beta)+1}$, $\eta = \mu + \arg\{\rho^2\cos(2\beta)+1+i\rho^2\sin(2\beta)\}$, $\gamma = \mu+\beta$, $0 \leq \mu, \beta < 2\pi$, $0 \leq \rho < 1$, $\kappa > 0$ and $I_0(\rho) = \int_0^{2\pi}\exp[\rho\cos(\phi-\mu)]d\phi$ is the modified Bessel function of the first kind and order zero.

ML estimates were used to fit considered models to data. All the computations were done using the function `maxLik`, which is available at the R statistical software R Core Team (2017).

The dataset consists of 73 pairs of wind directions obtained by a Texas weather station, at 6.00 am and noon, on consecutive days, from May 20 to July 31, inclusive, 2003. The data are part of a larger dataset which is taken from the Codiac data archive, where the considered station is denoted by C28_ 1 and is available at `http://data.eol.ucar.edu/codiac/dss/id=85.034`. The dataset was the same used in Kato and Jones (2010), in order to compare the results. The independence of the variables was tested using the statistic r^2 proposed by Jupp and Mardia (1980). Under independence, $nr^2 \sim \chi^2_4$, where n is the sample size. Since $nr^2 = 56.69$ and $\chi^2_4 = 9.49$, there is strong evidence for dependence.

Figure 4.3(a) shows a plot of the data and the estimated regression curves which seems to describe the relationship between wind directions reasonably well. The residuals,

$$\widehat{\text{Arg}(\epsilon_i)} = \text{Arg}\left\{\frac{y_i(1+\bar{\widehat{\beta}}_1 x_i)}{\widehat{\beta}_0(x_i+\widehat{\beta}_1)}\right\},$$

expressed in terms of radians and the fitted EC distribution are displayed in the Figure 4.3(b). The q-q plot in the Figure 4.3(c) also evidences clearly that the angular errors are distributed as EC distribution.

Table 4.1 shows the ML estimates, the standard errors, the maximised log-likelihood, AIC and BIC values for the considered models. It is important to note that the values found for the vMM distribution are discordant to those in Kato and Jones (2010). Standard errors were calculated using the jackknife procedure. The jackknife procedure delivers a more accurate asymptotic inference than the analytic standard errors. According to the AIC and BIC, our model presented

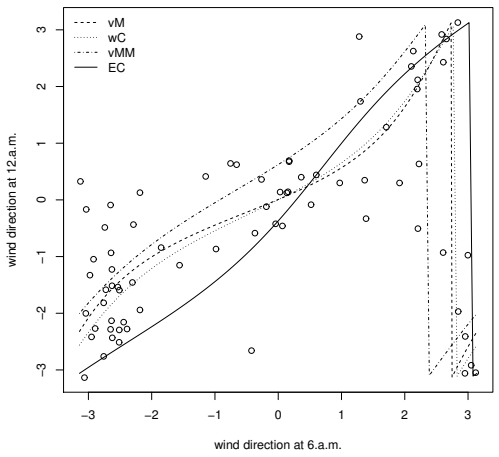

(a) Plot of the wind directions at 6 a.m. and noon with the estimated regression curves.

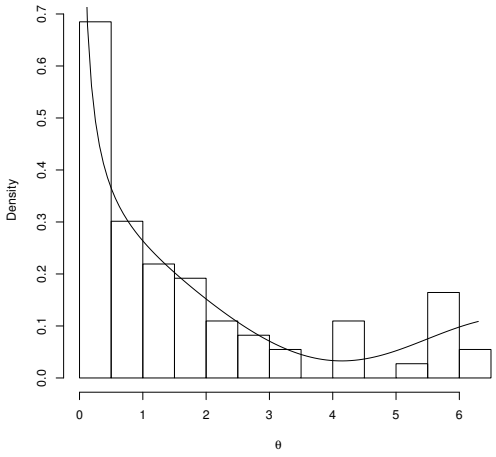

(b) Histogram of the residuals and the fitted EC density.

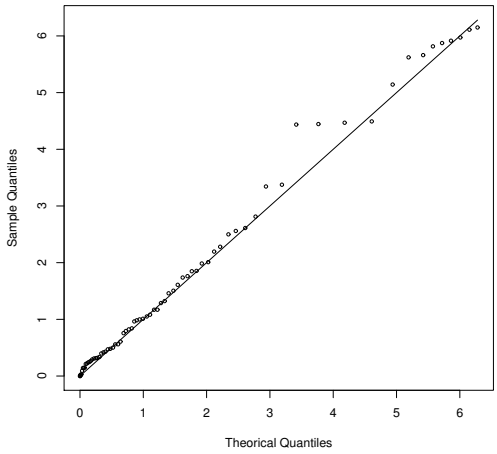

(c) Q-q plot.

Figure 4.3: Plots of the special functions.

the best result.

The Figure 4.4 shows the spokeplot, representation introduced by *et al.* Hussain *et al.* (2007) and consists of outer (on which response variable angles, say θ_1 are marked) and inner (for predicted response variable angles, say θ_2) rings, on which lines are used to conect the pair (θ_1, θ_2) at the same index. The short lines between θ_1 and θ_2 indicates good fit of the model. Thus, qualitative evidence seem to recomend our model to this database, according to the spokeplot

Table 4.1: ML estimates e (SEs) of the models parameters for the datasets.

Model	$\arg(\hat{\beta}_0)$	$\lvert\hat{\beta}_1\rvert$	$\arg(\hat{\beta}_1)$	$\hat{\kappa}$	$\hat{\rho}$	$\hat{\beta}$	$\hat{\mu}$	log$L$	AIC	BIC
vM	0.2797	0.3839	5.7852	1.7944	-	-	-	-97.5	203.1	212.2
	(0.1121)	(0.0792)	(0.1623)	(0.2985)						
wC	0.2158	0.2990	5.8135	-	0.6091	-	-	-97.7	203.5	212.6
	(0.1021)	(0.0770)	(0.1625)		(0.0482)					
vMM	0.8407	0.2035	5.6109	2.3531	0.6153	3.9666	0.8407	-93.5	194.9	204.1
	(0.1271)	(0.0486)	(0.1738)	(0.8494)	(0.1082)	(0.2549)	(0.1271)			
EC	6.1671	0.1703	3.8559	–	0.3225	0.5000	0.9800	-91.7	191.4	200.6
	(0.0000)	(0.0000)	(0.0000)	–	(0.0000)	(0.0000)	(0.0000)			

obtained using the mathematics dynamic software Geogebra (Hohenwarter, 2008).

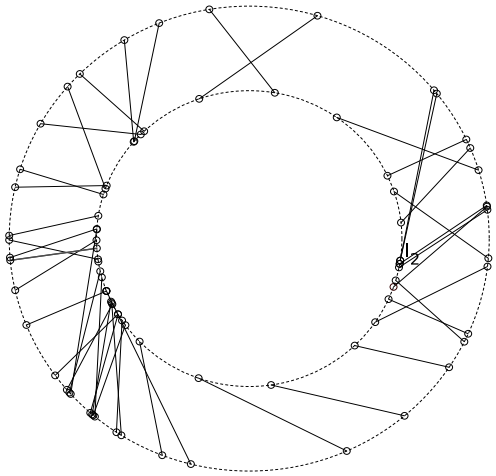

Figure 4.4: Spokeplot.

4.6 Concluding remarks

A circular-circular regression model has been proposed using the MT as link function and the exponentiated Cardioid distribution as model for its angular error. We have derived the complex distribution associated to the EC model and expressions for the score vector which yields support to the likelihood-based estimation procedure for regression parameters. Finally, an application to real wind data was made and results have indicated that the proposed model may outperform the other models that use the vM, wC, vMM distributions for the angular error.

5 Distribution Generators Applied to the Cardioid Model: Experiments on Circular Data

Resumo

A distribuição Cardioide (C) é um dos modelos mais importantes para dados circulares. Embora algumas propriedades de C tenham sido derivadas, esta distribuição não é apropriada para fenômenos assimétricos e multimodais no círculo e extensões são necessárias. Este capítulo propõe quatro extensões de C com base nos geradores β-G, Kw-G, Γ-G e MO-G. Nós derivamos Algumas propriedades matemáticas para esses novos modelos: extensões e momentos trigonométricos. Procedimentos de inferência para seus parâmetros também são fornecidos. Executamos duas aplicações para dados reais, em que os novos modelos são comparados com a distribuição C e uma de suas extensões propostas no Capítulo 2.

Palavras-chave: Cardioide extendida. Dados circulares. Função peso. Momentos trigonométricos.

Abstract

The Cardioid (C) distribution is one of the most important model for circle data. Although some C properties have been derived, this distribution is not appropriate for asymmetry and multimodal phenomena in the circle and extensions are required. This chapter proposes four C extensions based on the β-G, Kw-G, Γ-G and MO-G generators. We derive some mathematical properties for these new models: extensions and trigonometric moments. Inference procedures

for their parameters are provided as well. We perform two applications to real data, on which the new models are compared to the C distribution and one of its extensions proposed in the Chapter 2.

Keywords: Circular data. Extended Cardioid. Trigonometric moments. Weight function.

5.1 Introduction

Fitting densities to data has a long history. Traditionally families of curves have been developed to aid in fitting densities. Statistical distributions are very useful in describing and predicting real world phenomena. Numerous classical distributions have been extensively used over the past decades for modeling data in several disciplines, in particular, in reliability engineering, survival analysis, demography, actuarial study and others. Recent developments address definitions of new families that extend well-known distributions and, at the same time, provide great flexibility in modelling real data. Adding parameters to a well-established distribution is a time honored device for obtaining more flexible new families of distributions. In fact, several classes of distributions have been introduced by adding one or more parameters to generate new distributions in the statistical literature. The well-known generators are the Marshall-Olkin-G (MO-G) (Marshall and Olkin, 1997), beta-G (β-G) (Eugene *et al.*, 2002), gamma-G (Γ-G) (Zografos and Balakrishnan, 2009), Kumaraswamy-G (Kw-G) (Cordeiro and de Castro, 2011), exponentiated generalized (Cordeiro *et al.*, 2013), type I half-logistic-G (Cordeiro *et al.*, 2016), Burr X-G (Yousof *et al.*, 2016) and exponentiated Weibull-H (Cordeiro *et al.*, 2017), among others.

The two-parameter Cardioid (C) distribution was introduced by Jeffreys (1961) for describing directional spectra of ocean waves. This model has cumulative distribution function (cdf), $G(\theta) = G(\theta;\mu,\rho)$, and probability density function (pdf), $g(\theta) = g(\theta;\mu,\rho)$, given by, respectively, (for $0 \leq \theta \leq 2\pi$)

$$G(\theta) = \frac{\theta}{2\pi} + \frac{\rho}{\pi}\left[\sin(\theta-\mu) + \sin(\mu)\right] \tag{5.1}$$

and

$$g(\theta) = \frac{1}{2\pi}\left[1 + 2\rho\cos(\theta - \mu)\right], \tag{5.2}$$

where $0 < \mu \leq 2\pi$ is a location parameter and $|\rho| \leq 0.5$ represents concentration index.

Some works have addressed to extend the C distribution. A novel circular distribution was proposed by Wang and Shimizu (2012), who applied the Möbius transformation to the C model. The Papakonstantinou's family studied by Abe *et al.* (2009) also extends (5.1). However, these extensions present hard analytic formulas for their densities. The Chapter 2 have proposed a simple extended C distribution called exponentiated Cardioid (EC) distribution. The last was derived from the exp-G generator and can describe asymmetric and some bimodal cases, beyond those behaviors described by the C model.

In this chapter, we derive four extensions for the C model through the β-G, Kw-G, Γ-G and MO-G generators, which extend the exp-G. We propose four new circular distributions called beta Cardioid (βC), Kumaraswamy Cardioid (KwC), gamma Cardioid (ΓC) and Marshall-Olkin Cardioid (MOC). These distributions are rewritten like special cases into a new family, which is the result of weighting the term $[1 + 2\rho\cos(\theta - \mu)]$ in (5.2). Some of properties of new models are derived: extensions and trigonometric moments. A brief discussion about likelihood-based estimation procedures is provided. Finally, two applications to real data are performed to illustrate the flexibility of our proposals.

The remainder of this chapter is organized as follows. New models are proposed in Section 5.2. Section 5.3 discusses about some of their properties; while an estimation procedure is presented in Section 5.4. Applications are performed in Section 5.5. Main conclusions are listed in Section 5.6.

5.2 Generalized Cardioid Models

Next, we provide some three- and four-parameter distributions by transforming the C distribution, according to four generator. Let $G(\theta)$ be the cdf of a baseline distribution with p parameters,

a) the β-G cdf proposed by Eugene *et al.* (2002) is

$$F_{\beta-G}(\theta) \,=\, \mathbb{I}_{G(\theta)}(a,b)\,; = \,\frac{1}{B(a,b)}\int_0^{G(\theta)} \omega^{a-1}\,(1-\omega)^{b-1}\,\mathrm{d}\omega, \tag{5.3}$$

where $a, b > 0$ are two additional parameters, $\mathbb{I}_{G(\theta)}(a,b)$ is the incomplete beta function ratio evaluated at $G(\theta)$ and $B(a,b) = \int_0^{G(\theta)} \omega^{a-1}(1-\omega)^{b-1}\mathrm{d}\omega$ is the complete beta function;

b) the Kw-G cdf introduced by Cordeiro and de Castro (2011) is

$$F_{Kw-G}(\theta) = 1 - \{1 - G(\theta)^a\}^b\,; \tag{5.4}$$

c) the Γ-G cdf proposed by Zografos and Balakrishnan (2009) is

$$F_{\Gamma-G}(\theta) = \frac{\gamma\left(a, -\log\left[1-G(\theta)\right]\right)}{\Gamma(a)} = \frac{1}{\Gamma(a)}\int_0^{-\log[1-G(\theta)]} t^{a-1}\exp(-t)\mathrm{d}t, \tag{5.5}$$

where $a > 0$, $\Gamma(a) = \int_0^{\infty}\, t^{a-1}\,\mathrm{e}^{-t}\,\mathrm{d}t$ denotes the gamma function, and $\gamma(a,z) = \int_0^z t^{a-1}\,\mathrm{e}^{-t}\,\mathrm{d}t$ denotes the incomplete gamma function;

d) the MO-G cdf proposed by Marshall and Olkin Marshall and Olkin (1997) is

$$F_{MO-G}(\theta) = 1 - \frac{a[1-G(\theta)]}{1-(1-a)[1-G(\theta)]} = \frac{a[1-G(\theta)]}{G(\theta)+a[1-G(\theta)]}, \tag{5.6}$$

For the two first generators, given one baseline cdf as input, one has new $(p+2)$-parameter models; whereas for remainder generators, $(p+1)$-parameter distributions are furnished.

5.2.1 *Beta Cardioid*

From applying (5.1) in (5.3), the βC distribution is introduced having cdf, $F_1(\theta) := F_1(\theta; a, b, \mu, \rho)$, given by

$$F_1(\theta) \,=\, \mathbb{I}_{\frac{\theta}{2\pi}+\frac{\rho}{\pi}[\sin(\theta-\mu)+\sin(\mu)]}(a,b).$$

This case is denoted by $\Theta \sim \beta C(a,b,\mu,\rho)$. By differentiating the last equation, the βC pdf, $f_1(\theta) := f_1(\theta; a, b, \mu, \rho)$, is given by

$$f_1(\theta) \,=\, \underbrace{\frac{h_1(\theta)}{2\pi\, B(a,b)}}_{:=\dot{h}_1(\theta)}\,[1+2\rho\cos(\theta-\mu)] \tag{5.7}$$

where

$$h_1(\theta) := h_1(\theta; a, b, \mu, \rho) = \frac{\left\{\frac{\theta}{2\pi} + \frac{\rho}{\pi}\left[\sin(\theta-\mu)+\sin(\mu)\right]\right\}^{a-1}}{\left\{1 - \frac{\theta}{2\pi} - \frac{\rho}{\pi}\left[\sin(\theta-\mu)+\sin(\mu)\right]\right\}^{1-b}}.$$

Note that for $b = 1$ the βC model collapses in the EC distribution proposed in the Chapter 2.

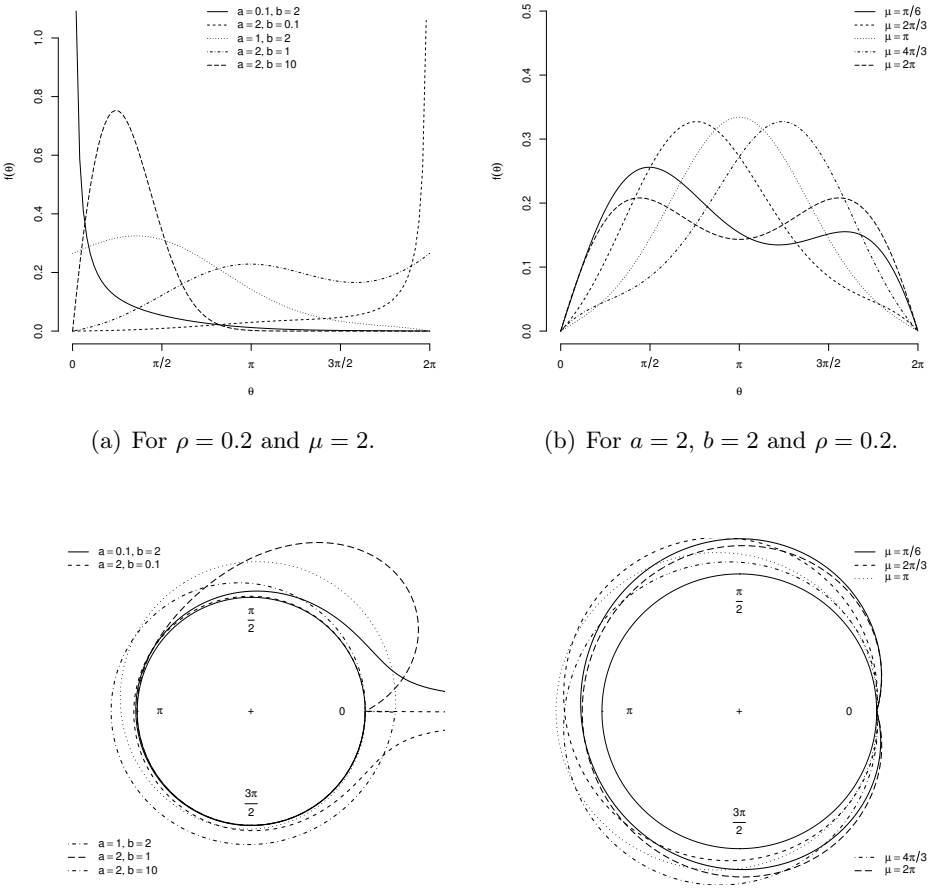

(a) For $\rho = 0.2$ and $\mu = 2$.

(b) For $a = 2$, $b = 2$ and $\rho = 0.2$.

(c) For $\rho = 0.2$ and $\mu = 2$.

(d) For $a = 2$, $b = 2$ and $\rho = 0.2$.

Figure 5.1: Theoretical and empirical βC densities for some parametric points.

5.2.2 *Kumaraswamy Cardioid*

From introducing (5.1) in (5.4), the KwC distribution is obtained having cdf, $F_2(\theta) := F_2(\theta; a, b, \mu, \rho)$, given by

$$F_2(\theta) \,=\, 1 \,-\, \left\{1 \,-\, \left(\frac{\theta}{2\pi} + \frac{\rho}{\pi}\left[\sin(\theta-\mu) + \sin(\mu)\right]\right)^{a}\right\}^{b}.$$

This case is denoted as $\Theta \sim KwC(a, b, \mu, \rho)$. Therefore, the KwC pdf is given by

$$f_2(\theta) \,=\, \underbrace{\frac{a\, b\, h_2(\theta)}{2\,\pi}}_{:=\dot{h}_2(\theta)}\left[1 + 2\rho\cos(\theta-\mu)\right], \tag{5.8}$$

where

$$h_2(\theta) \,:=\, h_2(\theta; a, b, \mu, \rho) \,=\, \frac{\left\{\frac{\theta}{2\pi} + \frac{\rho}{\pi}\left[\sin(\theta-\mu) + \sin(\mu)\right]\right\}^{a-1}}{\left\{1 \,-\, \left(\frac{\theta}{2\pi} + \frac{\rho}{\pi}\left[\sin(\theta-\mu) + \sin(\mu)\right]\right)^{a}\right\}^{1-b}}.$$

5.2.3 *Gamma Cardioid*

From evaluating (5.1) in (5.5), the ΓC distribution is obtained having cdf, $F_3(\theta) := F_3(\theta; a, \mu, \rho)$, given by

$$F_3(\theta) \,=\, \frac{\gamma\left(a, -\log\left\{1 \,-\, \frac{\theta}{2\pi} \,-\, \frac{\rho}{\pi}\left[\sin(\theta-\mu) + \sin(\mu)\right]\right\}\right)}{\Gamma(a)};$$

This case is denoted by $\Theta \sim \Gamma C(a, \mu, \rho)$. By differentiating the last equation, the ΓC density, $f_3(\theta) := f_3(\theta; a, \mu, \rho)$, becomes

$$f_3(\theta) \,=\, \underbrace{\frac{h_3(\theta)}{2\pi\,\Gamma(a)}}_{:=\dot{h}_3(\theta)}\left[1 + 2\rho\cos(\theta-\mu)\right], \tag{5.9}$$

where

$$h_3(\theta) \,:=\, h_3(\theta; a, \mu, \rho) \,=\, \left(-\log\left\{1 \,-\, \frac{\theta}{2\pi} \,-\, \frac{\rho}{\pi}\left[\sin(\theta-\mu) + \sin(\mu)\right]\right\}\right)^{a-1}.$$

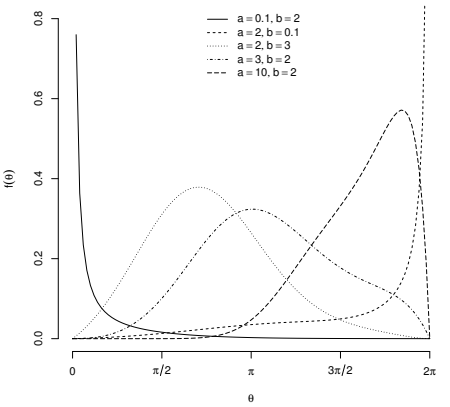

(a) For $\rho = 0.2$ and $\mu = 2$.

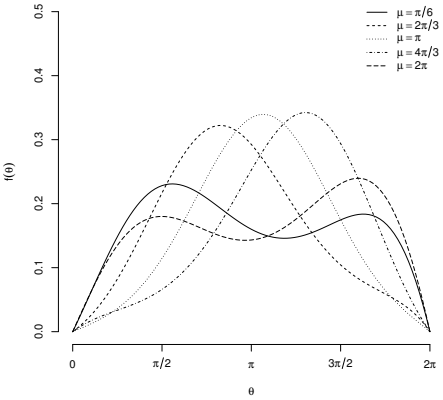

(b) For $a = 2$, $b = 2$ and $\rho = 0.2$.

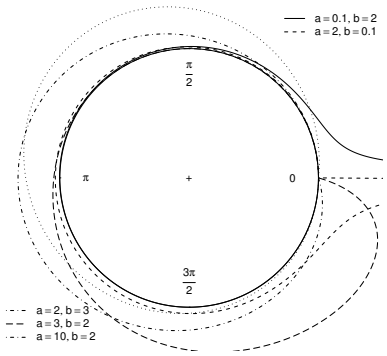

(c) For $\rho = 0.2$ and $\mu = 2$.

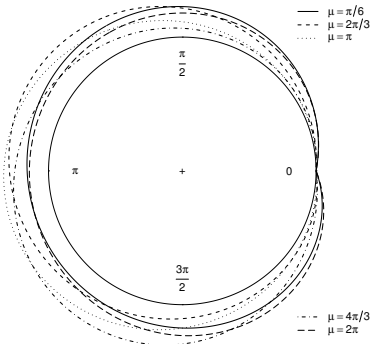

(d) For $a = 2$, $b = 2$ and $\rho = 0.2$.

Figure 5.2: Theoretical and empirical KwC densities for some parametric points.

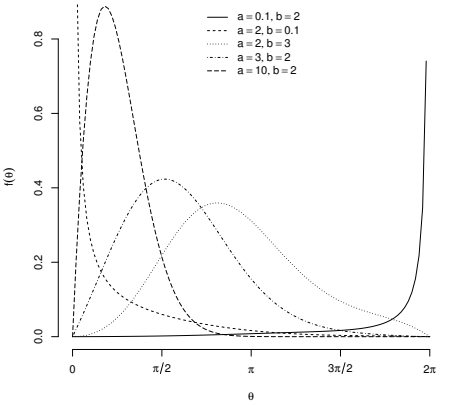

(a) For $\rho = 0.2$ and $\mu = 2$.

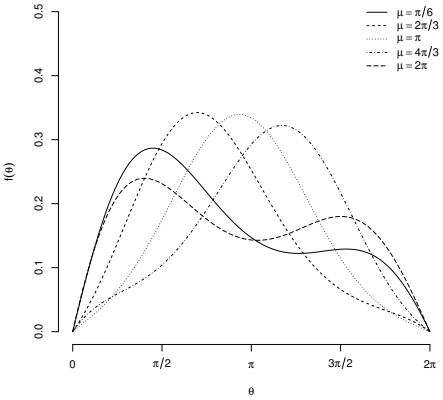

(b) For $a = 2$, $b = 2$ and $\rho = 0.2$.

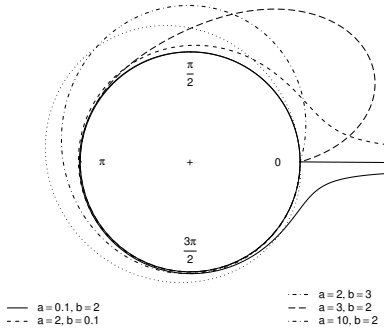

(c) For $\rho = 0.2$ and $\mu = 2$.

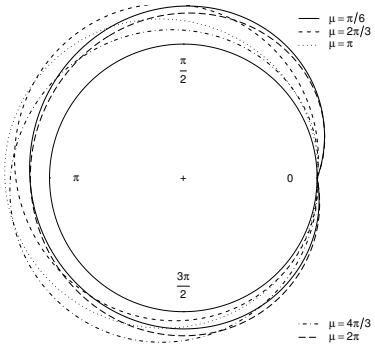

(d) For $a = 2$, $b = 2$ and $\rho = 0.2$.

Figure 5.3: Theoretical and empirical ΓC densities for some parametric points.

5.2.4 *Marshall-Olkin Cardioid*

From evaluating (5.1) in (5.6), we propose the MOC distribution having cdf, $F_4(\theta) := F_4(\theta; a, \mu, \rho)$, given by

$$F_4(\theta) = \frac{a\left\{1 - \frac{\theta}{2\pi} - \frac{\rho}{\pi}\left[\sin(\theta-\mu)+\sin(\mu)\right]\right\}}{\frac{\theta}{2\pi} + \frac{\rho}{\pi}\left[\sin(\theta-\mu)+\sin(\mu)\right] + a\left\{1 - \frac{\theta}{2\pi} - \frac{\rho}{\pi}\left[\sin(\theta-\mu)+\sin(\mu)\right]\right\}}.$$

This case is denoted by $\Theta \sim MOC(a, \mu\rho)$. Thus, the MOC density, $f_4(\theta) := f_4(\theta; a, \mu, \rho)$, becomes

$$f_4(\theta) = \underbrace{\frac{a\, h_4(\theta)}{2\pi}}_{:=\dot{h}_4(\theta)} \left[1 + 2\rho\cos(\theta-\mu)\right], \tag{5.10}$$

where

$$h_4(\theta) := h_4(\theta; a, \mu, \rho) = \left(1 - (1-a)\left\{1 - \frac{\theta}{2\pi} - \frac{\rho}{\pi}\left[\sin(\theta-\mu)+\sin(\mu)\right]\right\}\right)^{-2}.$$

5.2.5 *A general formula*

All four extensions have the same support of the C law and their densities may be rewritten in the general expression:

$$f_i(\theta) = \dot{h}_i(\theta)\left[1 + 2\rho\cos(\theta-\mu)\right], \quad \text{for} \quad i = 1, 2, 3, 4, \tag{5.11}$$

where $\dot{h}_i(\theta)$ is defined in the bellow table.

Models	C	βC	KwC	ΓC	MOC
Index (i)	•	1	2	3	4
Expressions	$(2\pi)^{-1}$	$\dot{h}_1(\theta)$	$\dot{h}_2(\theta)$	$\dot{h}_3(\theta)$	$\dot{h}_4(\theta)$

The new models may be understood as results of putting weights over the $[1 + 2\rho\cos(\theta-\mu)]$ term. Thus, illustrating $\dot{h}_i$ in (5.11) is a good activity to study the flexibility of the new models. Figure 5.5 illustrates the weight functions $\dot{h}_i(\theta)$. For this case, we fix $(\mu, \rho) = (2, 0.2)$ and assume $a = b \in (0, 100)$ for βC and KwC distributions, $a \in (0, 100)$ and $\theta \in [0, 2\pi]$. Note that although $\dot{h}_3$ and $\dot{h}_4$ have larger values, $\dot{h}_1$ and $\dot{h}_2$ present a larger domain region that result in considerable values. This fact can make ΓC and MOC more flexible.

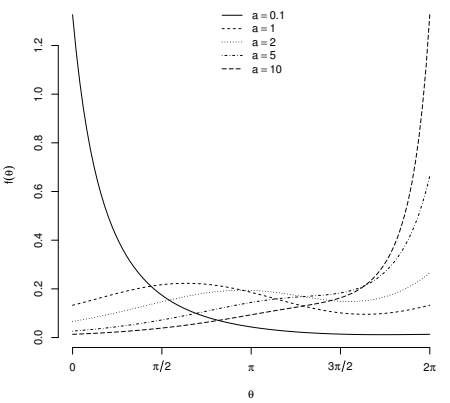

(a) For $\rho = 0.2$ and $\mu = 2$.

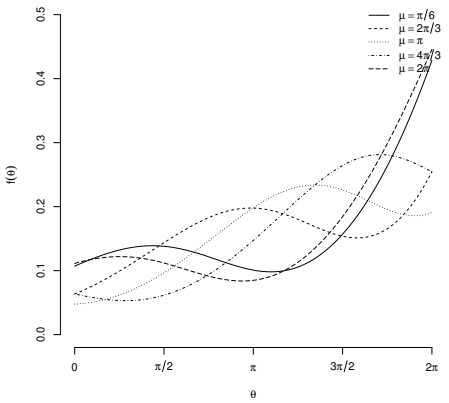

(b) For $a = 2$, $b = 2$ and $\rho = 0.2$.

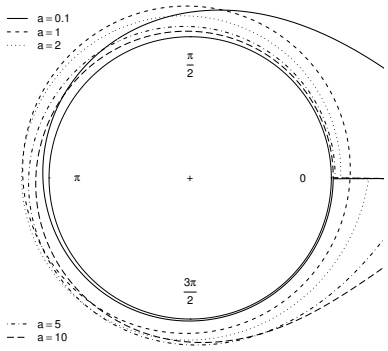

(c) For $\rho = 0.2$ and $\mu = 2$.

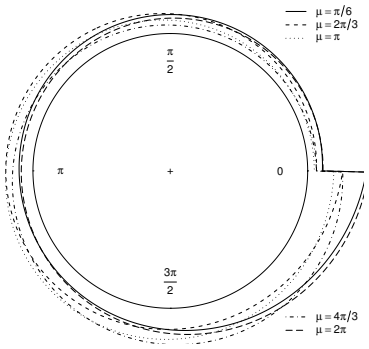

(d) For $a = 2$, $b = 2$ and $\rho = 0.2$.

Figure 5.4: Theoretical and empirical MOC densities for some parametric points.

It is important to note that the obtained models provide different asymmetry and modality scenarios, according to the Figures 5.1, 5.2, 5.3 and 5.4. Therefore, the proposed distributions can be attractive in the circular data modeling which, in many cases, are asymmetrically distributed with possible multimodality.

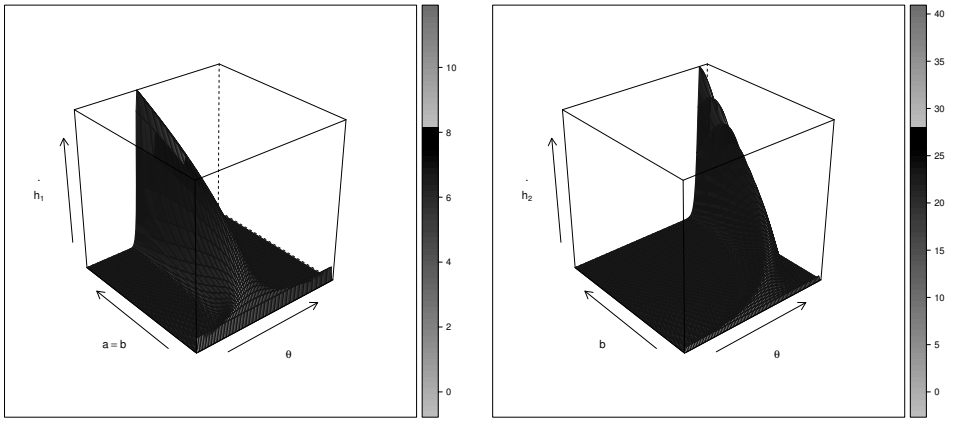

(a) Curve $\dot{h}_1$ (b) Curve $\dot{h}_2$

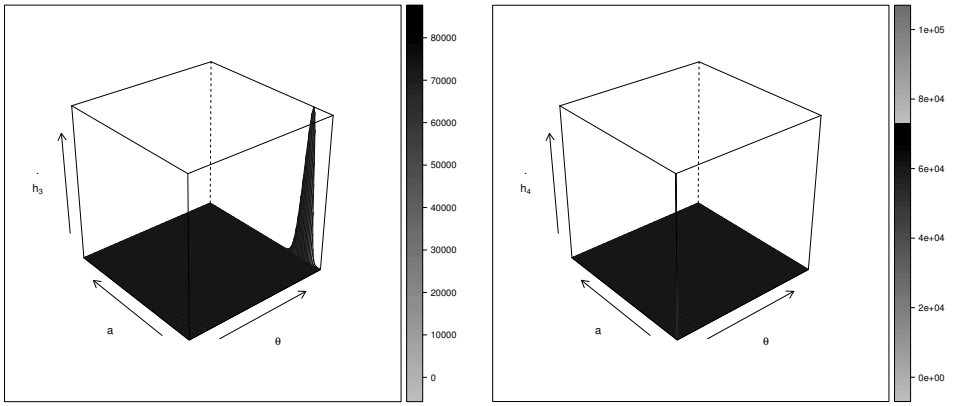

(c) Curve $\dot{h}_3$ (d) Curve $\dot{h}_4$

Figure 5.5: Weight curves for new models in family $f_i(\theta)$.

5.3 Mathematical properties

This section addresses the derivation of the trigonometric moments for new models. To that end, we derive expansions for $f_i(\theta)$ by means of the following results:

(Cordeiro and de Castro (2011)):

$$f_{\beta-G}(x) \;=\; [abB(a,b)]^{-1} g(x) \sum_{i=0}^{\infty} \underbrace{(-1)^i \, ab \binom{b-1}{i}}_{w_i} \, G(x)^{a+i-1}.\text{and}$$

and

$$f_{Kw-G}(x) \;=\; g(x) \sum_{i=0}^{\infty} \underbrace{(-1)^i ab \binom{b-1}{i}}_{w_i} \, G(x)^{a(i+1)-1}.$$

(Nadarajah *et al.* (2015)):

$$f_{\Gamma-G}(x) \;=\; \sum_{i=0}^{\infty} \underbrace{\frac{\binom{i+1-a}{k}}{(a+i)\Gamma(a-1)} \sum_{j=0}^{i} \frac{(-1)^{j+i}\binom{i}{j} p_{j,i}}{a-1-j}}_{b_i} \; h_{a+i}(x),$$

where $p_{j,i} = i^{-1} \sum_{m=1}^{i} [i - m(j+1)] c_m p_{j,i-m}$ and $c_i = (-1)^{i+1}(i+1)^{-1}$ for $k = 1, 2, \cdots$, $p_{j,0} = 1$, $h_{a+i}(x)$ denotes the pdf of the exp-G(a+i) distribution.

(Cordeiro *et al.* (2014)):

$$f_{MO-G}(x) \;=\; g(x) \sum_{i=0}^{\infty} \underbrace{a(-1)^i \sum_{k=0}^{j} \binom{j}{i} (j+1)(1-a)^j}_{d_i} \; G(x)^k.$$

.

(Consequence of the Theorem 2.3.1):

Let $\Theta \sim EC(\beta, \mu, \rho)$. The cdf of Θ, say $F(\theta) = F(\theta; \beta, \mu, \rho)$,

$$F(\theta) = \sum_{k=0}^{\infty} \sum_{s=0}^{k} v_{k,s}(\beta) \, \theta^{\beta-k} \, \Pi_{k,s}(\theta; \rho, \mu), \tag{5.12}$$

where $v_{k,s}(\beta) = \binom{\beta}{k}\binom{k}{s} (2\,\pi)^{k-\beta}$ and

$$\Pi_{k,s}(\theta; \rho, \mu) = \left(\frac{\rho}{\pi}\right)^k [\sin(\mu)]^s \, [\sin(\theta - \mu)]^s \left\{ [\sin(\theta - \mu)]^{k-2s} M_0 + [\sin(\mu)]^{k-2s} M_1 \right\}$$

depends only on the parameters of the Cardioid distribution. M_0 and M_1 are defined as in the Theorem 2.3.1.

5.3.1 *Beta Cardioid*

Theorem 5.3.1. *Let $a, b, \beta > 0$, $0 < \mu \leq 2\pi$ and $0 \leq \rho \leq 0.5$. The pdf of the βC model is given by*

$$f(\theta) = \frac{1}{2\pi abB(a,b)}[1 + 2\rho\cos(\theta - \mu)]\sum_{i=0}^{\infty}\sum_{k=0}^{a+i-1}\sum_{s=0}^{k} w_i v_{k,s}[a+i-1]\theta^{a+i-1-k}\Pi_{k,s}(\theta;\rho,\mu),$$

where

$$w_i = w_i(a,b) = (-1)^i ab\binom{b-1}{i}$$

and $\sum_{i=0}^{\infty} = 1$.

Corollary 5.3.2. *Let $\Theta \sim \beta C(\beta, \rho, \mu)$. The components of the first central trigonometric moment are given by*

$$\begin{aligned}\alpha_1 =& \frac{(2\rho)^{-1+z}}{2\pi abB(a,b)}\sum_{i=0}^{\infty}\sum_{k=0}^{a+i-1}\sum_{s=0}^{k} w_i t_{k,s}[a+i-1,\rho,\mu]\times \\ & \Big\{A[a+i-1-k,z,k-s]M_0 + [\sin(\mu)]^{k-2s}A[a+i-1-k,z,s]M_1\Big\}\end{aligned}$$

and

$$\begin{aligned}\beta_1 =& \frac{(2\rho)^{-1+z}}{2\pi abB(a,b)}\sum_{i=0}^{\infty}\sum_{k=0}^{a+i-1}\sum_{s=0}^{k} w_i t_{k,s}[a+i-1,\rho,\mu]\times \\ & \Big\{A[a+i-1-k,z-1,k-s+1]M_0 + [\sin(\mu)]^{k-2s}A[a+i-1-k,z-1,s+1]M_1\Big\}\end{aligned}$$

where $t_{k,s}$ is defined as in the Theorem 2.3.1, $z \in \{1, 2\}$ and

$$A(a,b,c) = \int_0^{2\pi} \theta^a[\cos(\theta-\mu)]^b[\sin(\theta-\mu)]^c d\theta.$$

.

5.3.2 *Kumaraswamy Cardioid*

Theorem 5.3.3. *Let $a, b, \beta > 0$, $0 < \mu \leq 2\pi$ and $0 \leq \rho \leq 0.5$. The pdf of the KwC model is given by*

$$f(\theta) = \frac{1}{2\pi}[1 + 2\rho\cos(\theta - \mu)]\sum_{i=1}^{\infty}\sum_{k=0}^{a(i+1)-1}\sum_{s=0}^{k} w_i v_{k,s}[a(i+1)-1]\theta^{a(i+1)-1-k}\Pi_{k,s}(\theta;\rho,\mu),$$

Corollary 5.3.4. *Let $\Theta \sim KwC(\beta, \rho, \mu)$. The components of the first central trigonometric moment are given by*

$$\alpha_1 = \frac{(2\rho)^{-1+z}}{2\pi} \sum_{i=0}^{\infty} \sum_{k=0}^{a(i+1)-1} \sum_{s=0}^{k} w_i t_{k,s}[a(i+1)-1, \rho, \mu] \times \left\{ A[a(i+1)-1-k, z, k-s] M_0 + [\sin(\mu)]^{k-2s} A[a(i+1)-1-k, z, s] M_1 \right\}$$

and

$$\beta_1 = \frac{(2\rho)^{-1+z}}{2\pi} \sum_{i=0}^{\infty} \sum_{k=0}^{a(i+1)-1} \sum_{s=0}^{k} w_i t_{k,s}[a(i+1)-1, \rho, \mu] \times \left\{ A[a(i+1)-1-k, z-1, k-s+1] M_0 + [\sin(\mu)]^{k-2s} A[a(i+1)-1-k, z-1, s+1] M_1 \right\},$$

where $z = 1, 2$.

5.3.3 *Gamma Cardioid*

Theorem 5.3.5. *Let $a, \beta > 0$, $0 < \mu \leq 2\pi$ and $0 \leq \rho \leq 0.5$. The pdf of the ΓC model is given by*

$$f(\theta) = \frac{1}{2\pi}[1 + 2\rho\cos(\theta - \mu)] \sum_{i=0}^{\infty} \sum_{k=0}^{a+i-1} \sum_{s=0}^{k} b_i v_{k,s}(a+i-1) \theta^{a+i-1-k} \Pi_{k,s}(\theta; \rho, \mu),$$

where

$$b_i = b_i(a) = \frac{\binom{i+1-a}{i}}{\Gamma(a-1)} \sum_{j=0}^{i} \frac{(-1)^{j+i}\binom{i}{j} p_{j,i}}{a-1-j}$$

and

$$p_{j,i} = i^{-1} \sum_{m=1}^{i} [i - m(j+1)] c_m p_{j,i-m}$$

for $i = 1, 2, \ldots$, $p_{j,0} = 1$ and $c_m = (-1)^{m+1}(m+1)^{-1}$.

Corollary 5.3.6. *Let $\Theta \sim \Gamma C(\beta, \rho, \mu)$. The components of the first central trigonometric moment are given by*

$$\alpha_1 = \frac{(2\rho)^{-1+z}}{2\pi} \sum_{i=0}^{\infty} \sum_{k=0}^{a+i-1} \sum_{s=0}^{k} b_i t_{k,s}[a+i-1, \rho, \mu] \times \left\{ A[a+i-1-k, z, k-s] M_0 + [\sin(\mu)]^{k-2s} A[a+i-1-k, z, s] M_1 \right\}$$

and

$$\beta_1 = \frac{(2\rho)^{-1+z}}{2\pi} \sum_{i=0}^{\infty} \sum_{k=0}^{a+i-1} \sum_{s=0}^{k} b_i t_{k,s}[a+i-1, \rho, \mu] \times \\ \Big\{ A[a+i-1-k, z-1, k-s+1] M_0 + [\sin(\mu)]^{k-2s} A[a+i-1-k, z-1, s+1] M_1 \Big\}$$

where $z = 1, 2$.

5.3.4 *Marshall-Olkin Cardioid*

Theorem 5.3.7. *Let* $a, \beta > 0$, $0 < \mu \leq 2\pi$ *and* $0 \leq \rho \leq 0.5$. *The pdf of the MOC model is given by*

$$f(\theta) = \frac{1}{2\pi}[1 + 2\rho\cos(\theta - \mu)] \sum_{i=0}^{\infty} \sum_{k=0}^{i} \sum_{s=0}^{k} d_i v_{k,s}(i) \theta^{i-k} \Pi_{k,s}(\theta; \rho, \mu),$$

where

$$d_i = d_i(a) = a(-1)^i \sum_{j=k}^{\infty} \binom{j}{i} (j+1)(1-a)^j.$$

Corollary 5.3.8. *Let* $\Theta \sim MOC(\beta, \rho, \mu)$. *The components of the first central trigonometric moment are given by*

$$\alpha_1 = \frac{(2\rho)^{-1+z}}{2\pi} \sum_{i=0}^{\infty} \sum_{k=0}^{i} \sum_{s=0}^{k} d_i t_{k,s}[i, \rho, \mu] \times \\ \Big\{ A[i-k, z, k-s] M_0 + [\sin(\mu)]^{k-2s} A[i-k, z, s] M_1 \Big\}$$

and

$$\beta_1 = \frac{(2\rho)^{-1+z}}{2\pi} \sum_{i=0}^{\infty} \sum_{k=0}^{i} \sum_{s=0}^{k} d_i t_{k,s}[i, \rho, \mu] \times \\ \Big\{ A[i-k, z-1, k-s+1] M_0 + [\sin(\mu)]^{k-2s} A[i, z-1, s+1] M_1 \Big\}$$

where $z = 1, 2$.

5.3.5 *General Forms*

The expansions found for the density function and moments of the proposed distributions can be written, in general, as

Theorem 5.3.9. *The pdf is given by*

$$f(\theta) = \frac{F}{2\pi}[1 + 2\rho\cos(\theta - \mu)] \sum_{i=0}^{\infty} \sum_{k=0}^{c_i} \sum_{s=0}^{k} D_i v_{k,s}(c_i) \theta^{c_i - k} \Pi_{k,s}(\theta; \rho, \mu).$$

Corollary 5.3.10. *The components of the first central trigonometric moment are given by*

$$\begin{aligned}\alpha_1 =& \frac{F(2\rho)^{-1+z}}{2\pi} \sum_{i=0}^{\infty} \sum_{k=0}^{c_i} \sum_{s=0}^{k} D_i t_{k,s}[c_i, \rho, \mu] \times \\ & \left\{ A[c_i - k, z, k - s] M_0 + [\sin(\mu)]^{k-2s} A[c_i - k, z, s] M_1 \right\}\end{aligned}$$

and

$$\begin{aligned}\beta_1 =& \frac{F(2\rho)^{-1+z}}{2\pi} \sum_{i=0}^{\infty} \sum_{k=0}^{c_i} \sum_{s=0}^{k} D_i t_{k,s}[c_i, \rho, \mu] \times \\ & \left\{ A[c_i - k, z - 1, k - s + 1] M_0 + [\sin(\mu)]^{k-2s} A[c_i, z - 1, s + 1] M_1 \right\},\end{aligned}$$

where $z = 1, 2$.

The quantities F, c_i and D_i are expressed in the Table 5.1, for each proposed distribution.

Table 5.1: The quantities F, c_i and D_i for each distribution.

Model	F	c_i	D_i
βC	$[abB(a,b)]^{-1}$	$a + i - 1$	w_i
KwC	1	$a(i+1) - 1$	w_i
ΓC	1	$a + i - 1$	b_i
MOC	1	i	d_i

5.4 Estimation

This section tackles a brief discussion about maximum likelihood estimation for parameters of the proposed family with density (5.11). Let $\theta_1, \ldots, \theta_n$ be an observed sample, outcomes obtained from a random variable having density (5.11). Thus, the associated log-likelihood function at

$\boldsymbol{\delta} = (a, b, \mu, \rho)^\top$ (omit b for three-parameter distributions) is given by (for $i = 1, 2, 3, 4$)

$$\ell_i(\boldsymbol{\delta}) \,=\, \sum_{j=1}^{n} \log f_i(\theta_j) \,=\, \sum_{j=1}^{n} \{\, \log \dot{h}_i(\theta_j) \,+\, \log[1 \,+\, 2\,\rho\, \cos(\theta_j \,-\, \mu)]\,\}.$$

The associated score vector for $\ell_i(\theta)$,

$$(U_{a,i},\, U_{b,i},\, U_{\mu,i},\, U_{\rho,i}) := \left(\frac{\mathrm{d}\,\ell_i(\boldsymbol{\delta})}{\mathrm{d}a}, \frac{\mathrm{d}\,\ell_i(\boldsymbol{\delta})}{\mathrm{d}b}, \frac{\mathrm{d}\,\ell_i(\boldsymbol{\delta})}{\mathrm{d}\mu}, \frac{\mathrm{d}\,\ell_i(\boldsymbol{\delta})}{\mathrm{d}\rho}\right),$$

is determined by

$$U_{a,i} \,=\, \sum_{j=1}^{n} \frac{\frac{\mathrm{d}\,\dot{h}_i(\theta_j)}{\mathrm{d}a}}{\dot{h}_i(\theta_j)}, \quad U_{b,i} \,=\, \sum_{j=1}^{n} \frac{\frac{\mathrm{d}\,\dot{h}_i(\theta_j)}{\mathrm{d}b}}{\dot{h}_i(\theta_j)},$$

$$U_{\mu,i} \,=\, \sum_{j=1}^{n} \left\{ \frac{\frac{\mathrm{d}\,\dot{h}_i(\theta_j)}{\mathrm{d}\mu}}{\dot{h}_i(\theta_j)} \,+\, \frac{2\,\rho\, \sin(\theta_j - \mu)}{1 \,+\, 2\,\rho\, \cos(\theta_j - \mu)} \right\}$$

and

$$U_{\rho,i} \,=\, \sum_{j=1}^{n} \left\{ \frac{\frac{\mathrm{d}\,\dot{h}_i(\theta_j)}{\mathrm{d}\rho}}{\dot{h}_i(\theta_j)} \,+\, \frac{2\, \cos(\theta_j - \mu)}{1 \,+\, 2\,\rho\, \cos(\theta_j - \mu)} \right\}.$$

Thus, the ML estimate for $\boldsymbol{\delta}$ is defined by $\widehat{\boldsymbol{\delta}} \,=\, \mathrm{argmax}_{\boldsymbol{\delta}\in\boldsymbol{\Delta}}\, \{\ell_i(\boldsymbol{\delta})\}$ for $\boldsymbol{\Delta}$ being the parametric space or, equivalently, as solutions of the system $U_{a,i} = U_{b,i}, = U_{\mu,i} = U_{\rho,i} = 0$.

5.5 Applications

In this section, we present two applications to illustrate and compare the flexibility of the generalized distributions of the Cardioid distribution.

The first dataset consists of 21 wind directions obtained by a Milwaukee weather station, at 6.00 am on consecutive days (Johnson and Wehrly, 1977). The second one corresponds to the directions taken by 76 turtles after treatment. This dataset was studied by Stephens (1969). The datasets present positive (0.4313) and negative (-0.0816) skewness, respectively. Besides comparing the models, the idea here is to verify the effect of the datasets skewness signal in the adjustment of the models.

First, the ML estimates and their SEs (given in parentheses) are evaluated and, subsequently, the values of the Kuiper (K) and Watson (W) statistics are obtained. These aderence measures may be found in Jammalamadaka and Sengupta (2002). ML estimates were used to fit considered

models to data. All the computations were done using function `maxLik` at the R statistical software (R Core Team, 2017). The obtained results for dataset 1 and 2, are given in Tables 5.2 and 5.3, respectively.

Table 5.2: ML estimates of the model parameters for the data, the corresponding standard errors (given in parentheses) and the Kuiper and Watson statistics.

Model	ρ	μ	a	b	Kuiper	Watson
C	0.2436	4.6708	–	–	1.1590	0.0711
	(0.1463)	(0.6835)	–	–		
EC	0.2164	1.1780	2.8755	–	0.7367	0.0257
	(0.1465)	(0.6168)	(0.8929)	–		
βC	0.2774	0.9093	3.9353	1.4044	0.8060	0.0247
	(0.0980)	(0.5030)	(2.6919)	(0.6641)		
Kw-C	0.2767	0.9381	3.6511	1.4144	0.8038	0.0240
	(0.0989)	(0.4933)	(2.1205)	(1.1213)		
ΓC	0.1364	1.7274	1.8563	–	0.8289	0.0328
	(0.1349)	(0.6820)	(0.2566)	–		
MOC	0.2007	2.0632	4.5765	–	0.8134	0.0327
	(0.1277)	(0.7659)	(1.8103)	–		

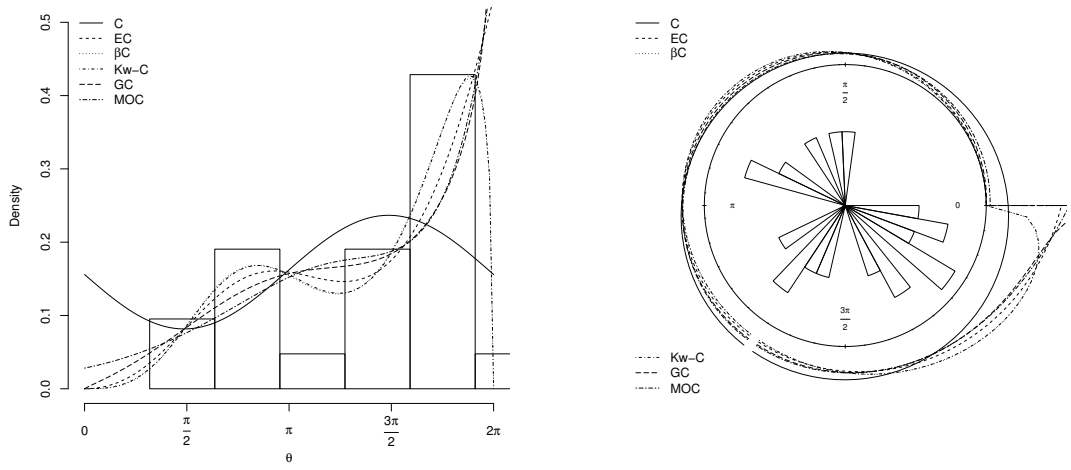

Figure 5.6: Fitted densities of the C, EC, βC, Kw-C, Γ-C and MOC models for the real data.

We emphasize that all generalized models fits the data better than the Cardioid model. For first dataset, the EC and KwC distributions stand out and the βC model fits the second dataset

better according to Kuiper and Watson.

Figures 5.6 and 5.7 presents empirical and fitted densities to data. The plots confirm what is concluded from Tables.

Table 5.3: ML estimates of the model parameters for the data, the corresponding standard errors (given in parentheses) and the Kuiper and Watson statistics.

Model	ρ	μ	a	b	Kuiper	Watson
C	0.3259	1.2022	–	–	2.4852	0.4855
	(0.0553)	(0.3337)	–	–		
EC	0.3067	1.6025	0.7688	–	2.3610	0.4443
	(0.1256)	(0.0829)	(0.5656)	–		
βC	0.3978	0.1441	1.8836	3.1088	1.2683	0.0917
	(0.0538)	(0.1892)	(0.4959)	(1.0142)		
Kw-C	0.3985	0.1712	1.6295	3.2205	1.3204	0.1007
	(0.0543)	(0.2713)	(0.3180)	(1.8769)		
ΓC	0.2829	1.5308	0.7788	–	2.3005	0.4006
	(0.0776)	(0.4744)	(0.0760)	–		
MOC	0.2160	1.9026	0.3880	–	1.9593	0.2614
	(0.1088)	(0.7594)	(1.1475)	–		

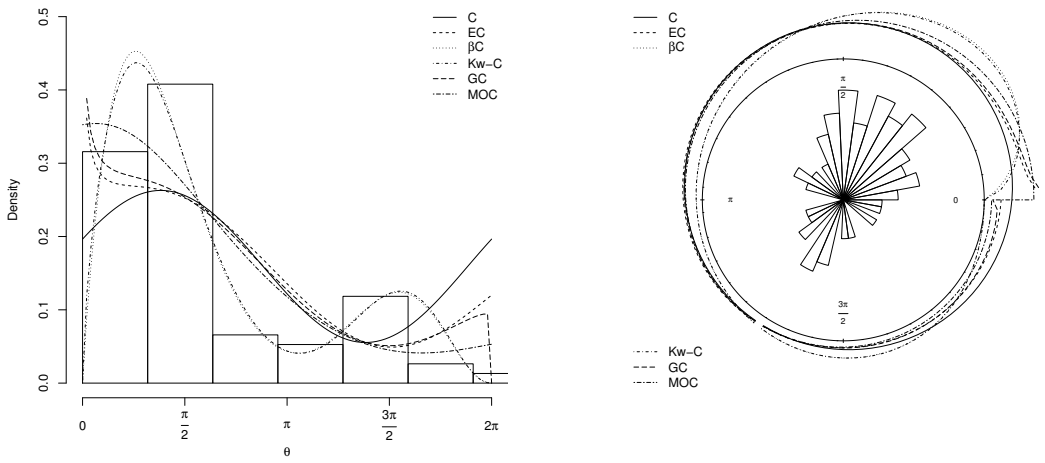

Figure 5.7: Fitted densities of the C, EC, βC, Kw-C, Γ-C and MOC models for the real data.

5.6 Conclusions

In this chapter, we propose four new distributions having support on the circle. These extensions to the Cardioid (C) distribution are obtained by applying it to the β-G, Kw-G, Γ-G and MO-G generators. Some properties for new models are proposed: expansions and trigonometric moments; which are reduced to the weighting of the $[1 + 2\rho\cos(\theta - \mu)]$ Cardioid pdf term. Further we also discuss the maximum likelihood estimation for their parameters. Two applications illustrate the flexibility of our proposals on real data. The βC and EC distributions stand out for the dataset with positive asymmetry and for the dataset with negative asymmetry, the KwC model is the best. The best performance of EC distribution when compared to the proposed models in this chapter, for the first considered dataset in the application, highlights the relevance of the proposed and studied model in this thesis.

6 Concluding remarks and future works

In this work, some advances in the field of circular statistics have been presented. Finding circular models that contemplate scenarios of asymmetry or multimodality and mathematically treatable properties is a challenge, as mentioned. In this sense, the method used to extend the Cardioid distribution, until then not used to the best of our knowledge in this field, proved to be efficient in the generation of a new model, the Exponentiated Cardioid. In Chapter 2, readers can see that the trigonometric moments of the EC distribution are well defined by special functions. In addition, the new model presents a lot of flexibility compared to the classical circular models, being more suitable for the data set considered.

In Chapter 3, the focus was on the inference on the parameters of the EC distribution in the sense of discriminating the new distribution of the distributions that are their particular cases, the Cardioid and uniform distributions. These hypothesis tests had not been used in the context of circular statistics and in the context of discrimination of circular distributions, as far as we know. The gradient or Wald tests presented better results. In addition, an advance in the field of circular distributions can be noticed, in the study of bootstrap versions of these tests, which also performed well. It is interesting to note also that the Fisher information matrix of the new model is presented by means of special functions and that they are well defined, as shown.

Chapter 4 introduces the EC model as distribution for the angular errors of the proposed circular-circular regression model using Möbius transformation. The proposed model proved to be more powerful than the other three models in the literature through its adjustments to wind direction real data. Another important contribution is the introduction of the complex version

of the EC distribution, named CEC distribution.

Four new circular distributions that extend the C distribution are introduced in Chapter 5, called beta Cardioid (βC), Kumaraswamy Cardioid (KwC), gamma Cardioid (ΓC) and Marshall-Olkin Cardioid (MOC). These distributions are rewritten as a family, which is a result of weighting the C pdf. General mathematical expressions for their trigonometric moments and the idea for estimating the parameters of the proposed models by the maximum likelihood method are presented. The usefulness of the new distributions is illustrated using two applications to real data. In the applications, the βC and EC distributions stand out for the dataset with positive asymmetry and for the dataset with negative asymmetry the KwC model is the best. The important contribution of this chapter, besides the presentation of four new flexible models for circular data, is the mathematical treatability of their trigonometric moments through the special functions presented in Chapter 2, for EC distribution.

Next, some future topics to be investigated are listed:

- In the Chapter 3 was noted the difficulty in the interpretation of the standard errors of the estimates obtained for the parameters of the distributions in question, in the applications. This is a problem in building confidence intervals, for example. Investigating this problem and proposing solutions and new methodologies is a topic of future research.

- Propose new circular distributions, by the methods used, using new baselines is intended in future researches.

- Proposed other regression models based on the EC distribution.

- Proposed methods of outliers identification to the presented regression model in this thesis.

References

Abe, T. and Pewsey, A. (2009). Sine-skewed circular distributions. *Statistical Papers* **52**, 683–707.

Abe, T., Pewsey, A. and Shimizu, K. (2009). On Papakonstantinou's extension of the Cardioid distribution. *Statistics and Probability Letters* **79**, 2138–2147.

Abe, T., Pewsey, A. and Shimizu, K. (2013). Extending circular distributions through transformation of argument. *Annals of the Institute of Statistical Mathematics* **65**, 833–858.

Ahlfors, L. V. (1979). *Complex Analysis: An Introduction to the Theory of Analytic Functions of One Complex Variable*, 3º edn. McGraw-Hill.

AL-Hussaini, E. K. and Ahsanullah, M. (2015). *Exponentiated Distributions*. Atlantic Press, Paris.

Azzalini, A. (1985). A class of distributions which includes the Normal ones. *Scandinavian Journal of Statistics* **12**, 171–178.

Batschelet, E. (1981). *Circular Statistics in Biology*. Academic Press, London.

Boles, L. C. and Lohmann, K. J. (2003). True navigation and magnetic maps in spiny lobsters. *Nature* **421**, 60–63.

Boomsma, W., Mardia, K. V., Taylor, C. C., Ferkinghoff-Borg, J., Krogh, A. and Hamelryck, T. (2008). A generative, probabilistic model of local protein structure. *Proceedings of the National Academy of Sciences of the United States of America* **105**, 8932–8937.

Box, G. E. P. and Pierce, D. A. (1970). Distribution of residual correlations in autoregressive-integrated moving average time series models. *Journal of the Royal Statistical Society* **65**, 1509–1526.

Brunsdon, C. and Corcoran, J. (2006). Using circular statistics to analyse time patterns in crime incidence. *Computers, Environment and Urban Systems* **30**, 300–319.

Chang, T. (1986). Spherical regression. *Encyclopedia of Statistical Sciences* .

Chu, X., Zhang, J., Wang, S. and Ji, Y. (2015). Algorithm to eliminate the wind direction ambiguity from the monostatic high-frequency radar backscatter spectra. *IET Radar, Sonar & Navigation* **9**(7), 758–762.

Coles, P., Dineen, P., Earl, J. and Wright, D. (2004). Phase correlations in cosmic microwave background temperature maps. *Monthly Notices of the Royal Astronomical Society* **350**(3), 989–1004.

Cordeiro, G. M. and de Castro, M. (2011). A new family of generalized distributions. *Journal of statistical computation and simulation* **81**(7), 883–898.

Cordeiro, G. M., Ortega, E. M. and da Cunha, D. C. (2013). The exponentiated generalized class of distributions. *Journal of Data Science* **11**(1), 1–27.

Cordeiro, G. M., Lemonte, A. J. and Ortega, E. M. (2014). The Marshall–Olkin family of distributions: Mathematical properties and new models. *Journal of Statistical Theory and Practice* **8**(2), 343–366.

Cordeiro, G. M., Alizadeh, M. and Diniz Marinho, P. R. (2016). The type i half-logistic family of distributions. *Journal of Statistical Computation and Simulation* **86**(4), 707–728.

Cordeiro, G. M., Afify, A. Z., Yousof, H. M., Pescim, R. R. and Aryal, G. R. (2017). The exponentiated Weibull-H family of distributions: Theory and applications. *Mediterranean Journal of Mathematics* **14**(4), 155.

Cribari-Neto, F. and Cordeiro, G. M. (1996). On Bartlett and Bartlett-type corrections. *Econometric Reviews* **15**, 339–367.

Cribari-Neto, F. and Queiroz, M. P. (2014). On testing inference in beta regressions. *Journal of Statistical Computation and Simulation* **84**, 186–203.

Davis, J. (ed) (1986). *Statistics and Data Analysis in Geology*, 2º edn. Wiley, New York.

Davison, A. C. and Hinkley, D. V. (2003). *Bootstrap Methods and Their Application*, 2º edn. Cambridge University Press, New York.

Downs, T. D. and Mardia, K. (2002). Circular regression. *Biometrika* **89**(3), 683–698.

Efron, B. (1979). Bootstrap methods: another look at the jackknife. *The Annals of Statistics* **7**, 1–26.

Eugene, N., Lee, C. and Famoye, F. (2002). Beta-normal distribution and its applications. *Communications in Statistics-Theory and methods* **31**(4), 497–512.

Fernandez, D. M., Graber, H. C., Paduan, J. D. and Barrick, D. E. (1997). Mapping wind direction with HF radar. *Oceanography* **10**(2), 93–95.

Fernández-Durán, J. J. (2004). Circular distributions based on nonnegative trigonometric sums. *Biometrics* **60**, 499–503.

Fisher, N. I. (1995). *Statistical Analysis of Circula Data*. Cambridge University Press.

Fisher, N. I. and Hall, P. (1990). On bootstrap hypothesis testing. *Australian Journal of Statistics* **32**, 177–190.

Fisher, N. I. and Hall, P. (1992). *Bootstrap Methods for Directional Data . In The Art of Statistical Science (K. V. Mardia, editor)*. Wiley, New York.

Flohr, F., Dumitru-Guzu, M., Kooij, J. F. and Gavrila, D. M. (2014). Joint probabilistic pedestrian head and body orientation estimation. Em: *2014 IEEE Intelligent Vehicles Symposium Proceedings*, IEEE, pp. 617–622.

Gatto, S. R. and Jammalamadaka, S. R. (2007). The generalized von Mises distribution. *Statistical Methodology* **4**, 341–353.

Guo, H., Guo, H. and Li, Y. (2010). A study on seasonal distribution of measles in Heping district, Shenyang, from 2001 to 2009. Em: *Biomedical Engineering and Informatics (BMEI), 2010 3rd International Conference on*, IEEE, vol 6, pp. 2446–2448.

Hardy, G. H. and Wright, E. M. (1979). *An introduction to the theory of numbers*. Oxford university press.

Hernández-Sánchez, E. and Scarpa, B. (2012). A wrapped flexible generalized skew-normal model for a bimodal circular distribution of wind directions. *Chilean Journal of Statistics (ChJS)* **3**(2).

Hohenwarter, M. (2008). Geogebra. .

Hussain, F., Zubairi, Y. Z. and Hussin, A. G. (2007). An alternative diagrammatical representation of wind data. Em: *Proceedings of the 12th WSEAS International Conference on Applied Mathematics*, World Scientific and Engineering Academy and Society (WSEAS), pp. 292–294.

Hussin, A., Fieller, N. and Stillman, E. (2004). Linear regression model for circular variables with application to directional data. *Journal of Applied Science and Technology* **9**(1), 1–6.

Jammalamadaka, S. R. and Kozubowsky, T. (2004). A new families of wrapped distributions for modeling skew circular data. *Communiation in Statistics-Theory and Methods* **33**, 2059–2074.

Jammalamadaka, S. R. and Sengupta, A. (2001). *Topics in Circular Statistics*, vol 5. World Scientific.

Jeffreys, H. (1961). *Theory of Probability*. Oxford University Press.

Jha, J. and Biswas, A. (2017). Multiple circular–circular regression. *Statistical Modelling* **17**(3), 142–171.

Johnson, R. A. and Wehrly, T. (1977). Measures and models for angular correlation and angular-linear correlation. *Journal of the Royal Statistical Society Series B (Methodological)* pp. 222–229.

Jones, M. (2004). The Möbius distribution on the disc. *Annals of the Institute of Statistical Mathematics* **56**(4), 733–742.

Jones, M. and Pewsey, A. (2005). A family of symmetric distributions on the circle. *Journal of the American Statistical Association* **100**(472), 1422–1428.

Jones, M. C. and Pewsey, A. (2012). Inverse Batschelet distributions for circular data. *Biometrics* **68**, 183–193.

Jupp, P. and Mardia, K. (1980). A general correlation coefficient for directional data and related regression problems. *Biometrika* **67**(1), 163–173.

Kato, S. and Jones, M. (2010). A family of distributions on the circle with links to, and applications arising from, Möbius transformation. *Journal of the American Statistical Association* **105**(489), 249–262.

Kato, S. and Jones, M. C. (2013). An extended family of circular distributions related to wrapped Cauchy distributions via Brownian motion. *Bernoulli* **19**, 154–171.

Kato, S., Shimizu, K. and Shieh, G. S. (2008). A circular–circular regression model. *Statistica Sinica* pp. 633–645.

Kucwaj, J. C., Reboul, S., Stienne, G., Choquel, J. B. and Benjelloun, M. (2017). Circular regression applied to GNSS-R phase altimetry. *Remote Sensing* **9**(7), 651.

Lehmann, E. L. and Casella, G. (2006). *Theory of Point Estimation*. Springer Science & Business Media.

Lemonte, A. J. and Ferrari, S. L. P. (2012). Local power and size properties of the LR, Wald, score and gradient tests in dispersion models. *Statistical Methodology* **9**, 537–554.

Li, J., Mahalingam, S. and Weise, D. R. (2017). Experimental investigation of fire propagation in single live shrubs. *International Journal of Wildland Fire* **26**(1), 58–70.

Malsimov, V. M. (1967). Necessary and sufficient statistics for the family of shifts of probability distributions on continuous bicompact groups. *Theory Of Probability And Its Applications* **12**, 267–280.

Mardia, K. V. (1972). *Statistics of Directional Data*. Academic Press, London.

Mardia, K. V. and Jupp, P. E. (1999). *Directional Statistics*. John Wiley, Chichester.

Mardia, K. V. and Sutton, T. W. (1975). On the modes of a mixture of two von Mises distributions. *Biometrika* **62**, 699–701.

Mardia, K. V., Taylor, C. C. and Subramaniam, G. K. (2007). Protein bioinformatics and mixtures of bivariate von Mises distributions for angular data. *Biometrics* **63**, 505–512.

Marshall, A. W. and Olkin, I. (1997). A new method for adding a parameter to a family of distributions with application to the exponential and Weibull families. *Biometrika* **84**(3), 641–652.

McCullagh, P. and *et al.* (1996). Möbius transformation and Cauchy parameter estimation. *The Annals of Statistics* **24**(2), 787–808.

Minh, D. L. and Farnum, N. R. (2003). Using bilinear transformations to induce probability distributions. *Communications in Statistics-Theory and Methods* **32**(1), 1–9.

Morellato, L. P. C., Alberti, L. F. and Hudson, I. L. (2010). Applications of circular statistics in plant phenology: a case studies approach. Em: Hudson, I. L. and Keatley, M. R. (Eds) *Phenological research: Methods for Environmental and Climate Change Analysis*, Springer, New York, pp. 339–359.

Nadarajah, S., Cordeiro, G. M. and Ortega, E. M. (2015). The zografos–balakrishnan-g family of distributions: mathematical properties and applications. *Communications in Statistics-Theory and Methods* **44**(1), 186–215.

Neyman, J. and Pearson, E. S. (1928). On the use and interpretation of certain test criteria for purposes of statistical inference. *Biometrika* **20**, 175–240.

Nocedal, J. and Wright, S. J. (2006). *Numerical Optimization*, 2º edn. Springer, New York, NY, USA.

Pan, L., Tomlinson, A. and Koloydenko, A. A. (2017). Time pattern analysis of malware by circular statistics. *2017 ACM/IEEE Symposium on Architectures for Networking and Communications Systems (ANCS)* pp. 119–130.

Pewsey, A. (2008). The wrapped stable family of distributions as a flexible model for circular data. *Computational Statistics Data Analysis* **52**, 1516–1523.

Pewsey, A., Neyhäuser, M. and Ruxton, G. D. (2014). *Circular Statistics in R*. Oxford University Press, United Kingdom.

R Core Team (2017). *R: A Language and Environment for Statistical Computing*. R Foundation for Statistical Computing, Vienna, Austria, URL `https://www.R-project.org/`.

Rao, A. V. D., Girija, S. V. S. and Phani, Y. (2011). Differential approach to Cardioid distribution. .

Rao, C. (1948). Large sample tests of statistical hypotheses concerning several parameters with applications to problems of estimation. *Mathematical Proceedings of the Cam- bridge Philosophical Society* **44**, 50–57.

Rao, J. S. and Sengupta, S. (1972). Mathematical techniques for paleocurrent analysis: Treatment of directional data. *Journal of the International Association for Mathematical Geology* **4**, 235–248.

Rivest, L. P. (1997). A decentred predictor for circular-circular regression. *Biometrika* **84**(3), 717–726.

Sarma, Y. and Jammalamadaka, S. (1993). Circular regression. *Statistical Science and Data Analysis* pp. 109–128.

SenGupta, A. and Kim, S. (2016). Statistical inference for homologous gene pairs between two circular genomes: a new circular–circular regression model. *Statistical Methods & Applications* **25**(3), 421–432.

SenGupta, A. and Pal, C. (2001). Optimal tests for no contamination in directional data. *Journal Applied Statistics* **28**, 129–143.

SenGupta, A., Kim, S. and Arnold, B. C. (2013). Inverse circular–circular regression. *Journal of Multivariate Analysis* **119**, 200–208.

Seshadri, V. (1991). A family of distributions related to the McCullagh family. *Statistics & probability letters* **12**(5), 373–378.

Solman, G. J. and Kingstone, A. (2014). Balancing energetic and cognitive resources: memory use during search depends on the orienting effector. *Cognition* **132**(3), 443–454.

Stephens, M. A. (1969). Techniques for directional data. Relatório Técnico, STANFORD UNIV CA DEPT OF STATISTICS.

Terrell, G. (2002). The gradient statistic. *Computing Science and Statistics* **34**, 206–215.

Tietjen, W. J. (1978). Tests for olfactory communication in four species of wolf spiders (araneae, lycosidae). *Journal of Arachnology* pp. 197–206.

Umbach, D. and Jammalamadaka, S. R. (2009). Building asymmetry into circular distributions. *Statistics and Probability Letters* **79**, 659–663.

Upton, G. J. G. and Fingleton, B. (1989). *Spatial Data Analysis by Example, Volume II: Categorical and Directional Data*. Wiley.

Viftrup, S. S., Kumarappan, V., Trippel, S. and Stapelfeldt, H. (2007). Holding and spinning molecules in space. *Physical Review Letters* **99**, 143.602.

Wald, A. (1943). Tests of statistical hypotheses concerning several parameters when the number of observations is large. *Transactions of the American Mathematical Society* **54**, 426–482.

Wang, M. z. and Shimizu, K. (2012). On applying Möbius transformation to Cardioid random variables. *Statistical Methodology* **9**(6), 604–614.

Yfantis, E. A. and Borgmann, L. E. (1982). An extension of the von Mises distribution. *Communications in Statistics* **11**, 1965–1706.

Yousof, H. M., Afify, A. Z., Hamedani, G. and Aryal, G. (2016). The Burr X generator of distributions for lifetime data. *Journal of Statistical Theory and Applications* **16**, 1–19.

Zografos, K. and Balakrishnan, N. (2009). On families of beta-and generalized gamma-generated distributions and associated inference. *Statistical Methodology* **6**(4), 344–362.

Appendix A - Theorem 2.2.1. proof

Let $\Theta \sim EC(\beta, \rho, \mu)$ and $\beta \geq 1$. Then,

$$\begin{aligned} f'(\theta) = 0 &\Rightarrow (\beta-1)F_C(\theta)^{\beta-1}\left[\frac{1}{2\pi} + \frac{\rho}{\pi}\cos(\theta-\mu)\right]^2 - F_C(\theta)^{\beta}\frac{\rho}{\pi}\sin(\theta-\mu) = 0 \\ &\Rightarrow (\beta-1)y(\theta)^{\beta-1}y'(\theta)^2 + y(\theta)^{\beta}y''(\theta) = 0, \end{aligned}$$

where F_C represents the Cardioid cdf.

The latter is an ordinary differential equation of the second order, whose general solution is $y(\theta) = c_2(\beta\theta + c_1)^{\frac{1}{\beta}}$, where $y(\theta) = F_C(\theta)$. Given that $\beta \geq 1$, then $y(0) = 0$ and $y(2\pi) = 1$. Thus, $c_1 = 0$ and $c_2 = (2\pi\beta)^{-\frac{1}{\beta}}$, where does it follow that $F(\theta) = \frac{\theta}{2\pi}$. Equivalence is demonstrated in a similar way.

Appendix B - First central trigonometric moment

In this appendix, the expression for the first central trigonometric moment of the EC distribution is derived in detail.

Theorem 6.0.1 (Binomial Theorem)**.** *For* $r \in \mathbb{R}$ *ou* $|\frac{x}{y}| < 1$.

$$(x+y)^r = \sum_{k=0}^{\infty} \binom{r}{k} x^k y^{r-k}.$$

First, consider also the following trigonometric inequalities and relation: For $x \in \mathbb{R}$, i) $|\sin x| < x$ and $|\cos x| < 1$ and ii) $\sin x + \cos y = 2\sin\left(\frac{x+y}{2}\right)\cos\left(\frac{x-y}{2}\right)$ hold and, consequently, one has that

$$\left|\frac{\frac{\rho}{\pi}[\sin(\theta-\mu)+\sin(\mu)]}{\frac{\theta}{2\pi}}\right| = \left|\frac{2\rho[\sin(\theta-\mu)+\sin(\mu)]}{\theta}\right| = \left|\frac{4\rho}{\theta}\sin\left(\frac{\theta}{2}\right)\cos\left(\frac{\theta-2\mu}{2}\right)\right|$$

$$< \left|\frac{4\rho}{\theta}\frac{\theta}{2}\cos\left(\frac{\theta-2\mu}{2}\right)\right| \leq 2\rho \leq 1.$$

Thus, from the binomial theorem, the EC cdf can be written as

$$\left\{\frac{\theta}{2\pi} + \frac{\rho}{\pi}[\sin(\theta-\mu)+\sin(\mu)]\right\}^{\beta} = \sum_{k=0}^{+\infty}\binom{\beta}{k}\left(\frac{\theta}{2\pi}\right)^{\beta-k}\left(\frac{\rho}{\pi}\right)^{k}[\sin(\theta-\mu)+\sin(\mu)]^k.$$

Further, the term $[\sin(\theta-\mu)+\text{sen}(\mu)]^k$ may be rewritten as

$$[\sin(\theta-\mu)]^k\left[1+\frac{\sin(\mu)}{\sin(\theta-\mu)}\right]^k M_0 + [\sin(\mu)]^k\left[1+\frac{\sin(\theta-\mu)}{\sin(\mu)}\right]^k M_1$$

$$= [\sin(\theta-\mu)]^k \sum_{s=0}^{+\infty}\binom{k}{s}\left[\frac{\sin(\mu)}{\sin(\theta-\mu)}\right]^s M_0 + [\sin(\mu)]^k \sum_{s=0}^{+\infty}\binom{k}{s}\left[\frac{\sin(\theta-\mu)}{\sin(\mu)}\right]^s M_1,$$

where, $M_0 = \mathbb{I}(|\sin(\theta-\mu)| \geq |\sin(\mu)|)$, $M_1 = \mathbb{I}(|\sin(\theta-\mu)| < |\sin(\mu)|)$, $\mathbb{I}(.)$ refers to the indicator function and the portion composed by the quotients are, in module, less than 1. Thus, from the Binomial Theorem, it follows that

$$F(\theta) = \sum_{k=0}^{+\infty}\sum_{s=0}^{k}\binom{\beta}{k}\binom{k}{s}\left(\frac{\theta}{2\pi}\right)^{\beta-k}\left(\frac{\rho}{\pi}\right)^{k}\left\{\frac{\sin(\mu)^s}{\sin(\theta-\mu)^{s-k}}M_0 + \frac{\sin(\theta-\mu)^s}{\sin(\mu)^{s-k}}M_1\right\}.$$

To simplify this expression, we adopt the notation

$$t_{k,s}(\beta,\rho,\mu)=\binom{\beta}{k}\binom{k}{s}\left(\frac{1}{2\pi}\right)^{\beta-k}\left(\frac{\rho}{\pi}\right)^{k}[\sin(\mu)]^{s}.$$

Thus,

$$F(\theta)=\sum_{k=0}^{+\infty}\sum_{s=0}^{k}t_{k,s}\theta^{\beta-k}[\sin(\theta-\mu)]^{s}\left\{[\sin(\theta-\mu)]^{k-2s}M_0+[\sin(\mu)]^{k-2s}M_1\right\}.$$

Now, using integration by parts, the EC pth central trigonometric moment is given by

$$\begin{aligned}\mu_p =&\mathbb{E}\{\cos[p(\Theta-\mu)]\}+i\mathbb{E}\{\sin[p(\Theta-\mu)]\}\\ =&\int_0^{2\pi}\cos[p(\theta-\mu)]dF(\theta)+i\int_0^{2\pi}\sin[p(\theta-\mu)]dF(\theta)\\ =&\cos(p\mu)+\int_0^{2\pi}p\{[\sin[p(\theta-\mu)]\}F(\theta)d\theta-i\left\{\sin(p\mu)+\int_0^{2\pi}p\{[\cos[p(\theta-\mu)]\}F(\theta)d\theta\right\}.\end{aligned}$$

The first moment is given by

$$\mu_1=\mathbb{E}[\cos(\Theta-\mu)]+i\mathbb{E}[\sin(\Theta-\mu)],$$

where

$$\mathbb{E}[\cos(\Theta-\mu)]=\cos(\mu)+\sum_{k=0}^{+\infty}\sum_{s=0}^{k}t_{k,s}\left\{A(\beta-k,0,k-s+1)M_0+[\sin(\mu)]^{k-2s}A(\beta-k,0,s+1)M_1\right\},$$

$$\mathbb{E}[\sin(\Theta-\mu)]=-\sin(\mu)-\sum_{k=0}^{+\infty}\sum_{s=0}^{k}t_{k,s}\left\{A(\beta-k,1,k-s)M_0-[\sin(\mu)]^{k-2s}A(\beta-k,1,s)M_1\right\}$$

and

$$A(a,b,c)=\int_0^{2\pi}\theta^{a}[\cos(\theta-\mu)]^{b}[\sin(\theta-\mu)]^{c}d\theta.$$

Appendix C - Theorem 3.2.1. proof

Let $\Theta \sim EC(\beta, \rho, \mu)$. Then,

$$\begin{aligned}\mathbb{E}\left\{\{F_C(\theta)\}^{-1}\right\} &= \beta\int_0^{2\pi}\{F_C(\theta)\}^{-1}\{F_C(\theta)\}^{\beta-1}f_C(\theta)d\theta = \beta\int_0^{2\pi}\{F_C(\theta)\}^{\beta-2}f_C(\theta)d\theta \\ &= \beta\frac{\{F_C(\theta)\}^{\beta-1}}{\beta-1}\Bigg|_0^{2\pi} = \frac{\beta}{\beta-1},\end{aligned}$$

for $\beta > 1$ and

$$\begin{aligned}\mathbb{E}\left\{\{F_C(\theta)\}^{-2}\right\} &= \beta\int_0^{2\pi}\{F_C(\theta)\}^{-2}\{F_C(\theta)\}^{\beta-1}f_C(\theta)d\theta = \beta\int_0^{2\pi}\{F_C(\theta)\}^{\beta-3}f_C(\theta)d\theta \\ &= \beta\frac{\{F_C(\theta)\}^{\beta-2}}{\beta-2}\Bigg|_0^{2\pi} = \frac{\beta}{\beta-2},\end{aligned}$$

for $\beta > 2$, where $F_C = \frac{\theta}{2\pi} + \frac{\rho}{\pi}[\text{sen}(\theta-\mu) + \text{sen}(\mu)]$ and $f_C(\theta) = \frac{1}{2\pi}\{1 + 2\rho\cos(\theta-\mu)\}$ is a Cardioid cdf and pdf, respectively.

Appendix D - Theorem 3.2.2. proof

The bellow corollary follows from Lehmann and Casella (2006).

Corollary 6.0.2. *Let $\Theta_1, \cdots, \Theta_n$ be a random sample which satisfies the regularity conditions on Lehmann and Casella (2006) and each Θ_i has observed information $\boldsymbol{J}_1$, the information of $\boldsymbol{\Theta} = (\Theta_1, \cdots, \Theta_n)$ is $\boldsymbol{J} = n\,\boldsymbol{J}_1$.*

Let $\Theta \sim EC(\beta, \rho, \mu)$. From the Theorem 3.2.1,

$$\begin{aligned}
\mathbb{E}[J_{12}] &= \mathbb{E}\left\{\frac{\sin(\Theta-\mu)+\sin(\mu)}{\Theta+2\rho[\sin(\Theta-\mu)+\sin(\mu)]}\right\} \\
&= \frac{\beta}{2\pi(\beta-1)}\int_0^{2\pi}[\sin(\theta-\mu)+\sin(\mu)]\,(\beta-1)\,\{G(\theta)\}^{\beta-2}\,g(\theta)\,\mathrm{d}\theta \\
&= \frac{\beta\sin(\mu)}{2\pi(\beta-1)} + \frac{\beta}{2\pi}\int_0^{2\pi}\sin(\theta-\mu)\;\{G(\theta)\}^{\beta-2}\,g(\theta)\,\mathrm{d}\theta \\
&= \frac{\beta}{2\pi}\left[\frac{\sin(\mu)}{\beta-1} + I_{0,1,2,1}(\beta,\rho,\mu)\right].
\end{aligned}$$

Thus, it follows from the Corollary 6.0.2 and the previous identity that

$$\mathbb{E}[J_{12}] = \frac{n\beta}{2\pi}\left[\frac{\sin(\mu)}{\beta-1} + I_{0,1,2,1}(\beta,\rho,\mu)\right].$$

The other FIM entries may be deducted in a similar way.

Appendix E - Derivation of the CEC pdf

Let $z = e^{i\theta}$ and $\phi = \rho e^{i\mu}$. The following equality holds

$$|z - \phi|^2 = 1 - 2\rho\cos(\theta - \mu) + \rho^2$$

and, therefore,

$$1 + 2\rho\cos(\theta - \mu) = -|z - \phi|^2 + 2 + \rho^2 \tag{6.1}$$

and

$$\cos(\theta - \mu) = \frac{-|z - \phi|^2 + 1 + \rho^2}{2\rho}. \tag{6.2}$$

.

From $\sin^2(\theta) + \cos^2(\theta) = 1$ and (6.2), we have

$$\sin(\theta - \mu) = \pm\sqrt{1 - \left(\frac{-|z - \phi|^2 + 1 + \rho^2}{2\rho}\right)^2}. \tag{6.3}$$

The $\sin(\theta - \mu)$ signal will depend on the circumference quadrant in which $\theta - \mu$ is located. In this case, the signal will positive and negative for $0 < \theta - \mu + 2k\pi \leq \pi$ and $\pi < \theta - \mu + 2k\pi \leq 2\pi$, respectively, considering $k = 0, 1$. Defining the indicator function $\mathbb{I}_1$ as

$$\mathbb{I}_1 = \begin{cases} 1, \text{if } \pi < \theta - \mu + 2k\pi \leq 2\pi, \text{for } k = 0, 1 \\ 0, \text{if } 0 < \theta - \mu + 2k\pi \leq \pi, \text{for } k = 0, 1 \end{cases},$$

Applying (6.1)-(6.3) in (4.2), we have

$$f(z) = -\beta\frac{|z - \phi|^2 + |1 - |\phi|^2| - 3}{(2\pi)^\beta} \times \left[\text{Arg}(\theta) + (-1)^{\mathbb{I}_1} 2\rho\left(\sqrt{1 - \left[\frac{-|z - \phi|^2 + 1 + |\phi|^2}{2|\phi|}\right]^2} + \sin[\text{Arg}(\phi)]\right)\right]^{\beta - 1},$$

with $0 < \rho \leq 0.5$, $0 < \theta, \mu \leq 2\pi$ and $|\cdot|$ and $\text{Arg}(\cdot)$ indicate the modulus and argument of a complex number, respectively.